Semiconductor Detectors

Simon Procz

University of Freiburg
FMF Freiburg Materials Research Center

UNIANDES PARTICLE DETECTOR SCHOOL
DECEMBER 13 - DECEMBER 15

Freiburg / Germany

Source: mofa-freiburg.de

Freiburg / Germany

250,000 residents

033,000 students

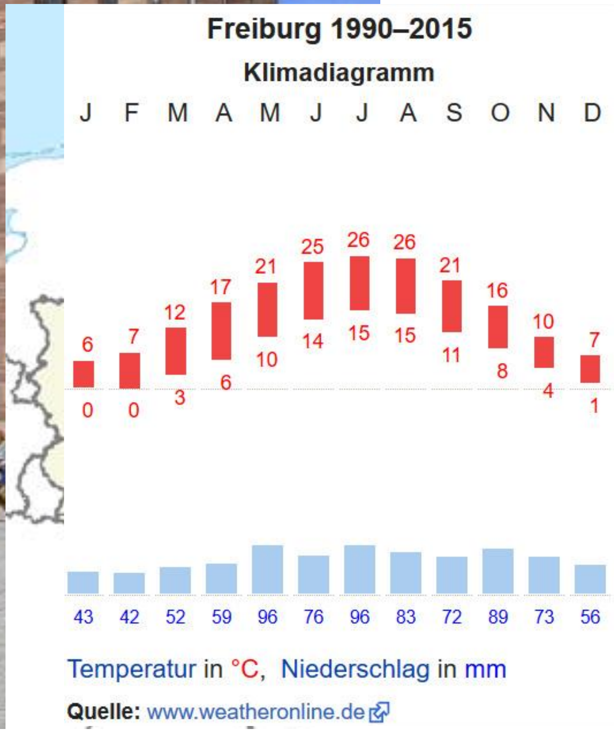

Outline

- Semiconductor Basics
- Growth of Silicon
- Non-Hybrid Semiconductor Detectors
- Signal Formation and Processing in Detectors
- Hybrid Pixel Detectors: Timepix & Medipix

Source:

Formation of Energy Bands in a Semiconductor

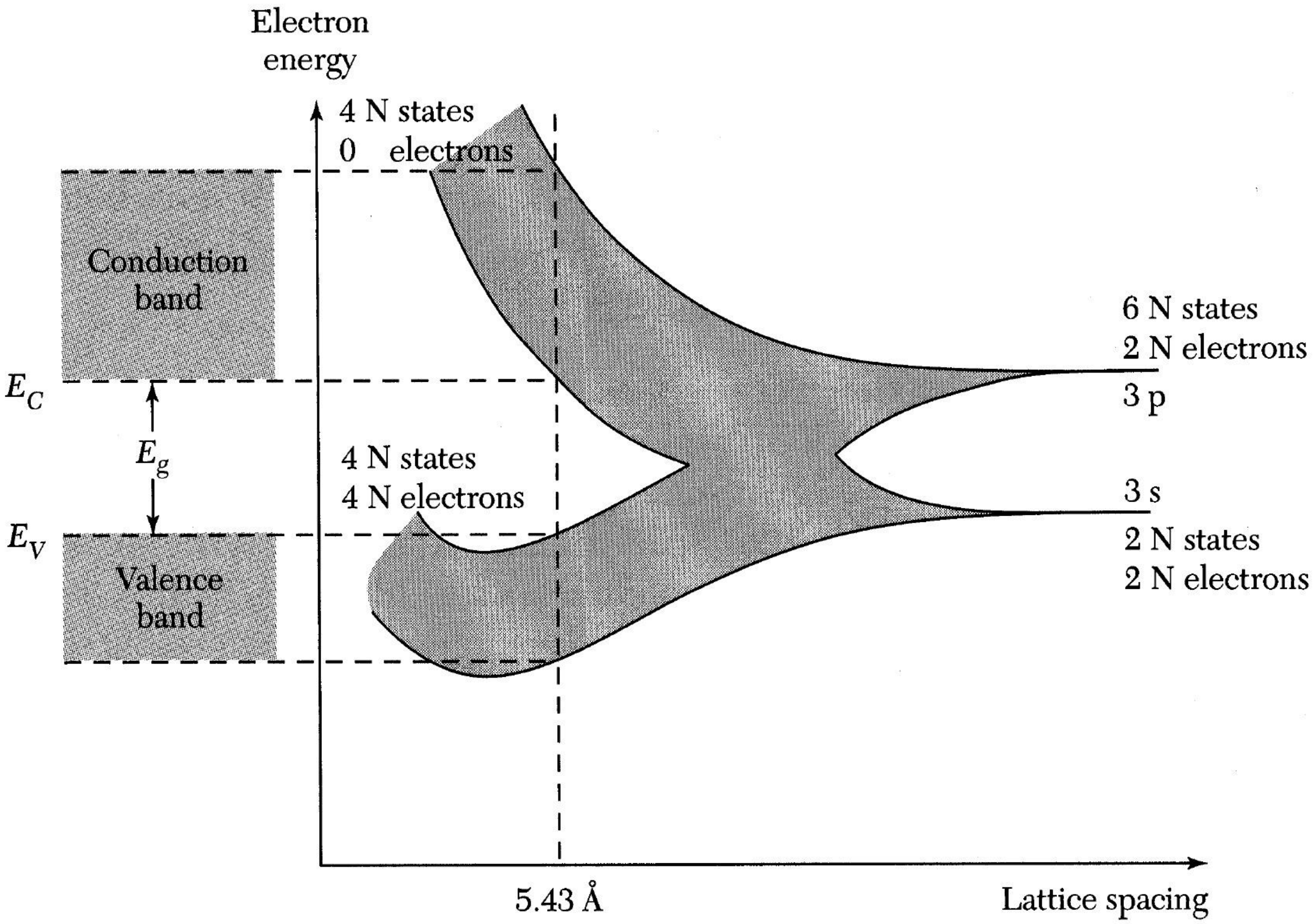

Source: Sze, Physics of Semiconductor Devices

Energy Bands in a Semiconductor

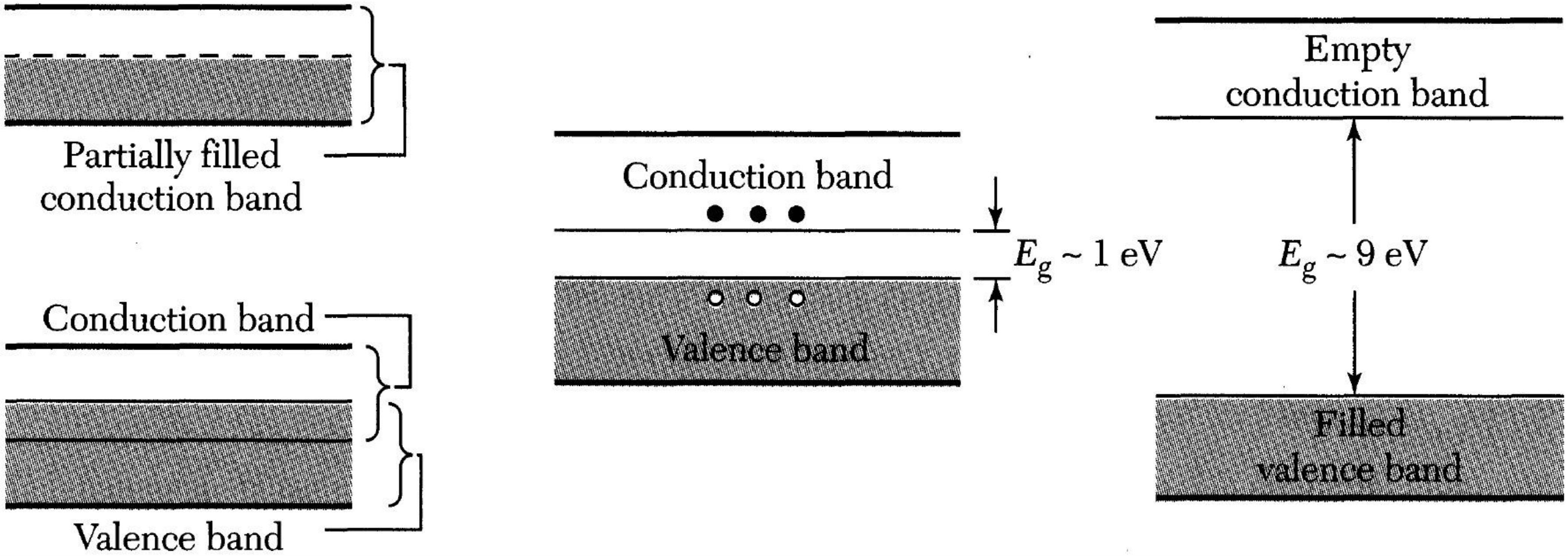

Metal Semiconductor Isolator

Source: Sze, Physics of Semiconductor Devices

Movement of Elektrons / Holes

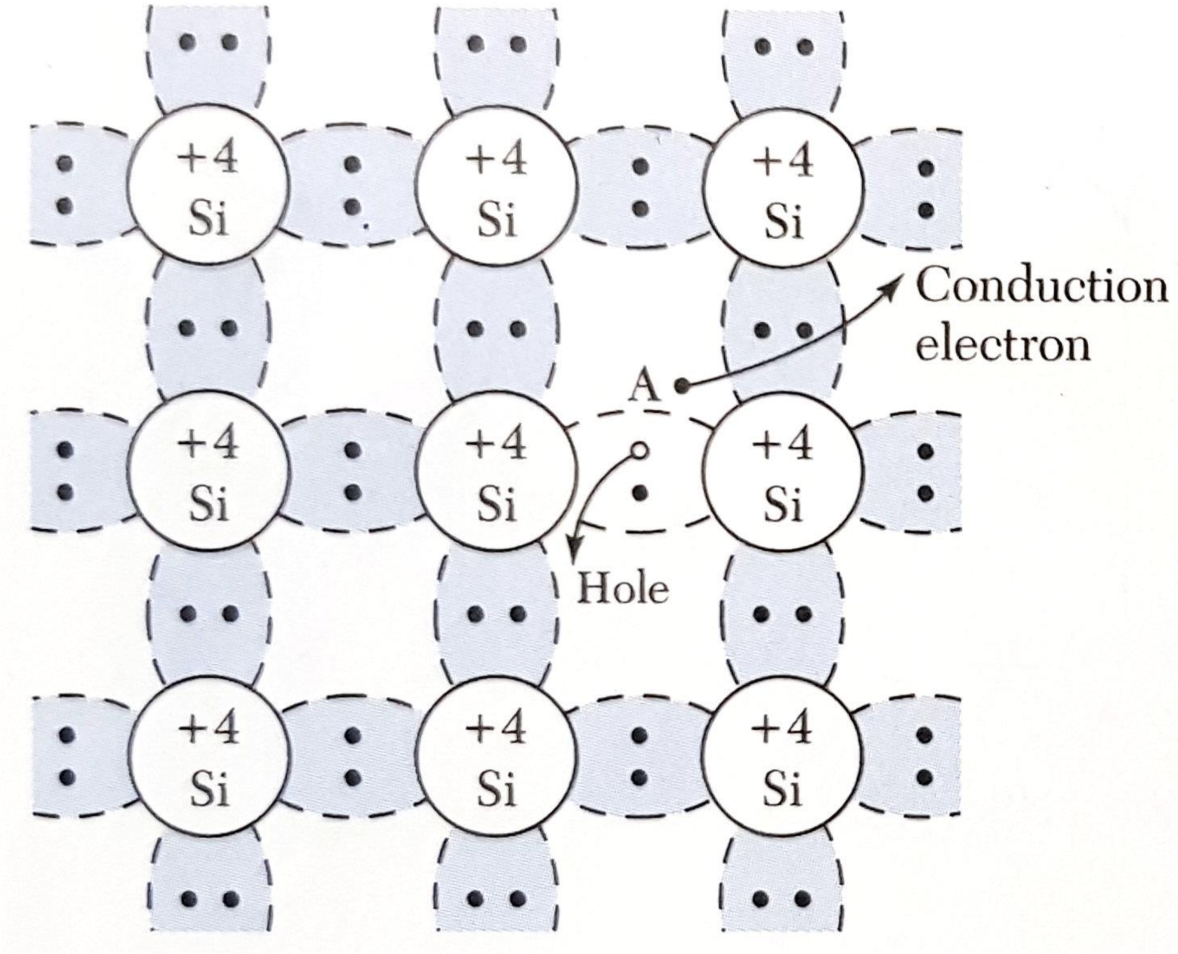

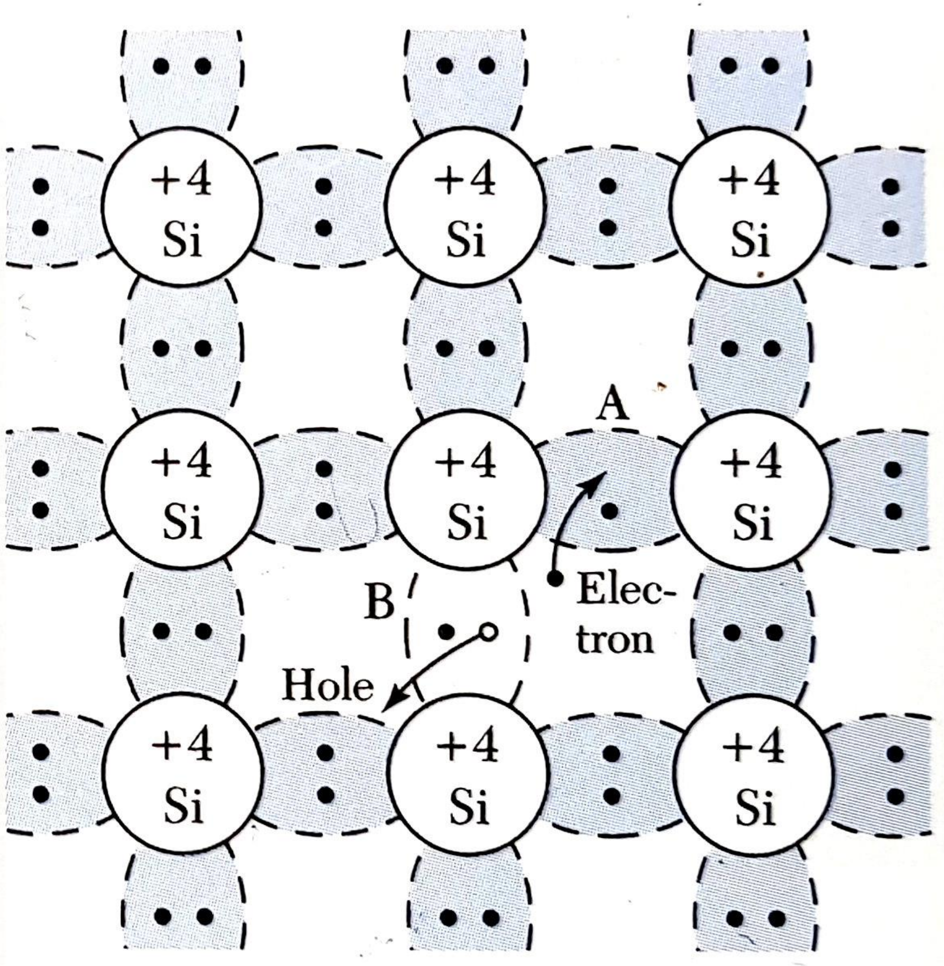

Semiconductor Band Diagramm

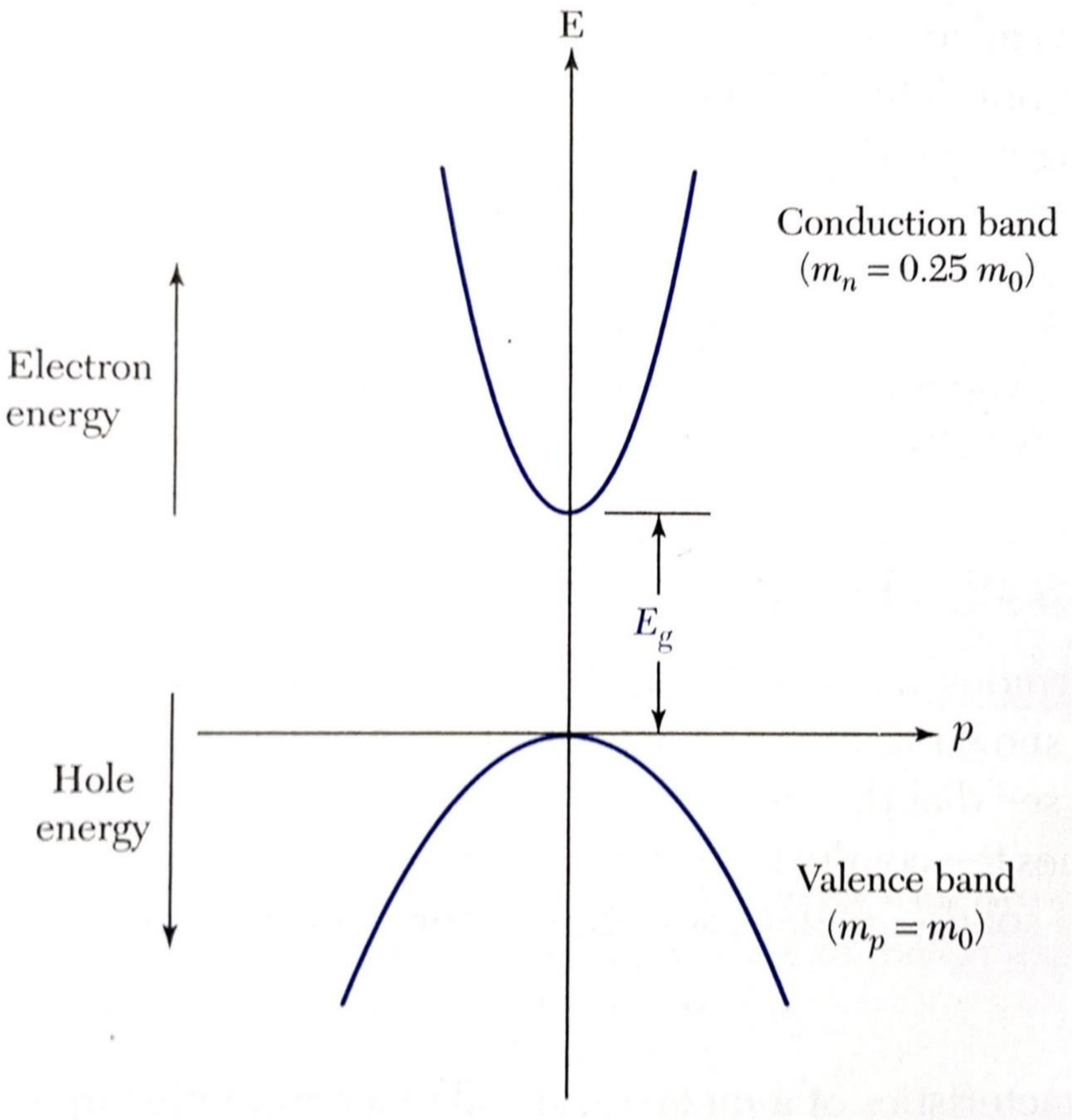

$$E = \frac{p^2}{2m_0},$$

$$m_n \equiv \left(\frac{d^2E}{dp^2} \right)^{-1}.$$

Semiconductor Band Diagramms

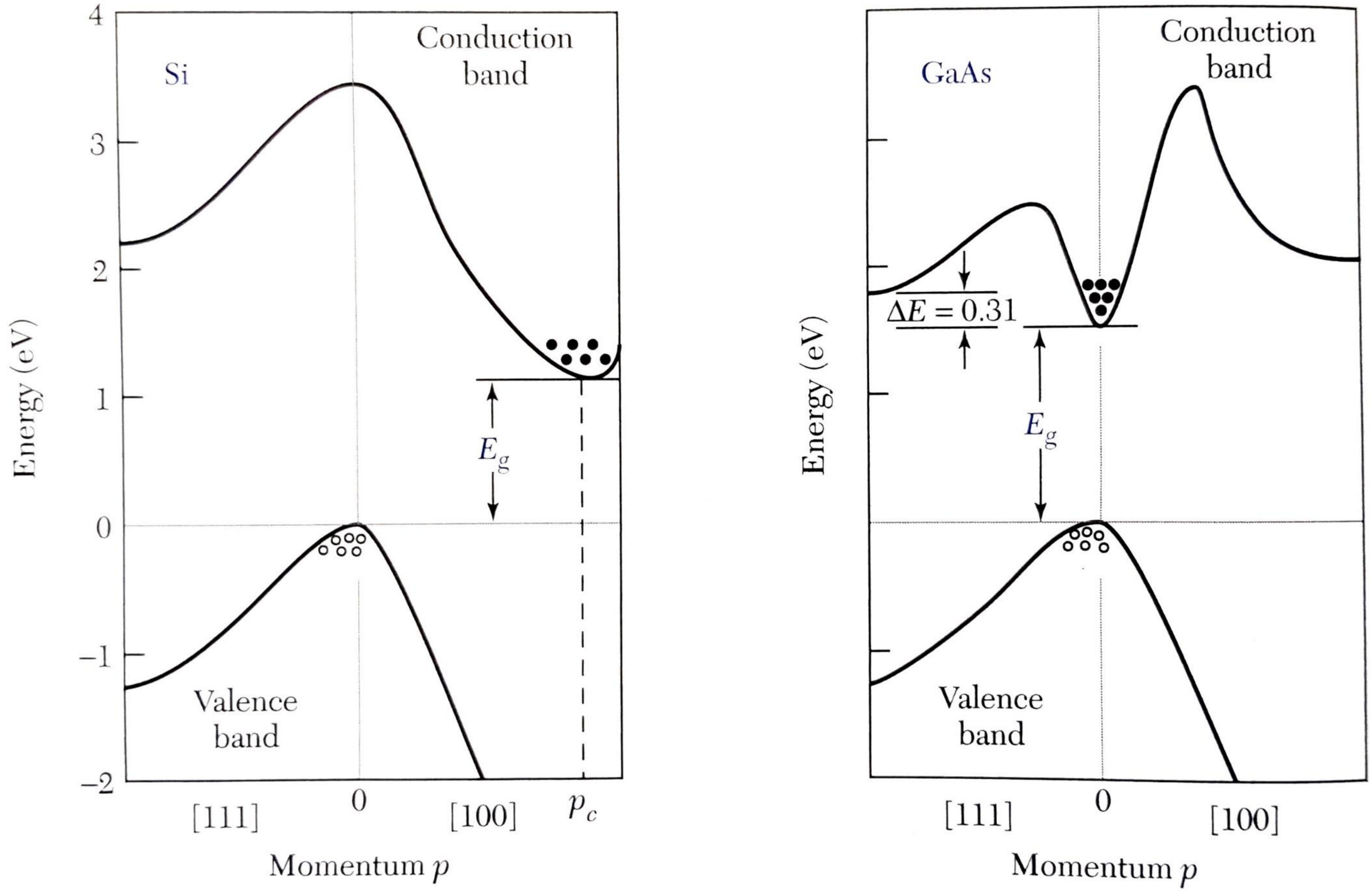

Source: Sze, Physics of Semiconductor Devices

Siemens Process

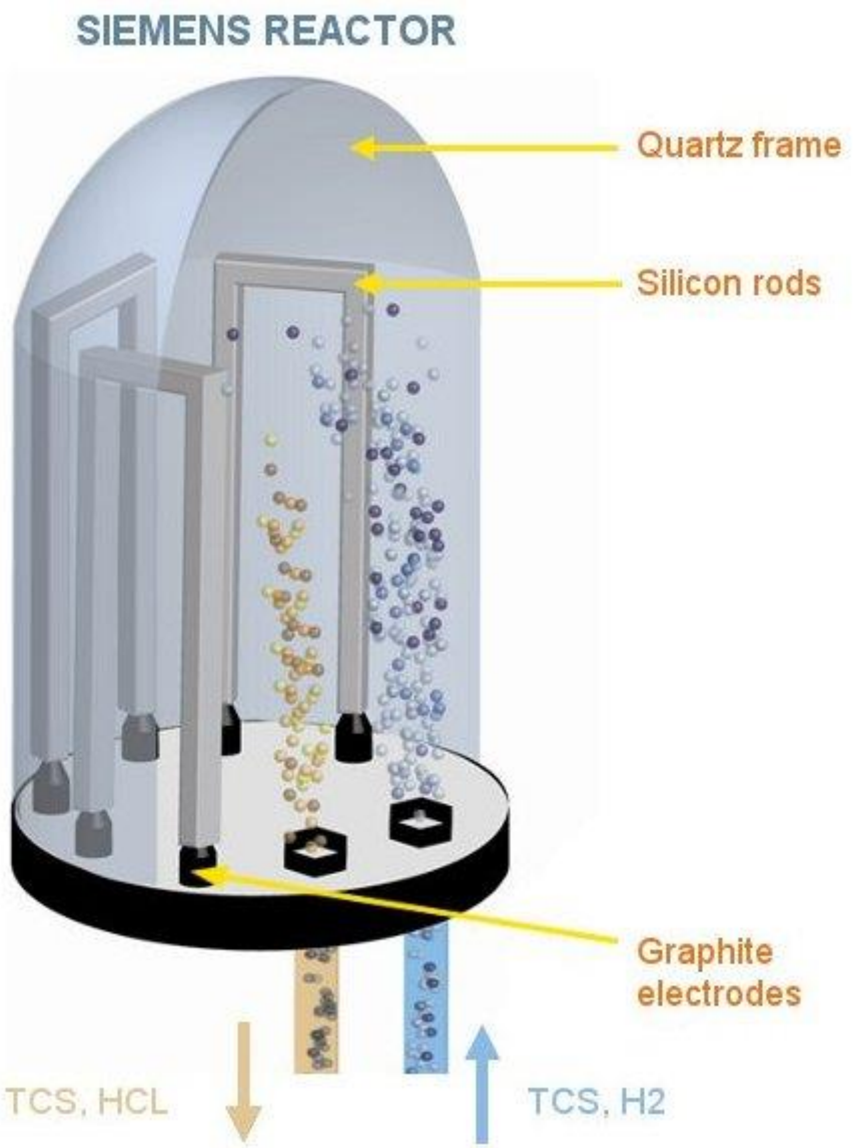

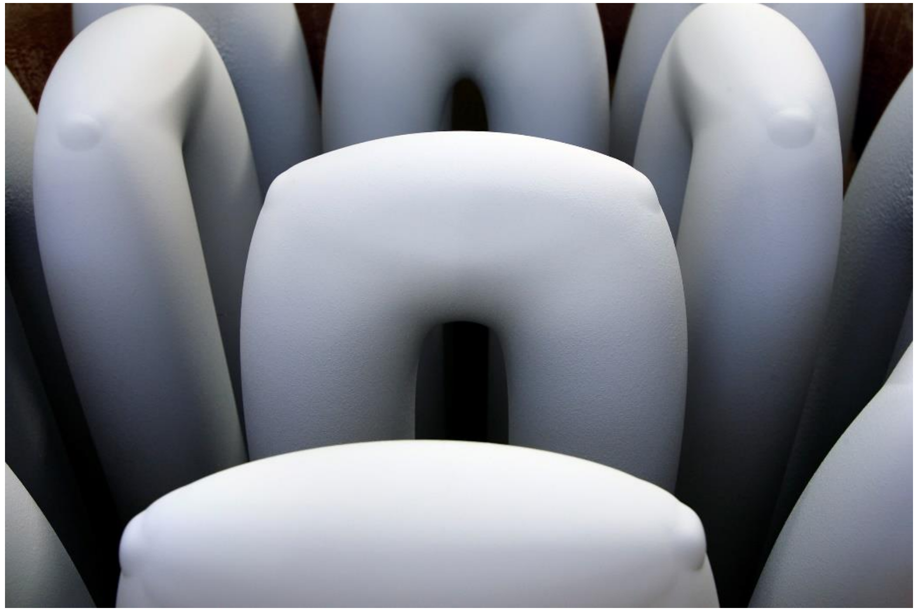

Silicon from Siemens Process

www.schott.com

Czochralski Growing

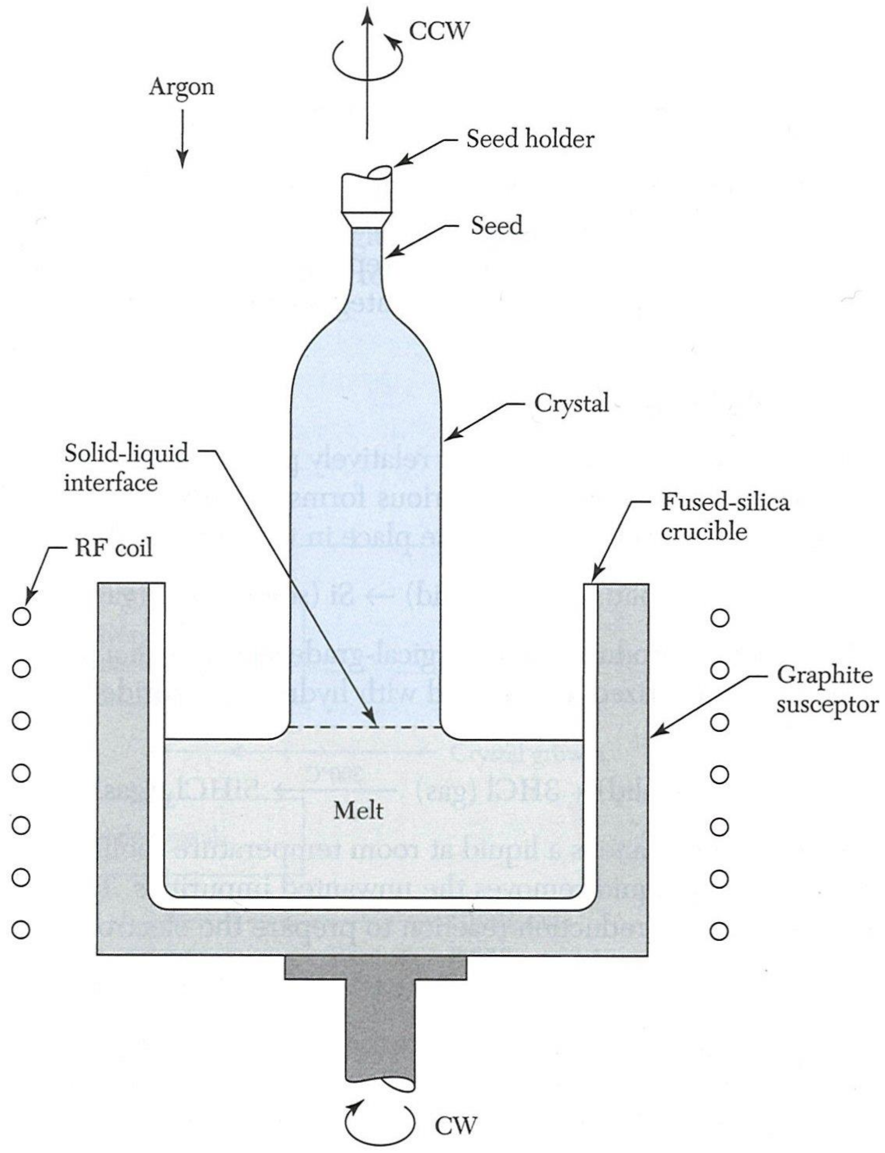

Fig. 2 Czochralski crystal puller. CW, clockwise; CCW, counter clockwise.

300mm Si Crystal by Czochralski

www.focus.de | Wacker Chemie

Silicon Dicing

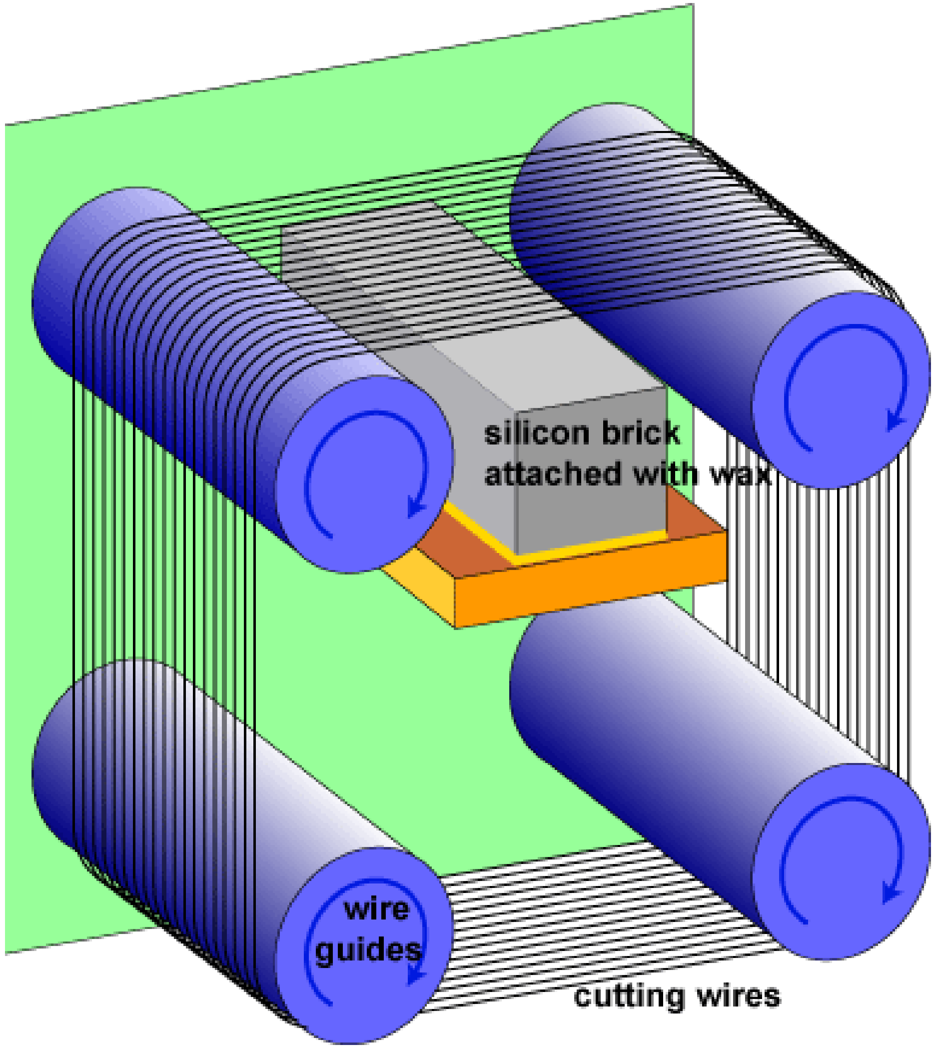

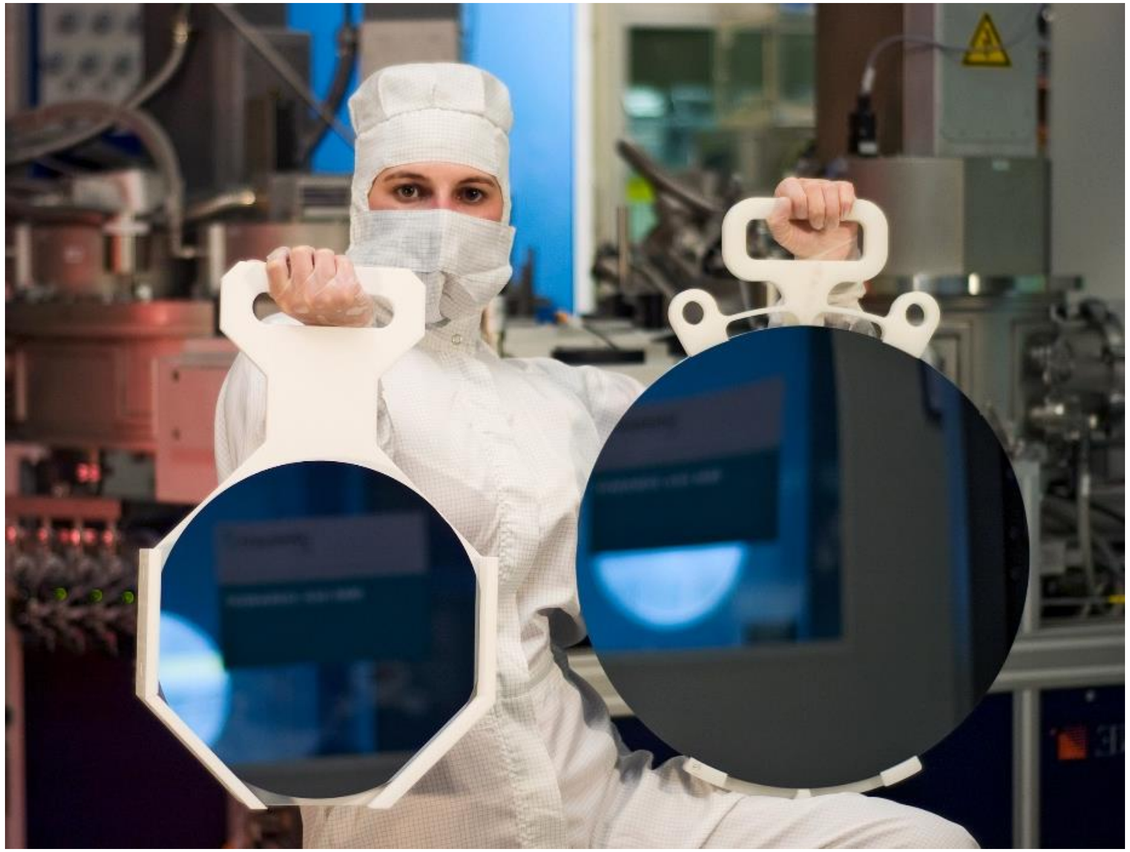

300mm vs 450mm wafer

http://www.pveducation.org/node/496 | http://wccftech.com/foundries-tsmc-companies-shift-300mm-wafers/

Attenuation Efficiency

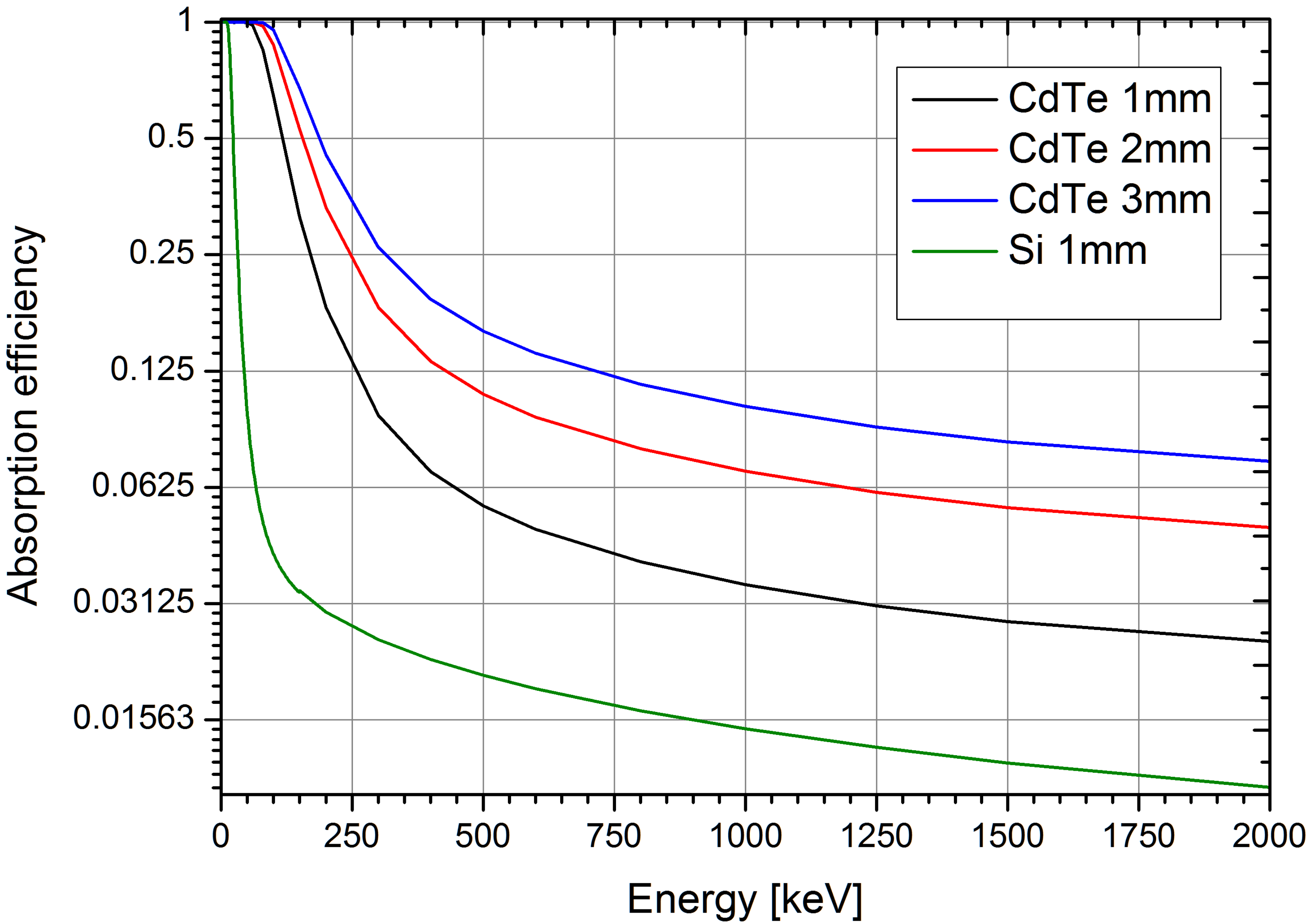

Attenuation Mechanisms in Si

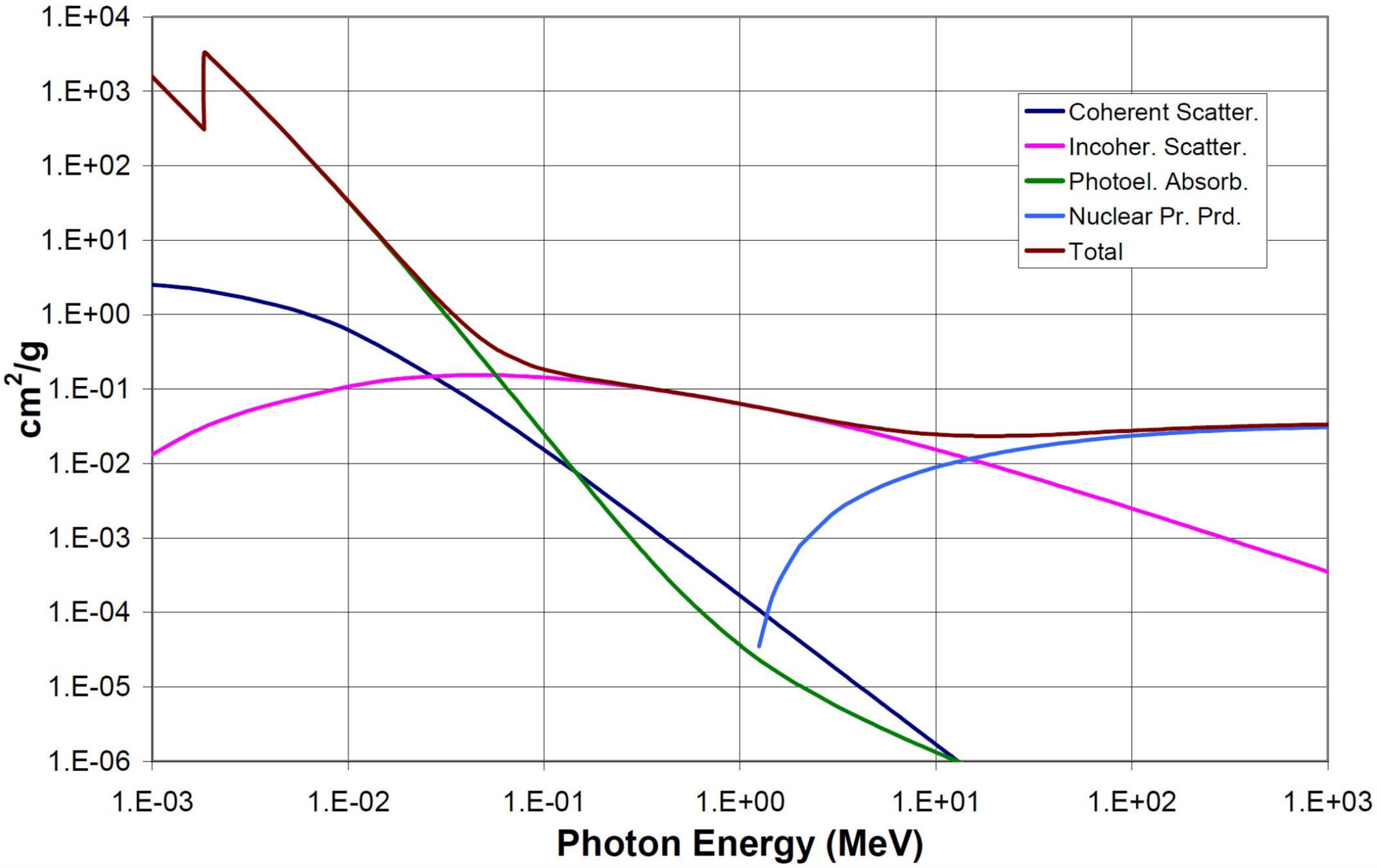

Source: R. Ballabriga / CERN & XCOM Database

Charge Coupled Device (CCD)

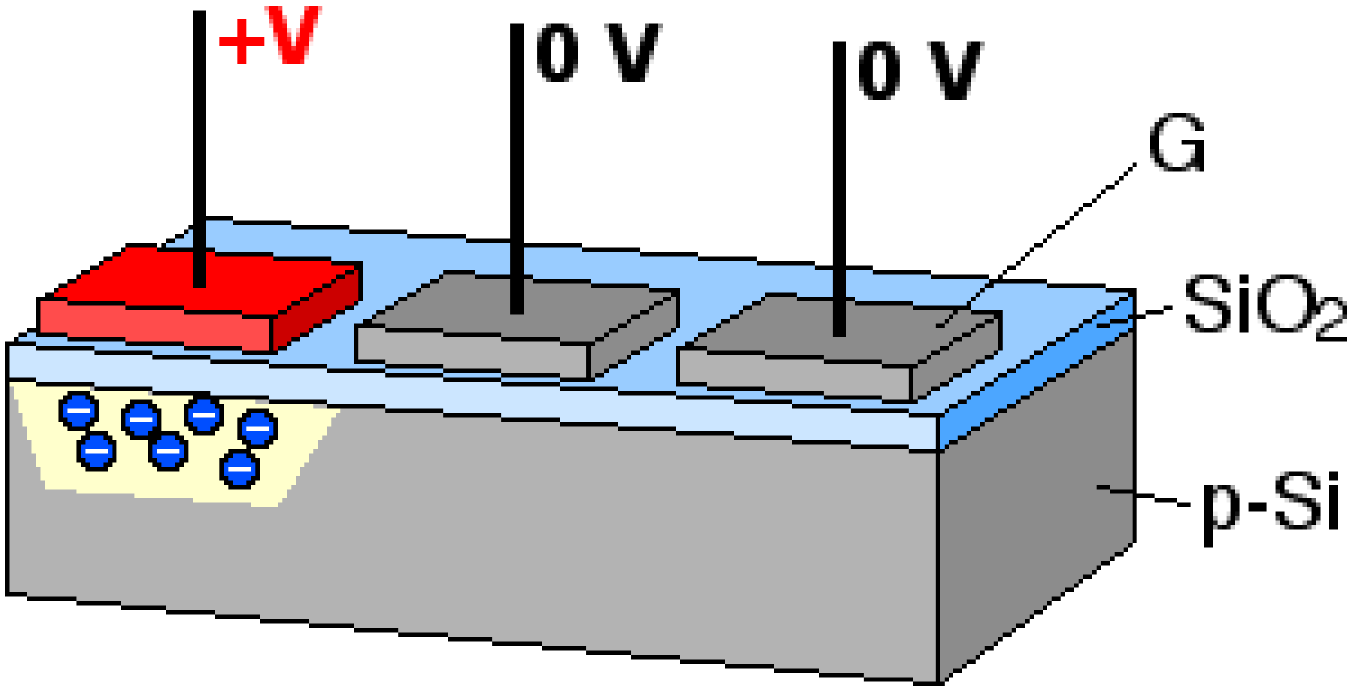

Microstrip Detector

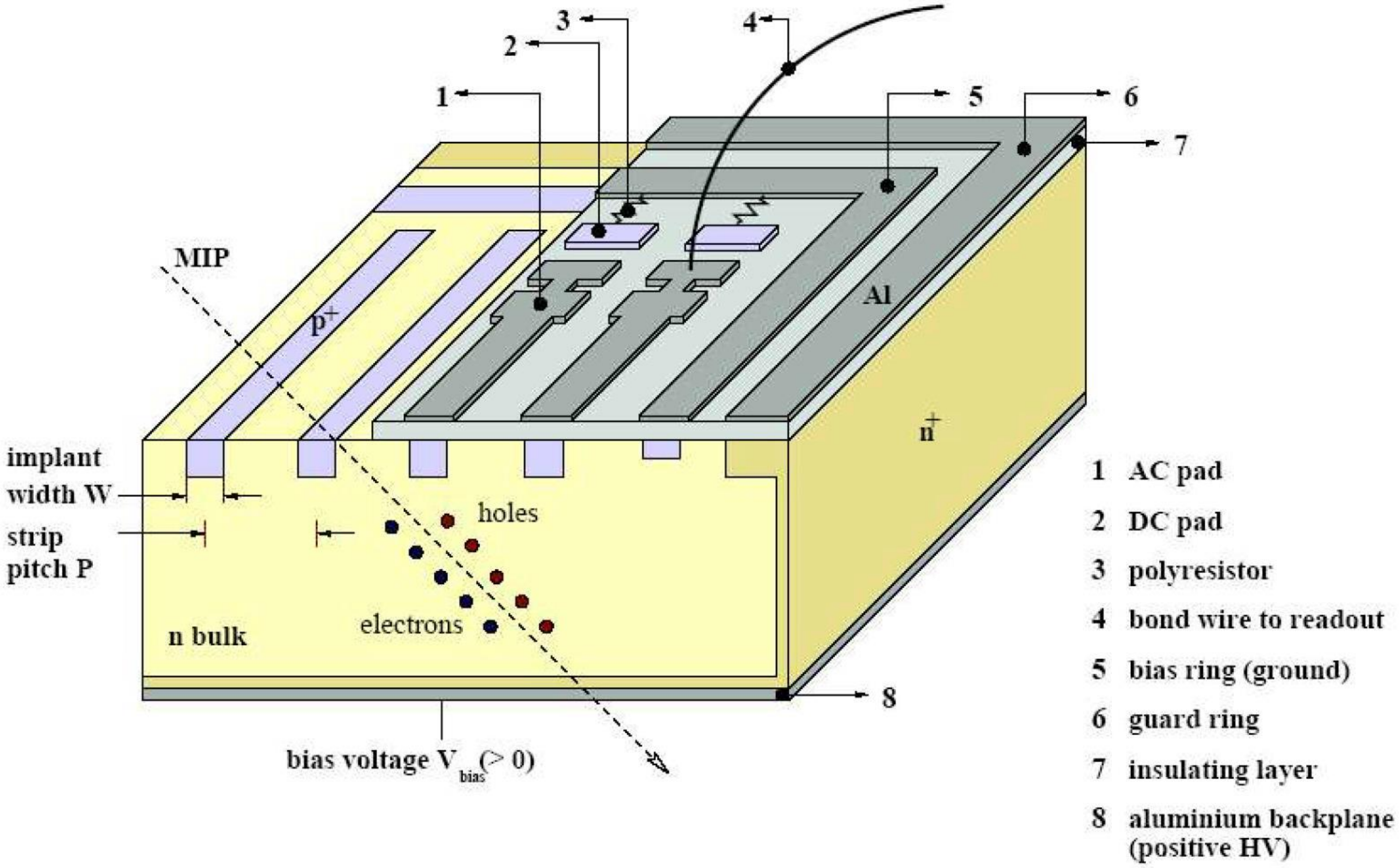

Microstrip Detector at CMS

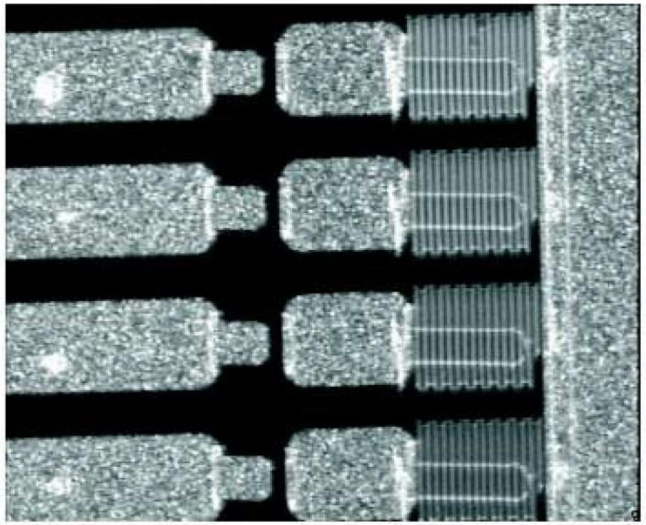

Quelle : CMS Collaboration, HEPHY Vienna

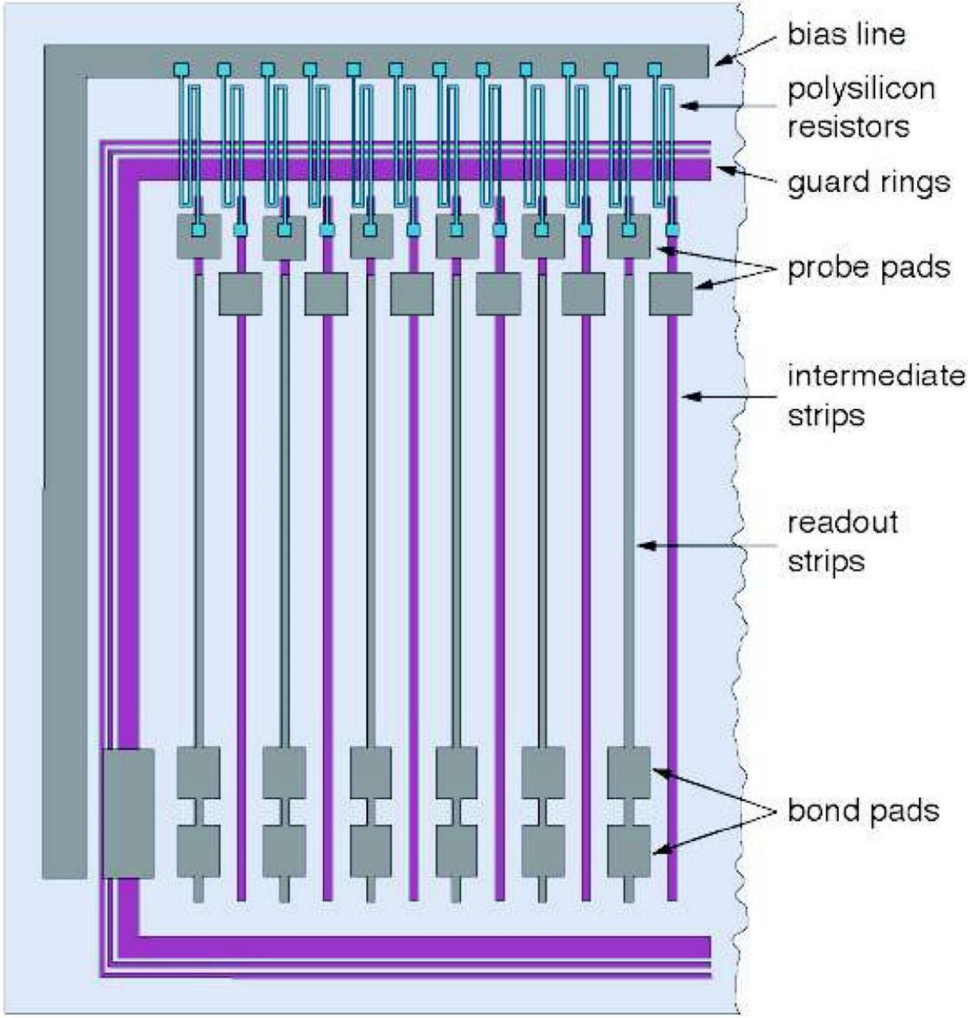

Use of Microstrip Detectors at CERN

H1

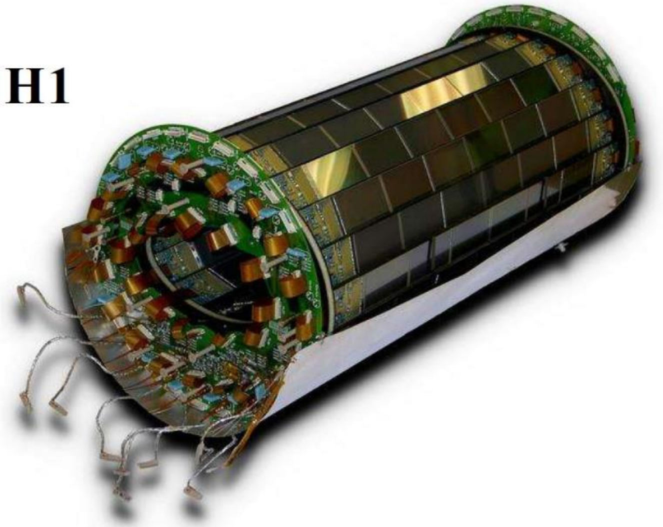

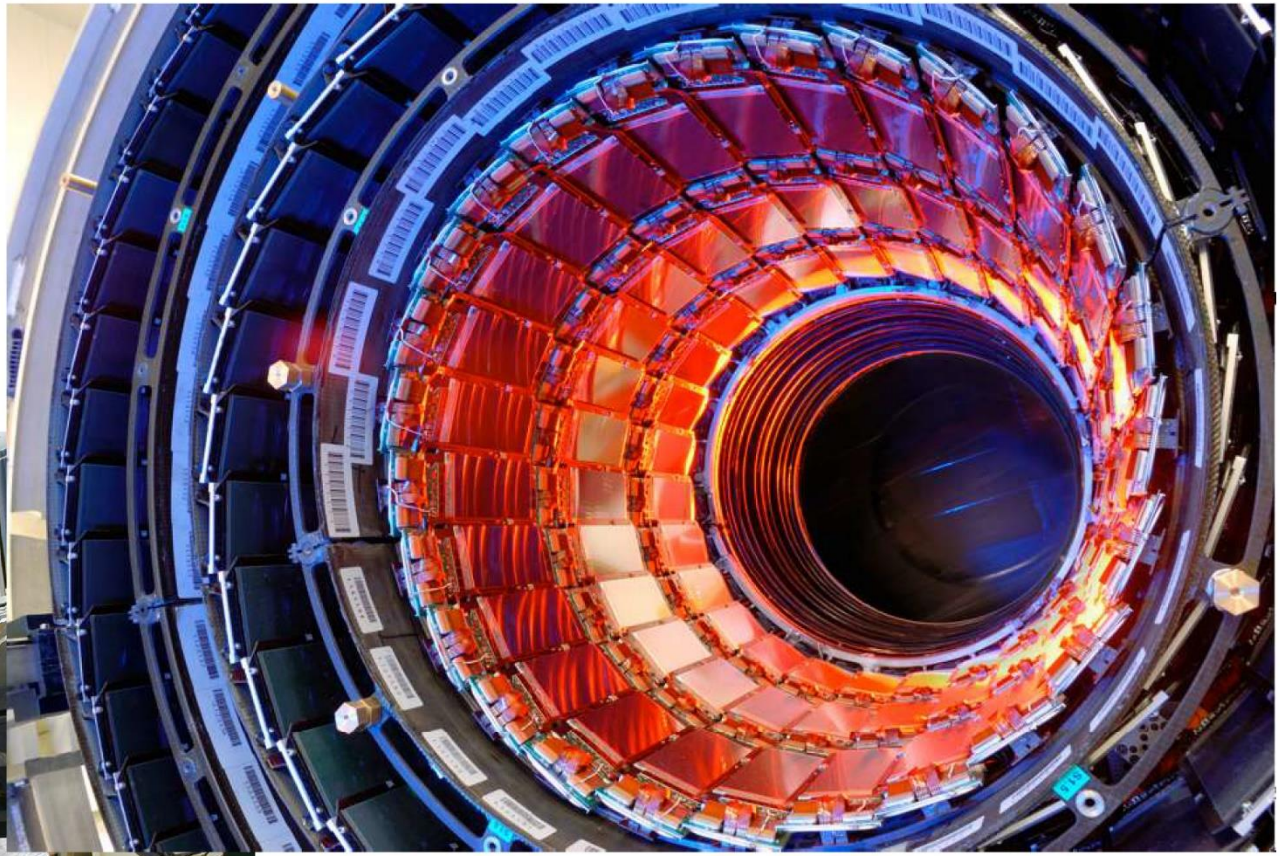

CMS

Hybrid Silicon Pixel Detectors

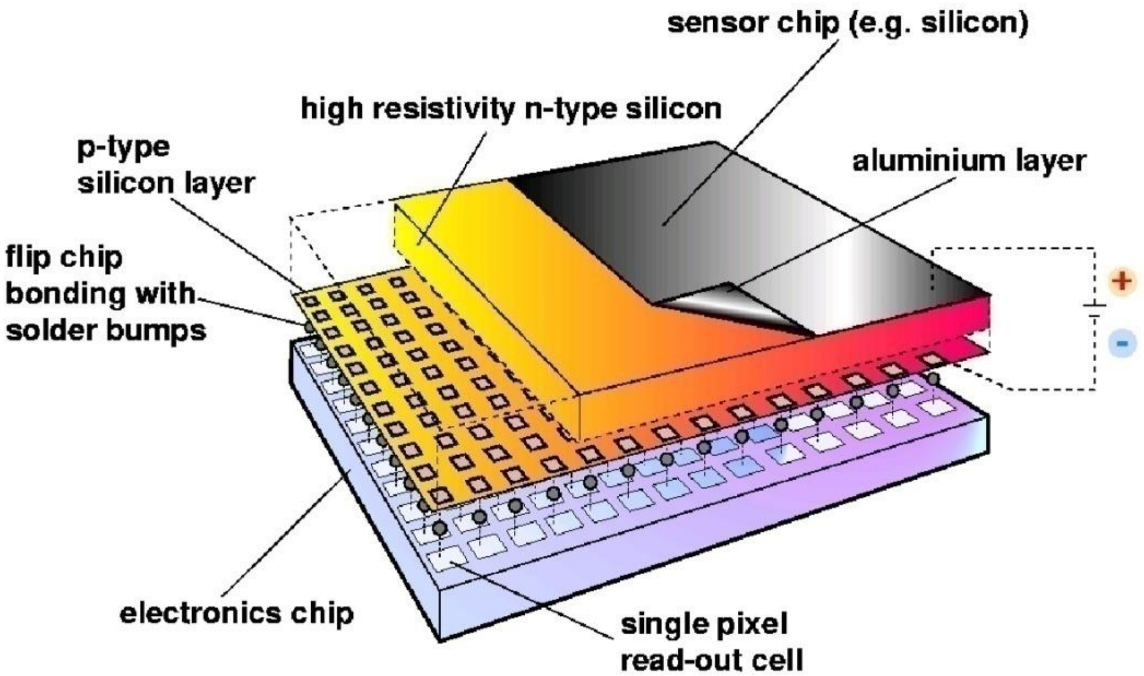

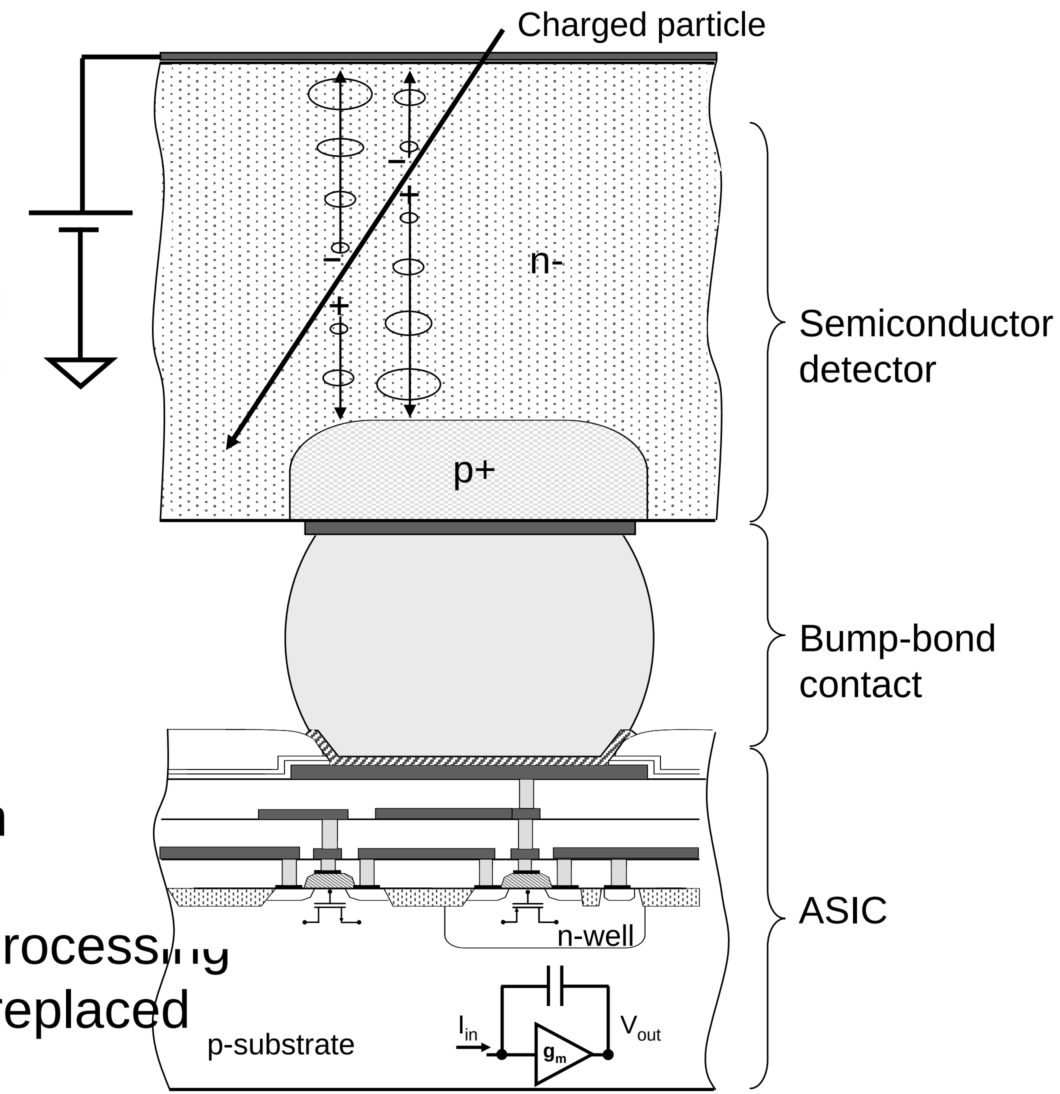

Fill factor is 100 % (away from periphery)
Full depletion of sensor allows prompt charge collection
Extremely high SNR easy to reach
Standard CMOS can be used allowing on-pixel signal processing
Sensor material can be changed (Si, GaAs, CdTe..) or replaced (Microchannel Plate, GEM, InGrid…)

But because of low volumes bump bonding is still expensive

Source: R. Ballabriga / CERN

Bump Bonding

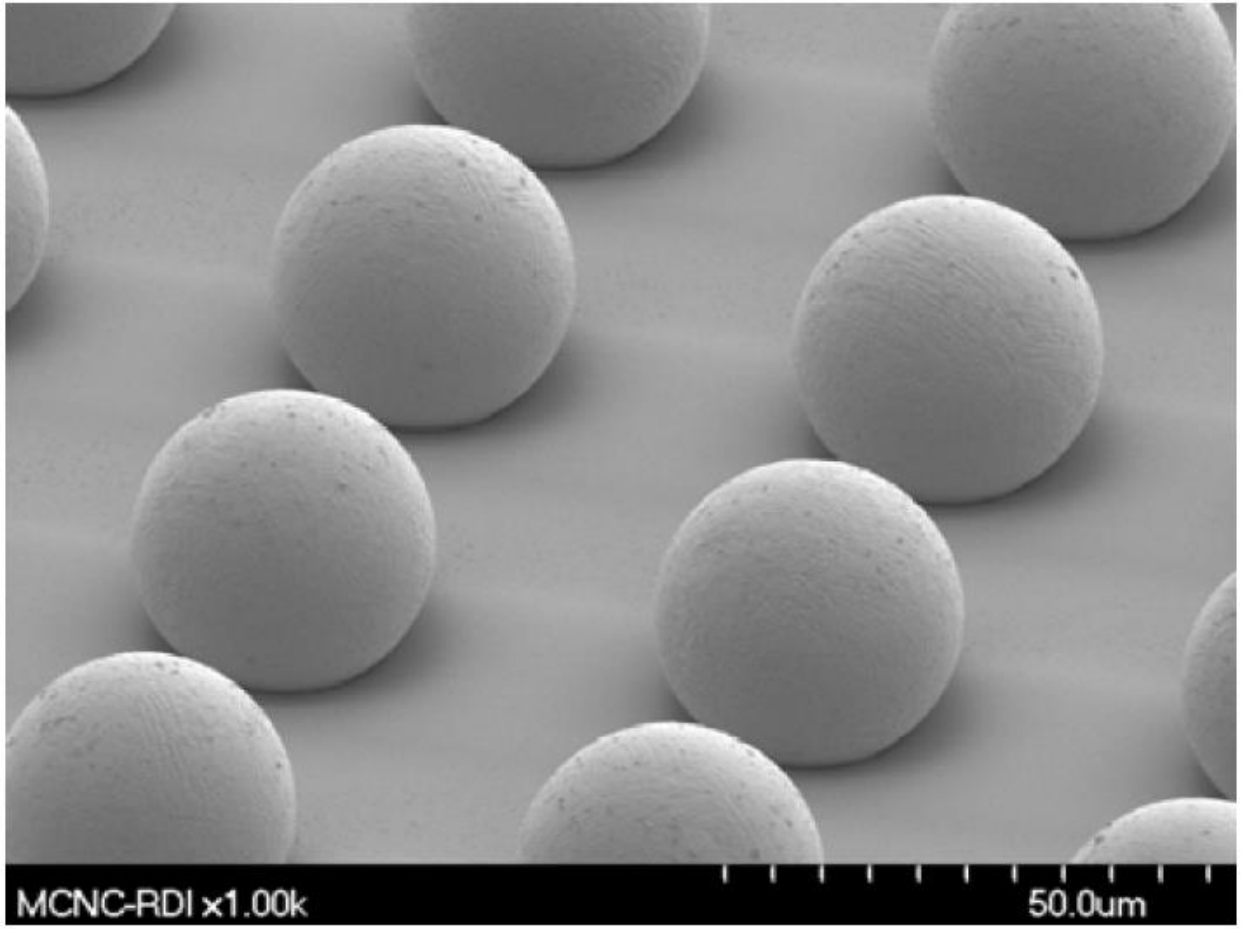

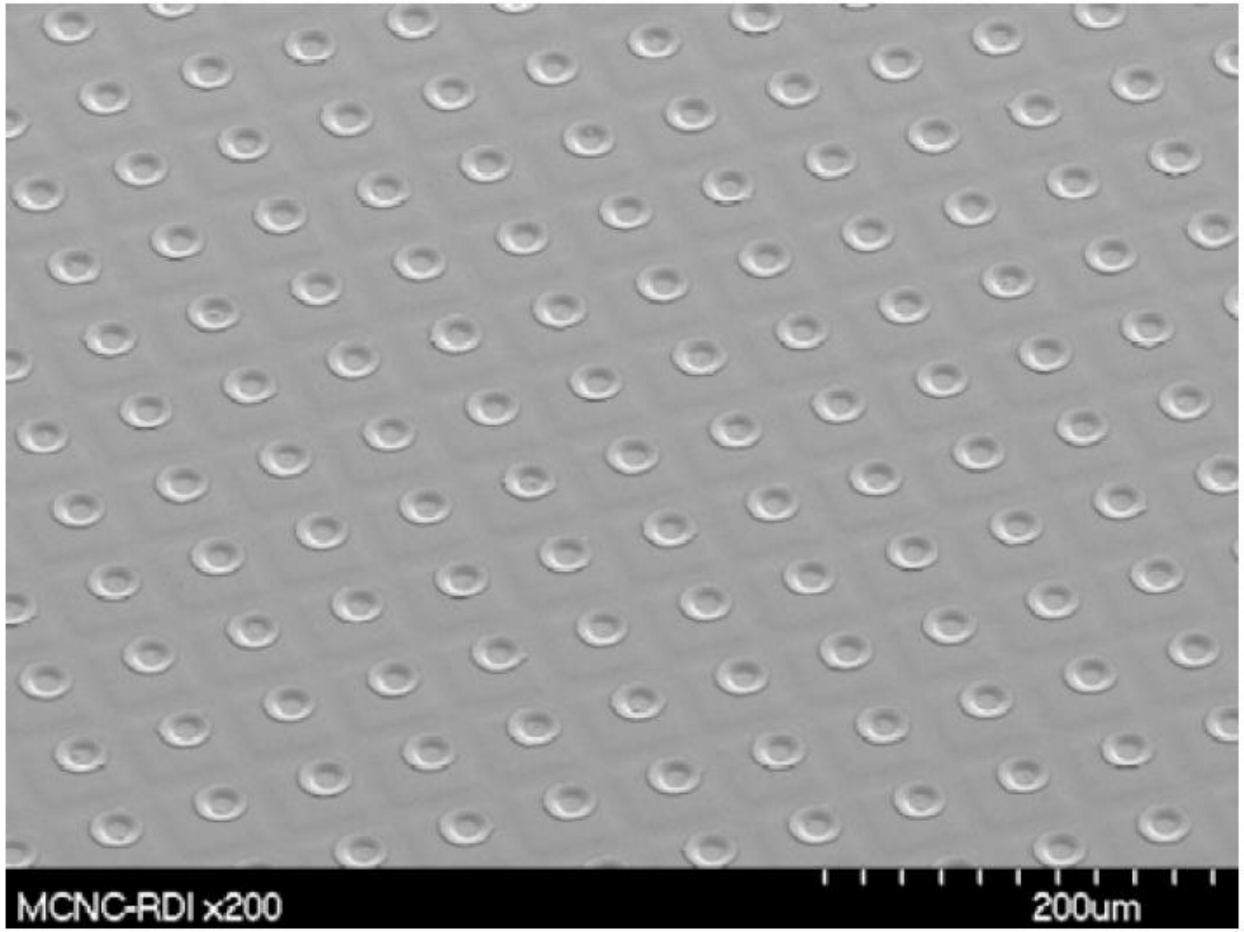

Semiconductor Sensor

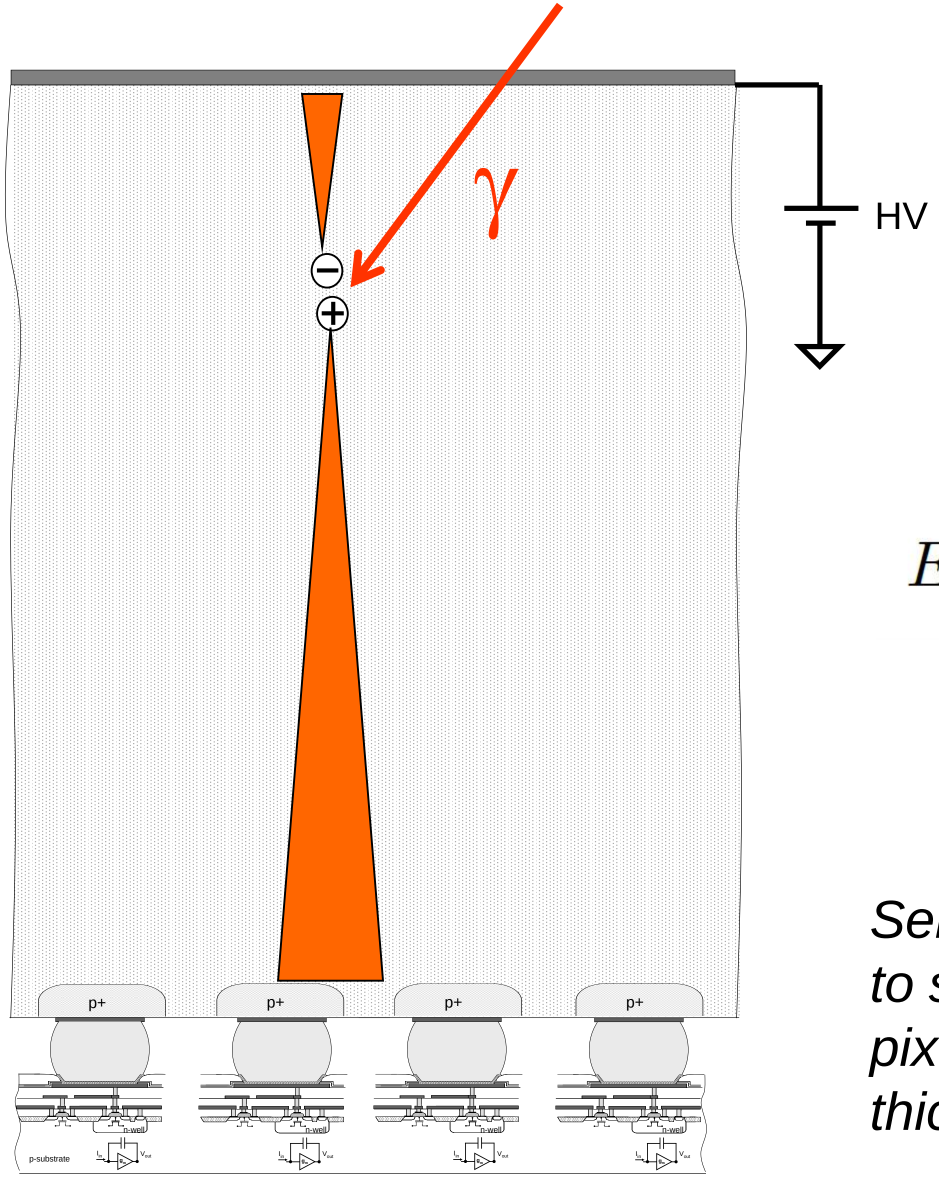

$$E_{pair} \approx 2.8 \times E_g + 0.6\ \text{eV}.$$

Sensor dimensions to scale (55μm pixel pitch, 300μm thick sensor)

Source: R. Ballabriga / CERN

Hybrid Pixel Detector

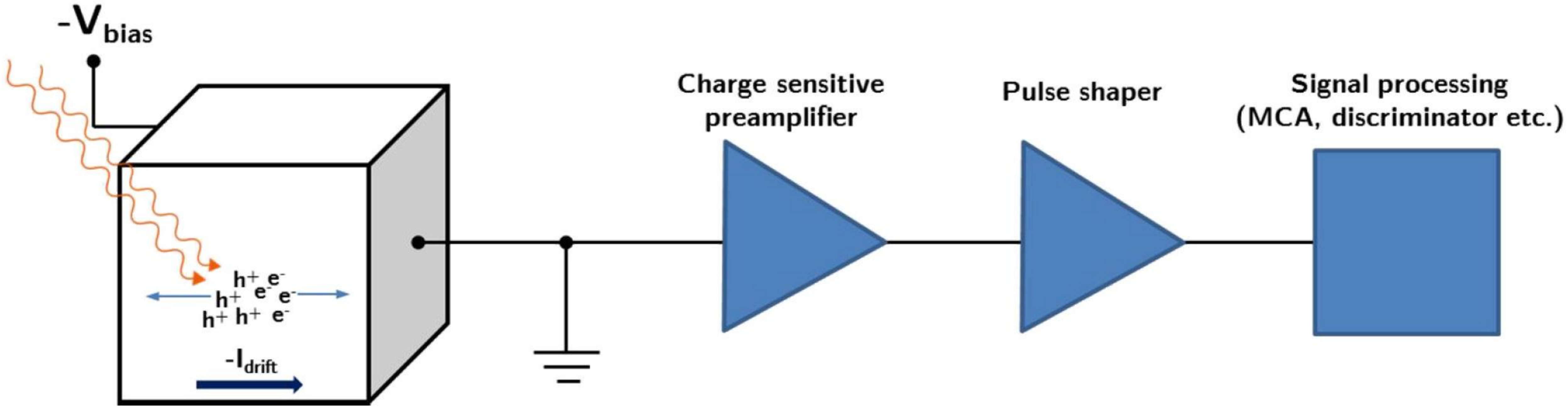

Photon Counting Detector (Medipix)

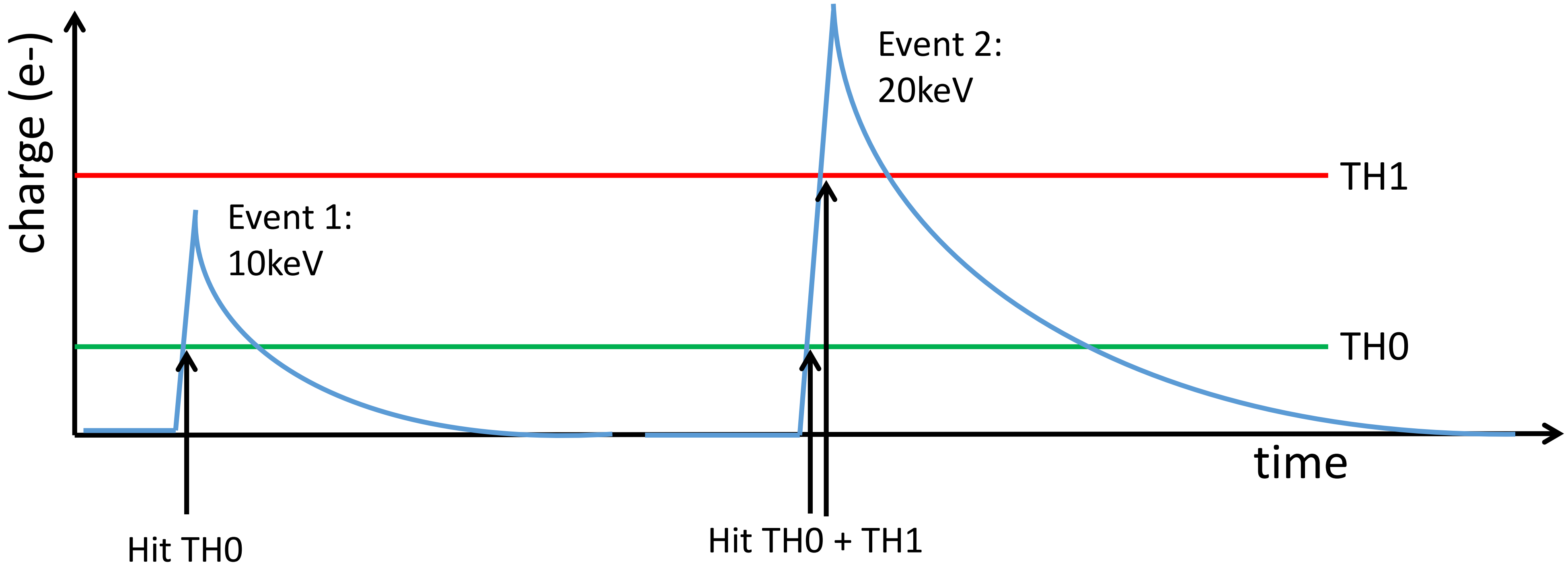

Induced Charge on Detector Electrodes

- Signals on detector electrodes arise from motion of charge carriers
- Induced current is derived from laws of electrostatics
- Method: Shockley-Ramo theorem: the instantaneous current induced on a given electrode is equal to

$$i = q\vec{v} \cdot \vec{E}_0$$

where q is the charge of the carrier, v is its velocity and E_0 *is the weighting field*

- The induced charge (*Q*) on the electrode is given by

$$Q = q\Delta\varphi_0$$

where $\Delta\varphi_0$ *is the weighting potential from the beginning to the end of the carrier path*

S.Ramo, Proc. IRE, 27 (1939) p.584
W.Shockley, J. Appl. Phys. 9, 635 (1938)
V. Radeka Ann. Rev. Nucl. Part. Sci. 1988 38: 217-277
Gatti et al., NIMA 193 (1982) 651

Signal induction in the pixel electrodes

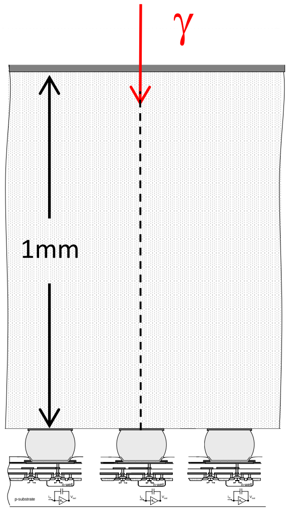

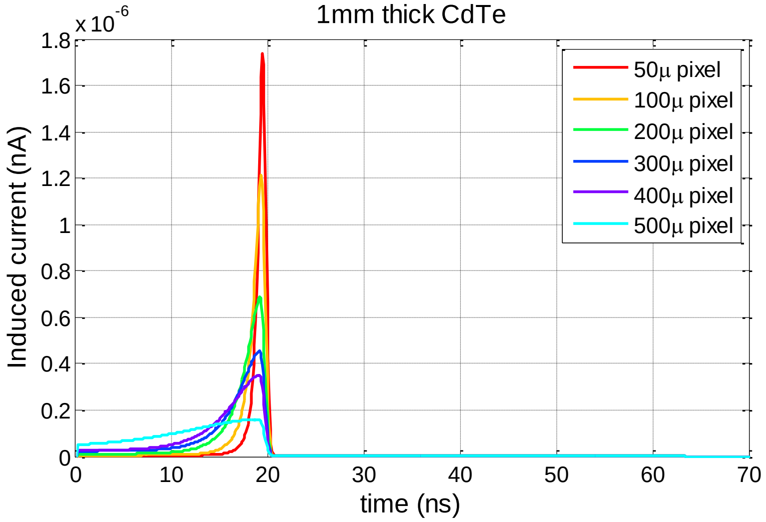

- 1mm CdTe
- 60keV photons
- 600V sensor bias
- Energy deposition at z=240μm
- (No charge trapping, charge sharing included in simulation)

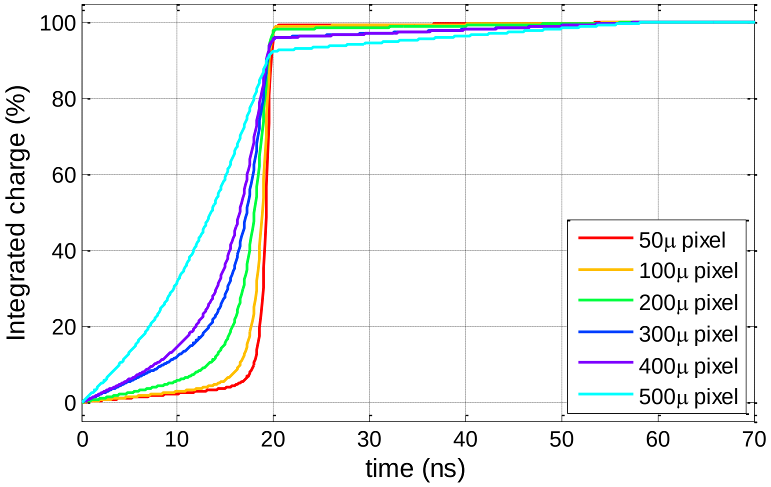

Signal shape depends on detector geometry

Pixel pitch

Time to integrate a given percentage of the charge

	$t_{90\%}$	$t_{97.5\%}$
50μm	2.4ns	13.5ns
300μm	14.7ns	38.2ns

If we assume $t_{90\%}=t_p$ and $\tau=2\tau_p$

$$\frac{1}{\tau}\frac{1}{pixel\ area}\left[Mcps/mm^2\right]$$

Pixel Detectors

Name	Matrix	Channel size (μm²)	Energy thresholds	Peaking time (ns)	Buttable sides	Technology (μm)	Specific information	References
Medipix3 *(1)*	256x256	55x55	2	120	3	0.13	Fine Pitch mode, Single Pixel mode, Compatibility with Through Silicon Vias (TSVs)	[33,34,35,36]
Medipix3 *(2)*	256x256	55x55	2	120	3	0.13	Fine Pitch mode, Charge summing and hit allocation algorithm, TSVs	[33,34,35,36]
Timepix3 *(3)*	256x256	55x55	10bits	30	3	0.13	Data push mode, Time-over-Threshold (ToT) energy measurement, charge sharing correction possible off-chip	[37]
Pixirad Pixie II *(4)*	512x476	52x60	2	300	2	0.18	Hexagonal pixels, equivalent pixel pitch of 55.6μm	[38]
Samsung PC *(5)*	128x128	60x60	3	NS	0	0.13	On-pixel successive approximation Analog to Digital Converter (ADC)	[39]
Pixirad Pixie III *(6)*	512x402	62x62	2	125	2	0.16	Large area ASIC (31.7x25mm²), Charge summing algorithm	[40]
Eiger *(7)*	256x256	75x75	1	30	3	0.25	Radiation hard electronics design	[41]
PXD23K (AGH) *(8)*	128x184	75x75	2	48	3	0.13		[42]
X-Counter PC *(9)*	256x256	100x100	2	NS	3	NS	Charge summing algorithm	[43]
PXD18K (AGH) *(10)*	96x192	100x100	2	30	3	0.18		[44]
FPDR90 (AGH) *(11)*	40x32	100x100	2	28	3	0.09		[45]
AGH_Fermilab *(12)*	18x24	100x100	2	48	0	0.04	Charge summing algorithm	[46]
Medipix3 *(13)*	128x128	110x110	8	120	3	0.13	Spectroscopic mode, Single Pixel mode, TSVs	[33,34,35,36]
Medipix3 *(14)*	128x128	110x110	8	120	3	0.13	Spectroscopic mode, Charge summing algorithm, TSVs	[33,34,35,36]
XPAD3 *(15)*	80x120	130x130	2	150	3	0.25		[47,48]
Pilatus 2 *(16)*	60x97	172x172	1	110.00	3	0.25	Radiation hard design	[49,50]
Pilatus 3 *(17)*	60x97	172x172	1	110.00	3	0.25	Radiation hard design, instant retrigger technology	[51]
Telesystems *(18)*	40x40	200x200	4	300-500	3	0.25		[52]
Dosepix *(19)*	16x16	220x220	16	300	3	0.13	ToT energy measurement, 16 digital thresholds	[53]
Siemens PC *(20)*	64x64	225x225	2	20	NS	NS	Pile-up trigger method	[54,55,56,57]
Hexitec *(21)*	80x80	250x250	14bits	2000	3	0.35	Digitization of pulse amplitude with off-chip ADC, TSVs	[58]
CIX 0.2 *(22)*	8x8	500x250	1	NS	1	0.35	Simultaneous charge integration and photon counting measurement	[59,60]
Philips Chromaix *(23)*	16x16	300x300	4	20	2	0.18		[61]
Ajat-0.35 (PC) *(24)*	32x64	350x350	1	1000	3	0.35		[62,63]
Ajat-0.35 (ADC) *(25)*	32x64	350x350	64	1000	3	0.35	On-pixel ADC	[62,63]
DxRay-Interon *(26)*	16x16	500x500	4	10	NS	NS		[2,64]
Ajat-0.5 *(27)*	44x22	500x500	2	1000-2000	3	0.35		[65]

Source: R. Ballabriga / CERN

Pixel Detectors

Name	Max count rates (Mcps/pixel)	Max count rates (Mcps/mm²)	Electronics noise (e^- r.m.s.)	Energy resolution (FWHM)	Power/pixel (μW)
Medipix3 (FPM-SPM) *(1)*	2.50	826	80	1.37keV @ 10keV, 300um Si	7.5
Medipix3 (FPM-CSM) *(2)*	0.50	164	174	2.03keV @ 10keV, 300um Si	9.3
Timepix3 *(3)*	1.3E-3	0.43	62	4.07keV @ 59.5keV, 300um Si	15.2
Pixirad Pixie II *(4)*	0.5	162	50	1.73keV @ 60keV, CdTe	12.5
Samsung PC *(5)*	NS	NS	68	NS	4.6
Pixirad Pixie III *(6)*	1	260	50(SPM)/100(CSM)	2keV @ 20keV, CdTe	34
Eiger *(7)*	4.2	747	121/160/185	NS	8.8
PXD23K (AGH) *(8)*	8.55	1519	90	NS	25
X-Counter PC *(9)*	1.2	120	NS	10KeV @60keV, CdTe	NS
PXD18K (AGH) *(10)*	5.8	580	168	NS	23
FPDR90 (AGH) *(11)*	8.55	855	91	NS	42
AGH_Fermilab *(12)*	NS	NS	84 (SPM)/168 (CSM)	NS	34
Medipix3 (SM-SPM) *(13)*	4.55	376	80	1.43keV @ 10KeV, Si	30
Medipix3 (SM-CSM) *(14)*	0.34	28	174	4.4keV @60keV, 2mm CdTe	37.2
XPAD3 *(15)*	2	118	127	2.3keV @59.5keV CdTe	40
Pilatus 2 *(16)*	6	203	123	1keV @ 8keV	20.2
Pilatus 3 *(17)*	15	507	123	1keV @ 8keV	20.2
Telesystems *(18)*	0.8	20	NS	4.88keV @ 122keV	94.4
Dosepix *(19)*	1.64	34	150	3.12keV @ 35keV	14.6
Siemens PC *(20)*	40	790	NS	NS	NS
Hexitec *(21)*	0.001	0.02	NS	0.8keV @ 60keV	220
CIX 0.2 *(22)*	12	96	330	NS	3200
Philips Chromaix *(23)*	38	422	400	4.7keV @60keV (1 channel)	3000
Ajat-0.35 (PC) *(24)*	2.2	18	NS	4keV @122keV, CdTe	390.6
Ajat-0.35 (ADC) *(25)*	4.88E-5	4.E-04	NS	4keV @122keV, CdTe	390.6
DxRay-Interon *(26)*	13.25	53	NS	7keV @60keV, CdTe	NS
Ajat-0.5 *(27)*	NS	NS	NS	4.7keV @122KeV, CdTe (single channel)	413.2

Source: R. Ballabriga / CERN

Medipix Detectors

- Developed by Medipix2 / Medipix3 Collaborations @ CERN
- Medipix detector: Electronics chip (ASIC) + sensor

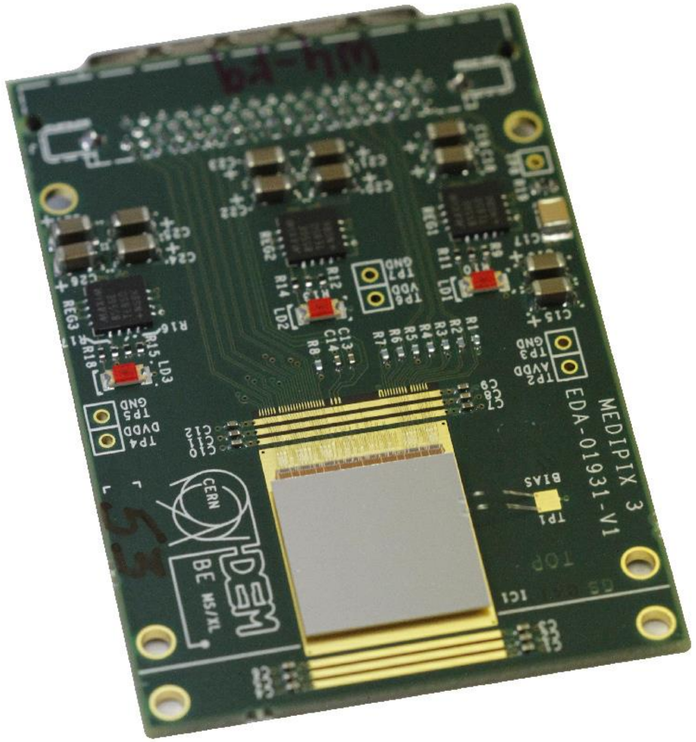

Medipix3 single 14x14 mm²

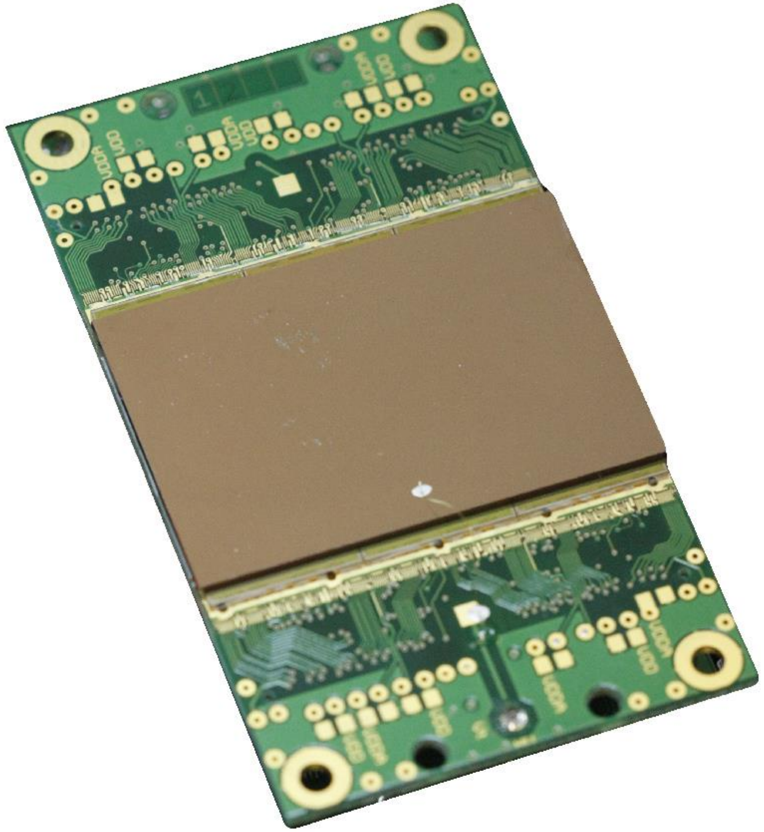

Medipix2 hexa 28x42 mm²

Medipix3 Collaboration

- University of Canterbury, Christchurch, New Zealand
- CEA, Paris, France
- CERN, Geneva, Switzerland,
- DESY-Hamburg, Germany
- Albert-Ludwigs-Universität, Freiburg, Germany
- University of Glasgow, Scotland, UK
- Leiden University, The Netherlands
- NIKHEF, Amsterdam, The Netherlands
- Mid Sweden University, Sundsvall, Sweden
- IEAP, Czech Technical University, Prague, Czechia
- ESRF, Grenoble, France
- Universität Erlangen-Nürnberg, Erlangen, Germany
- University of California, Berkeley, USA
- VTT, Information Technology, Espoo, Finland
- KIT/ANKA, Forschungszentrum Karlsruhe, Germany
- University of Houston, USA
- Diamond Light Source, Oxfordshire, England, UK
- Universidad de Los Andes, Bogota, Colombia
- University of Bonn, Germany
- AMOLF, Amsterdam, The Netherlands
- Technical University of Munich, Germany
- Brazilian Light Source, Campinas, Brazil

Source: M. Campbell / CERN

Medipix ASIC

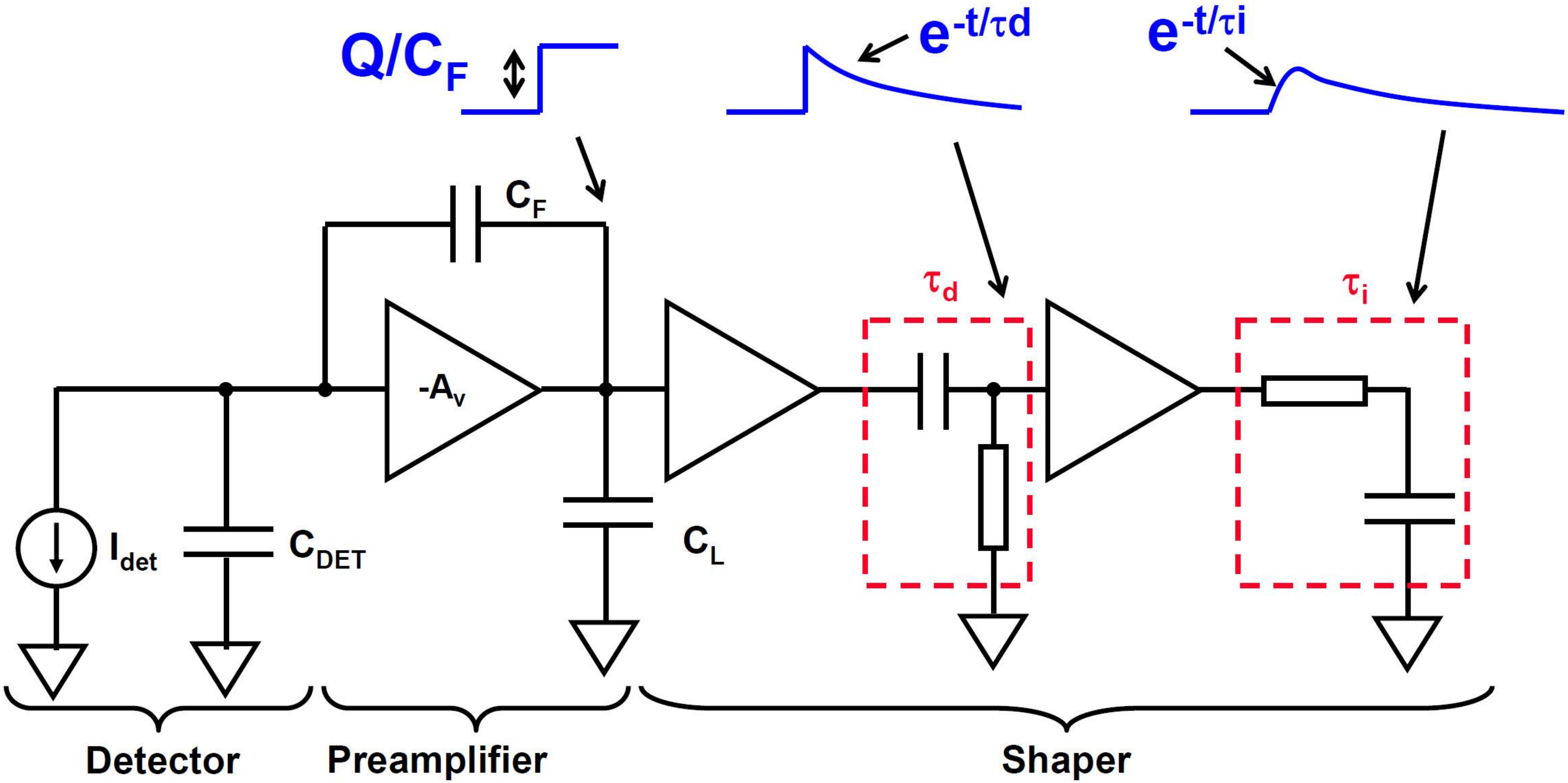

Source:
- Source: R. Ballabriga / CERN

Medipix 2 Pixel Cell

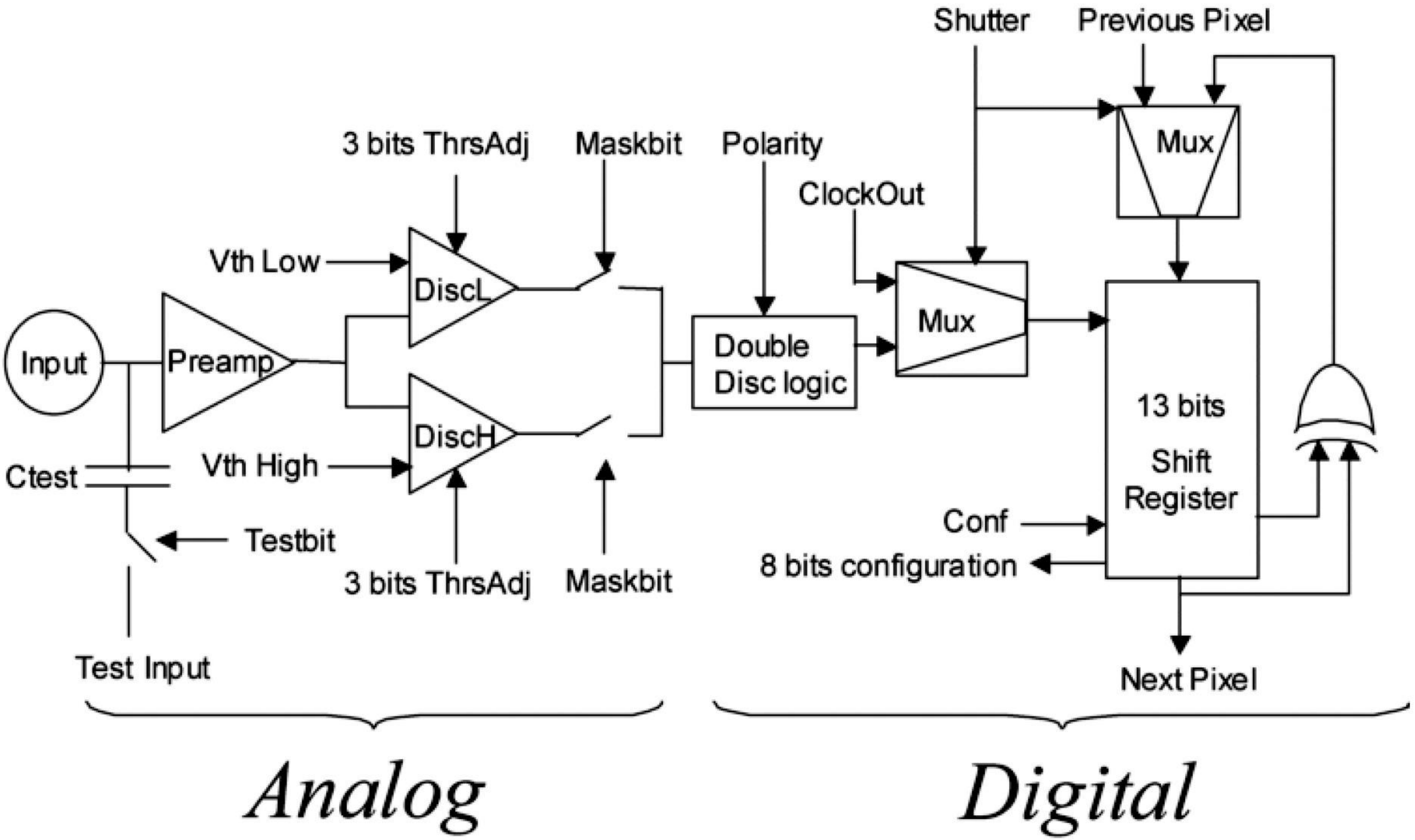

Source: R. Ballabriga / CERN

Photon Counting Detector - Applications

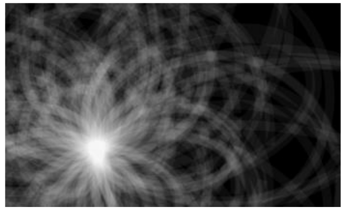

Compton Camera

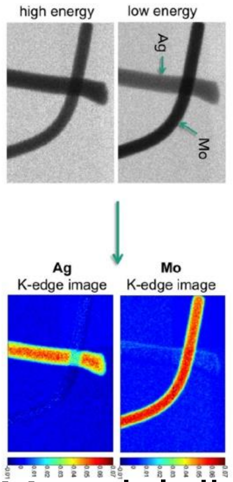

Material discrimination

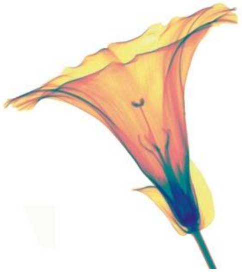

Low-Z imaging

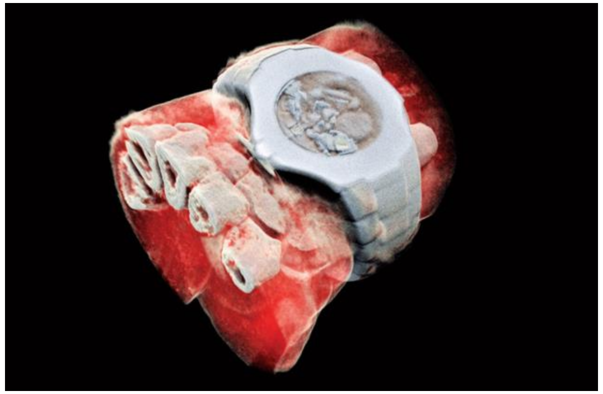

Spectral CT

High-Resolution medical Imaging

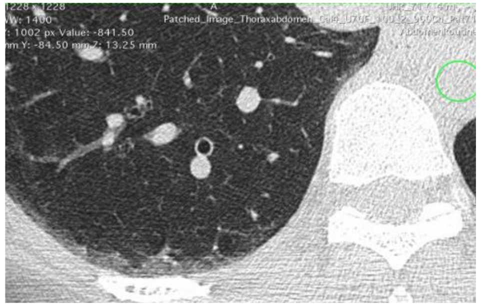

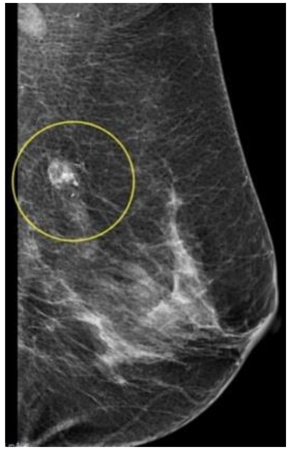

Dose reduction

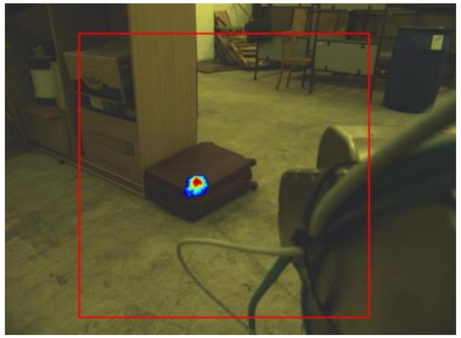

Gamma Camera

Photon Counting Detector

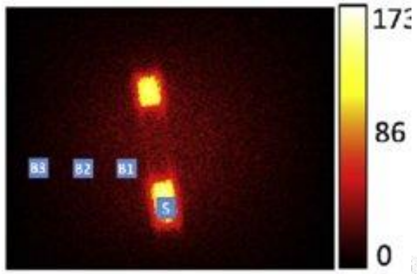

PET

ISS

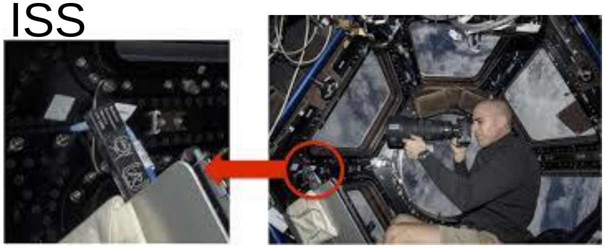

Synchrotron

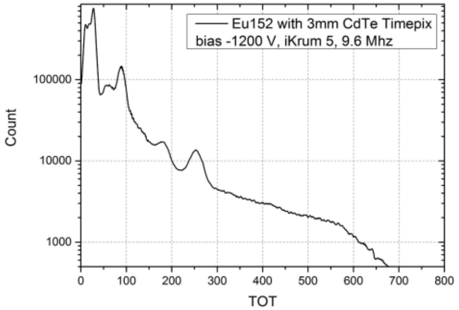

Radiation Monitoring

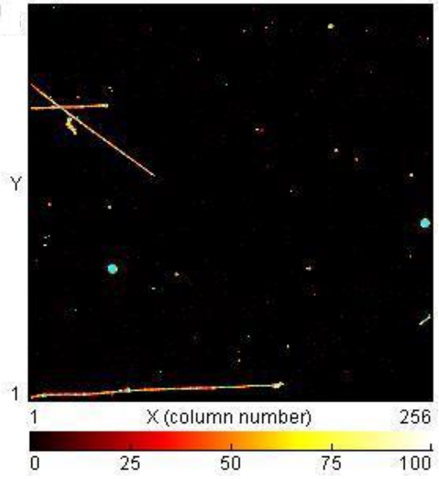

Particle Physics

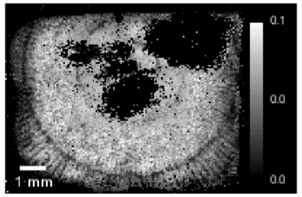

Neutron imaging

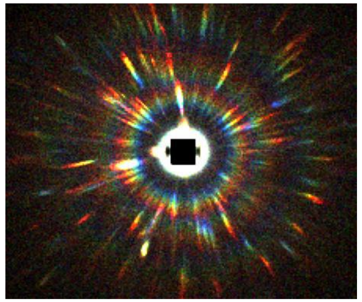

Energy Dispersive XRD

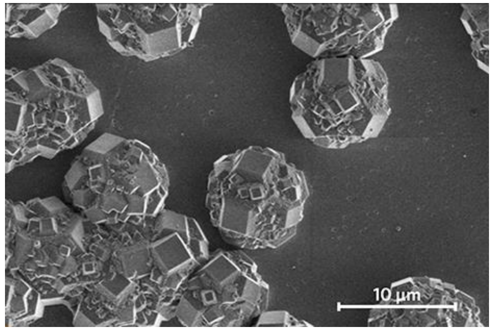

SEM

Imaging: Raw Image vs Flatfield Corrected Image

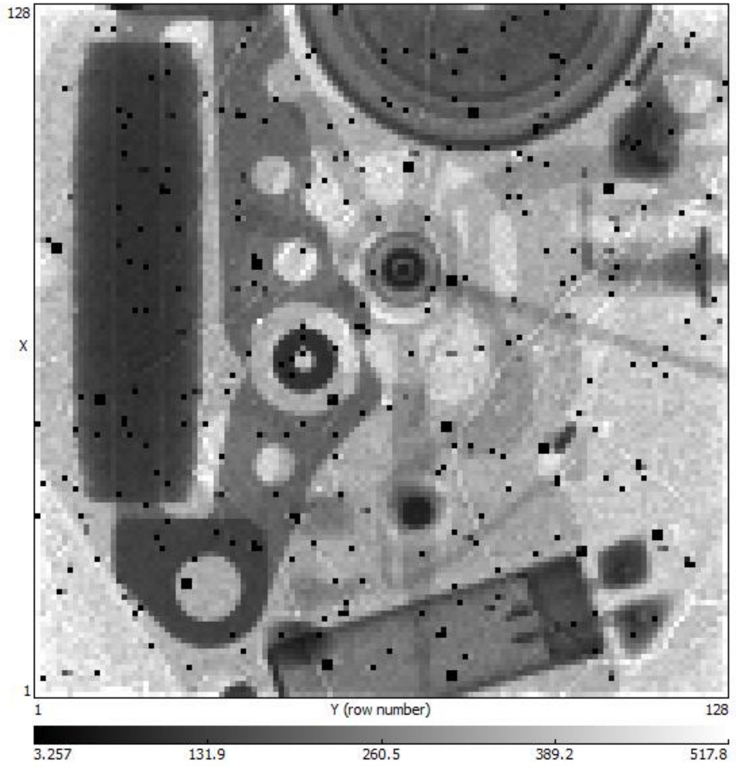

Raw Image

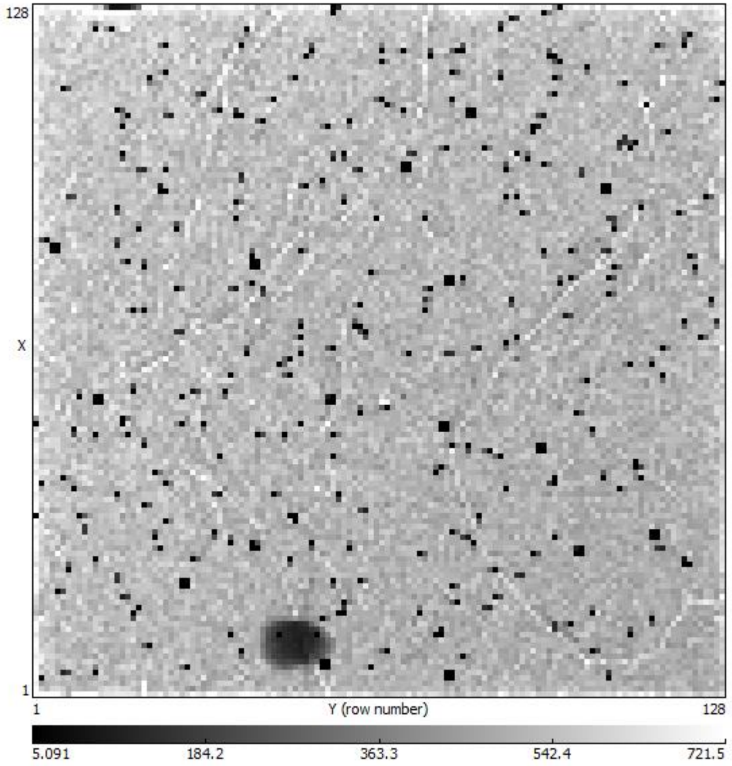

Flatfield Image

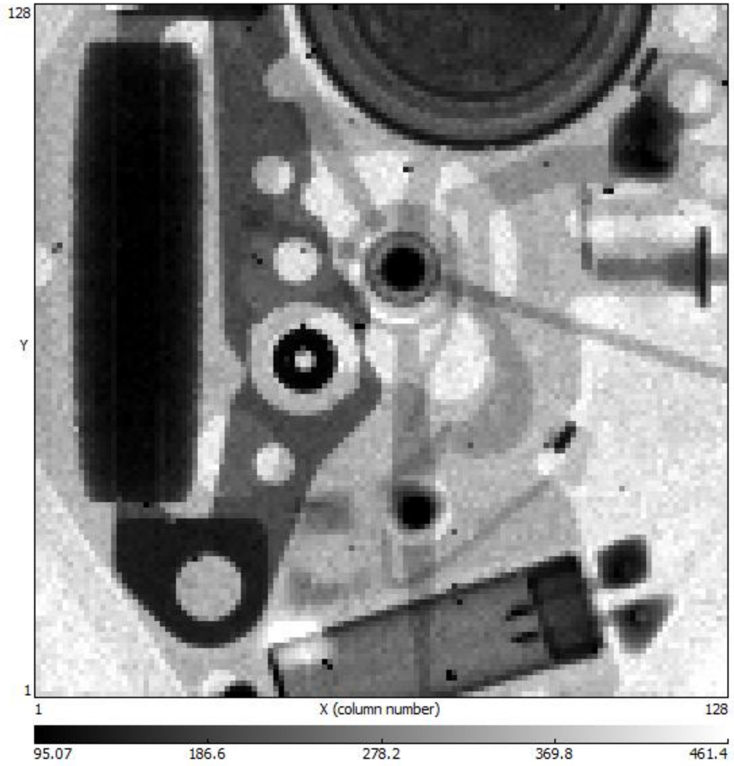

Division: Flatfield Correction

Medipix3 Biological Imaging: Dynamic Range

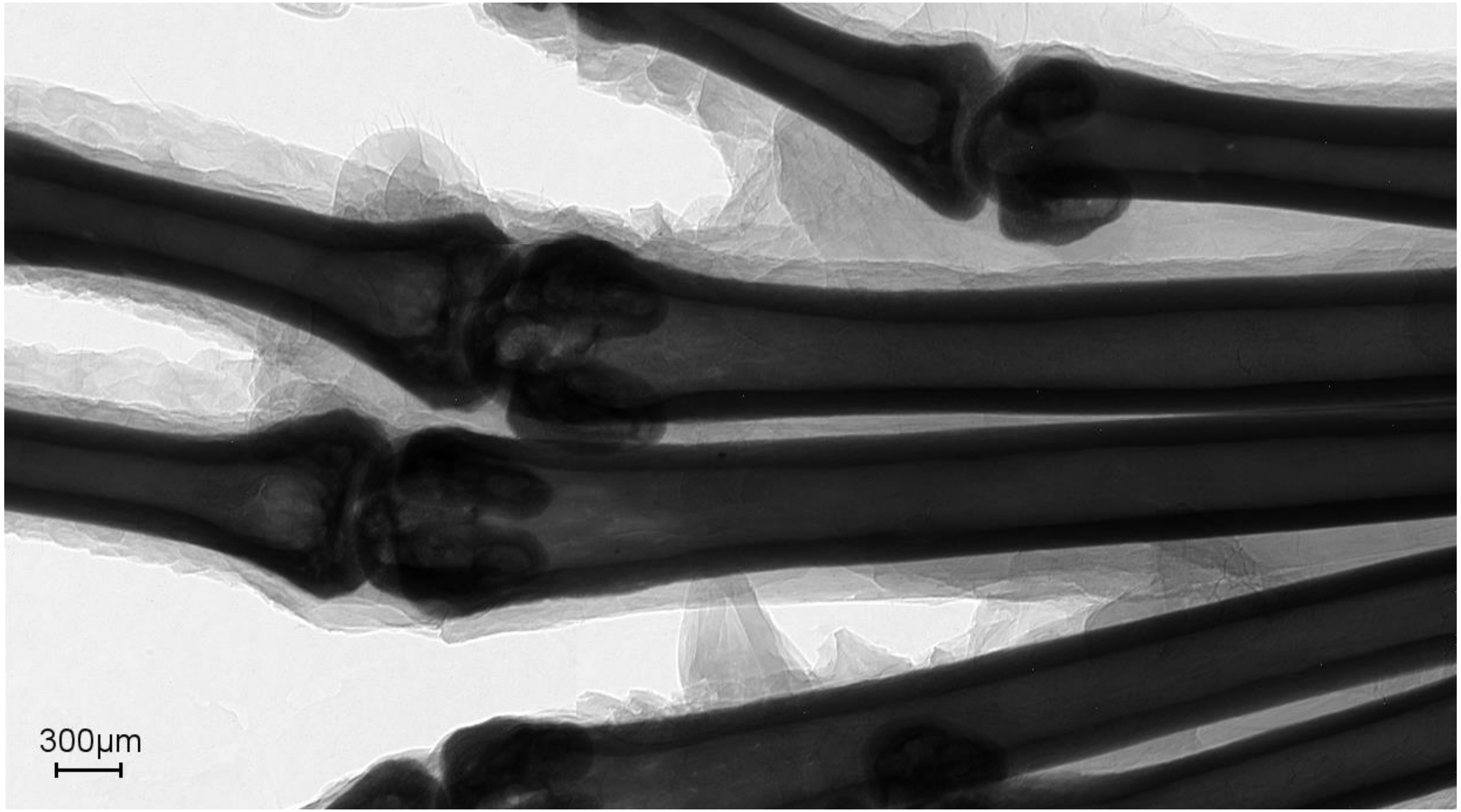

Histogramm range: 0 - 85 %

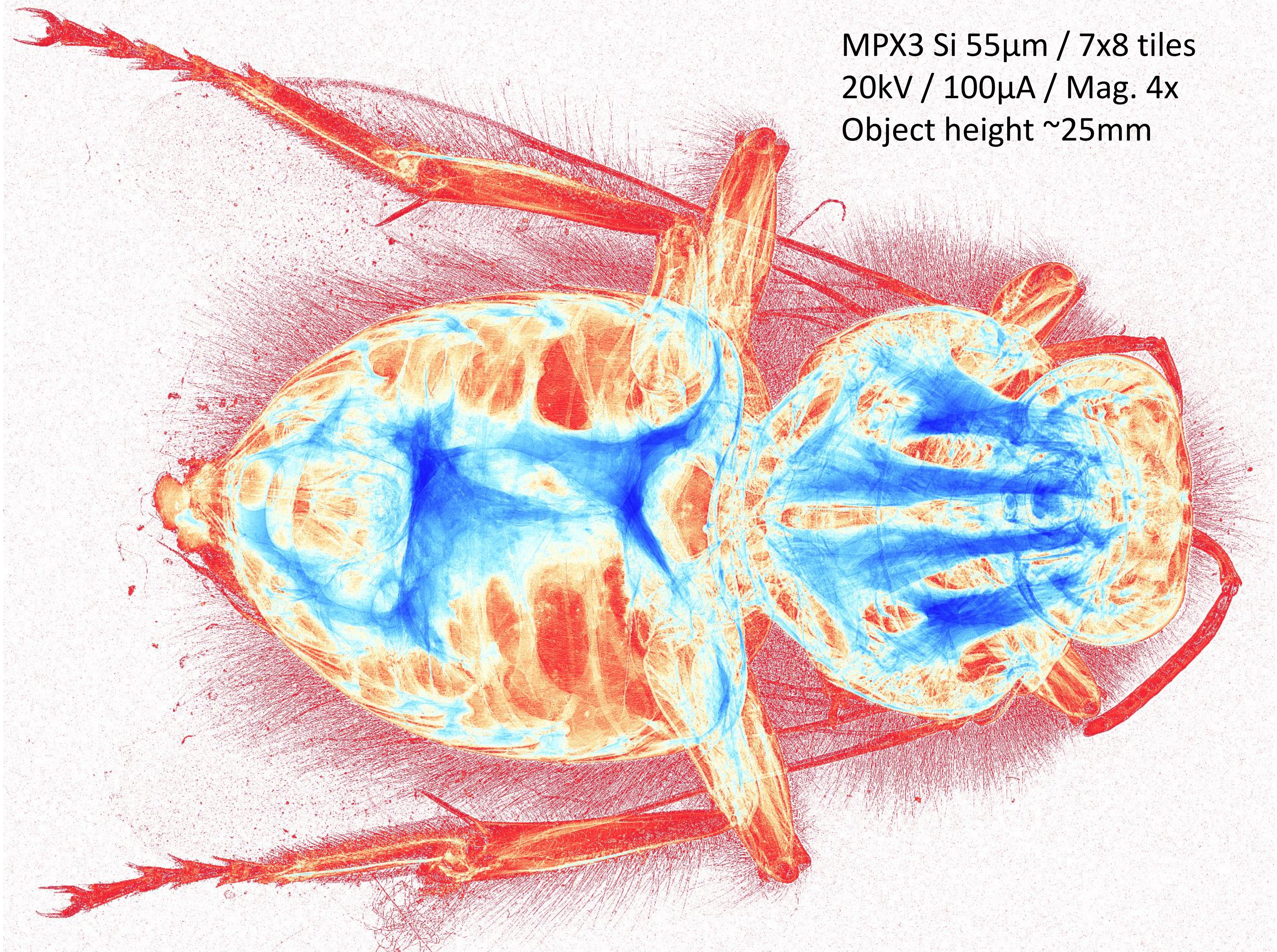

MPX3 Si 55µm / 7x8 tiles
20kV / 100µA / Mag. 4x
Object height ~25mm

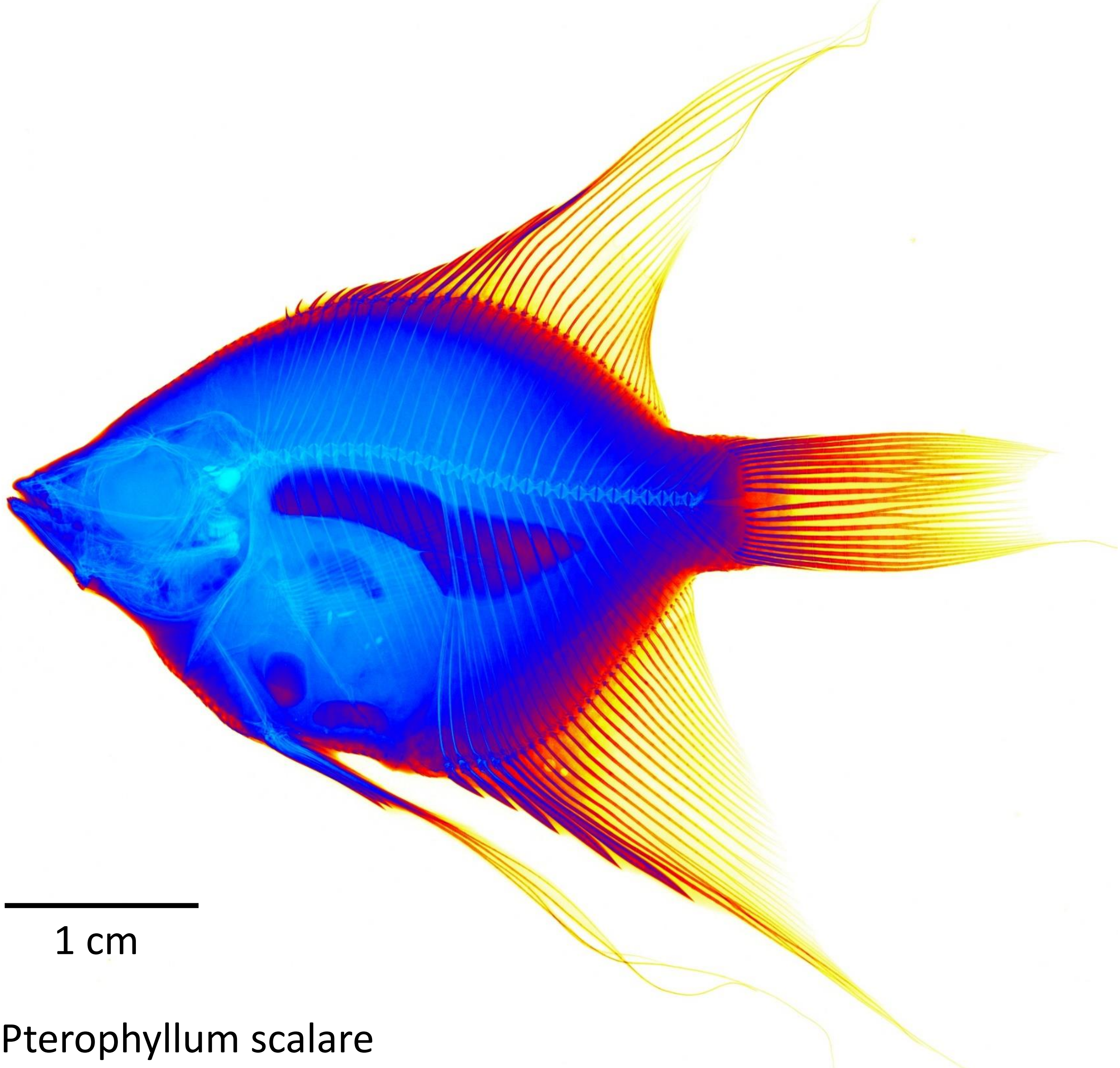

Pterophyllum scalare

MPX3RX 55 µm
SPM HGM

Si 300 µm
HV: +90 V

8x8 tiles
1.7x mag.

Medipix3 Biological Imaging: High Contrast Objects

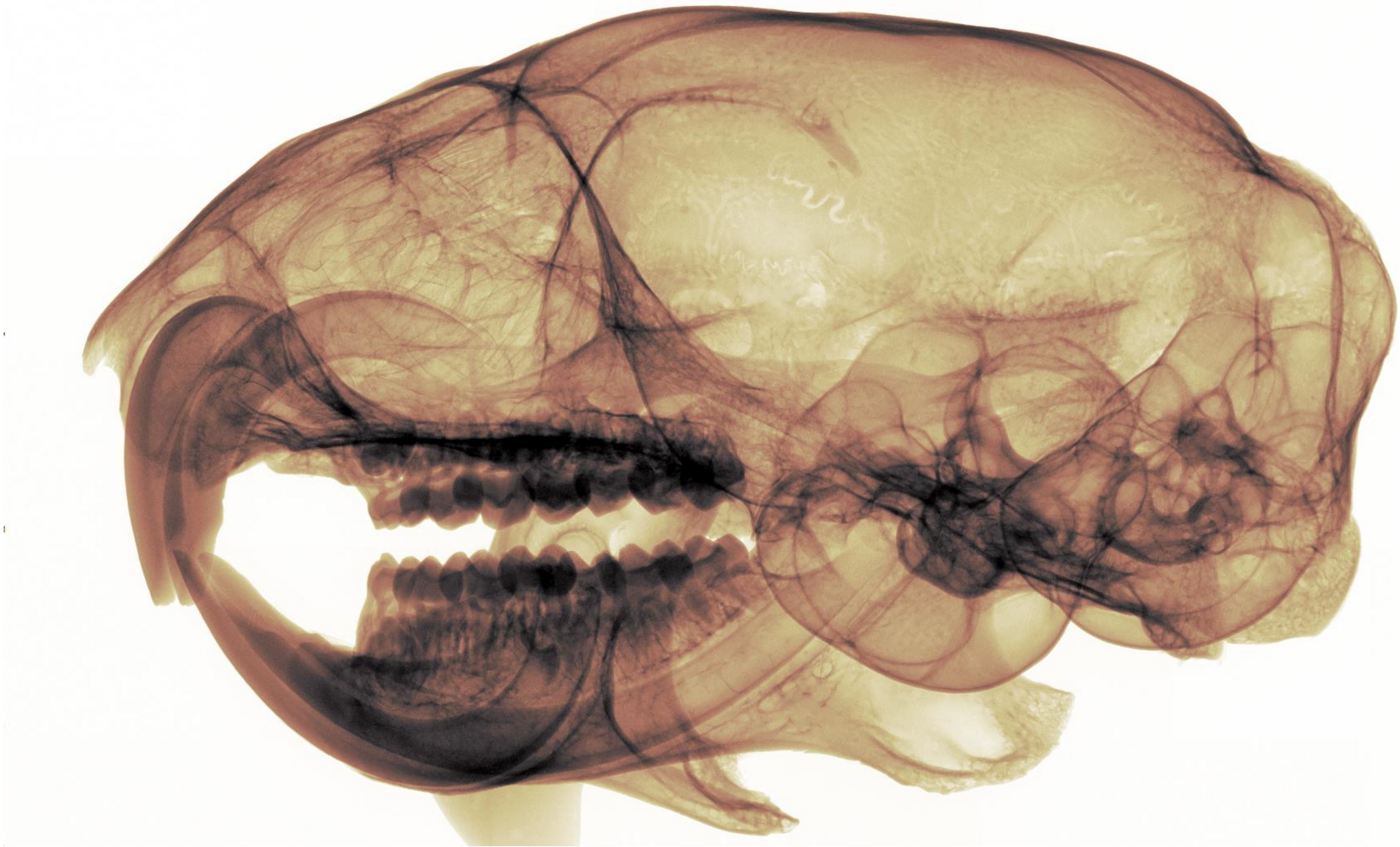

TPX, MPX-mode 55µm
GaAs 500µm
Bias: -230V
8x5 tiles, width 34mm

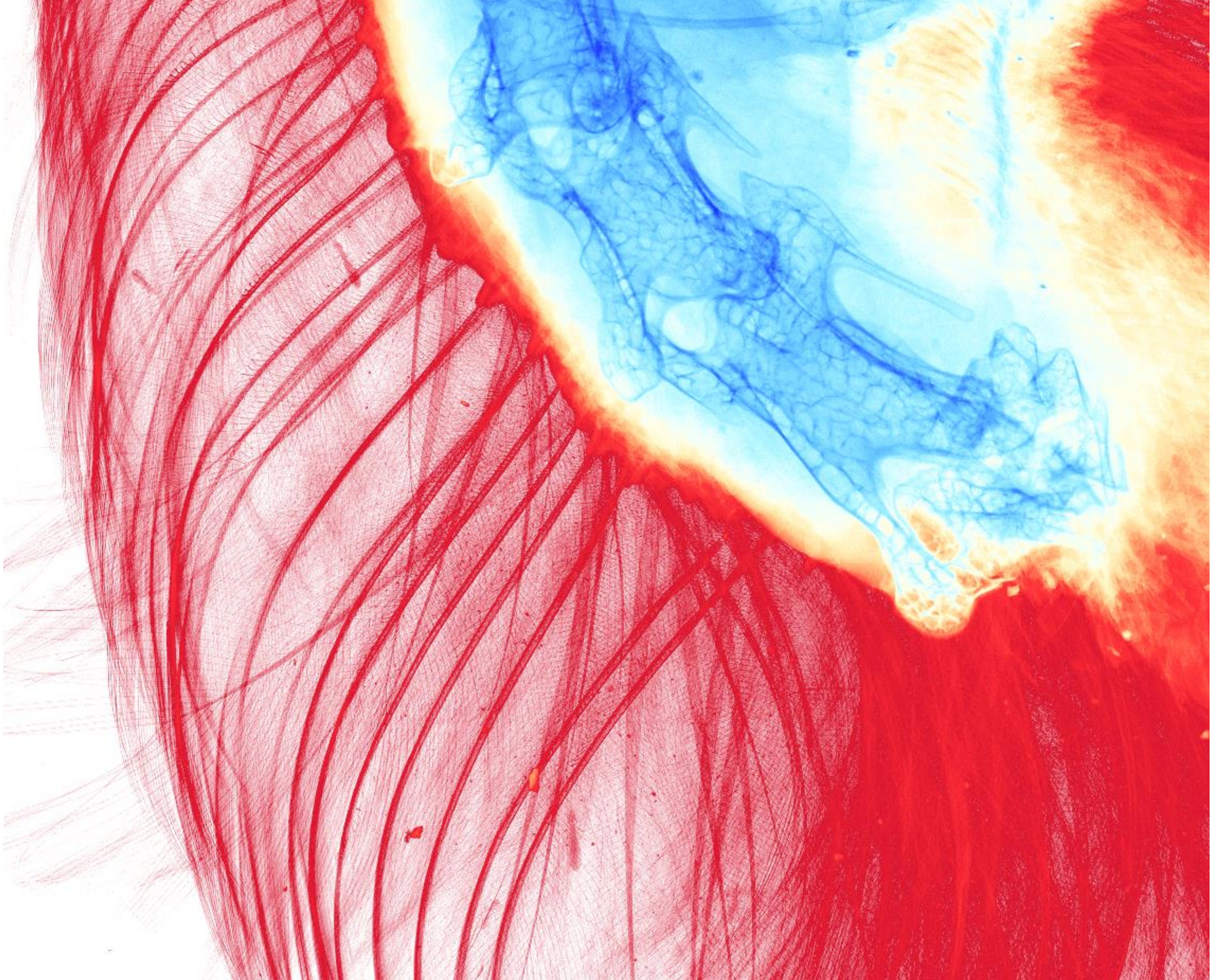

MPX3 Si 55µm
SPM HGM 24-Bit
8x8 tiles
27kV / 120µA
Mag. 2x

Object height
~50mm

Medipix3 Biological Imaging: High Frame Rates

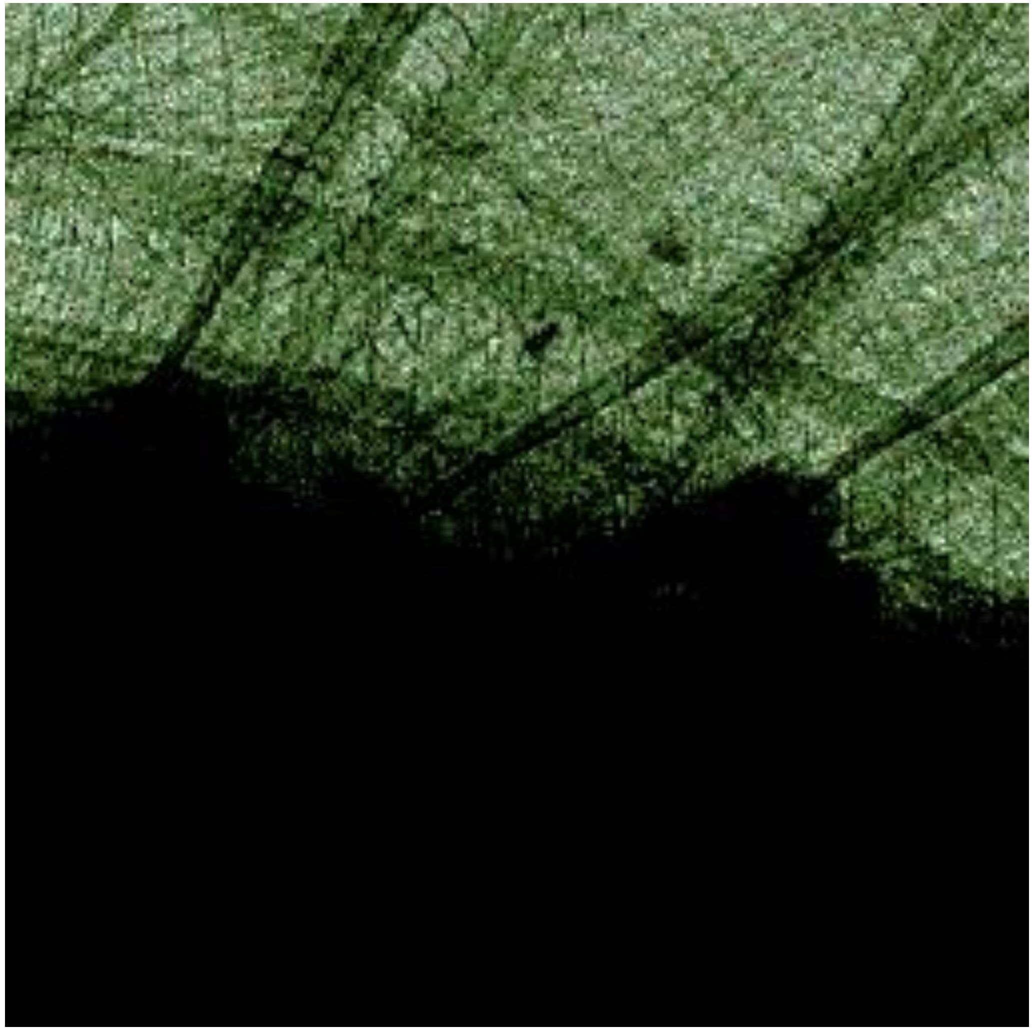

MPX3 Si 55µm
SPM HGM 12-Bit
1 tiles (256x256)
10 frames/s

45kV / 100µA
Mag. 3x-5x

Object height
~25mm

Energy Selective, Planar Imaging
MPX3 CdTe 1mm - Color Mode 110µm

Piezo Lighter

Magnification: 1.3x

Bias: -320V

MPX3 CdTe 1mm
Colour Mode
4x11 tiles

A: Logarithmic
grayscale sum

B: Coloured X-ray
image

C: Linear
grayscale sum

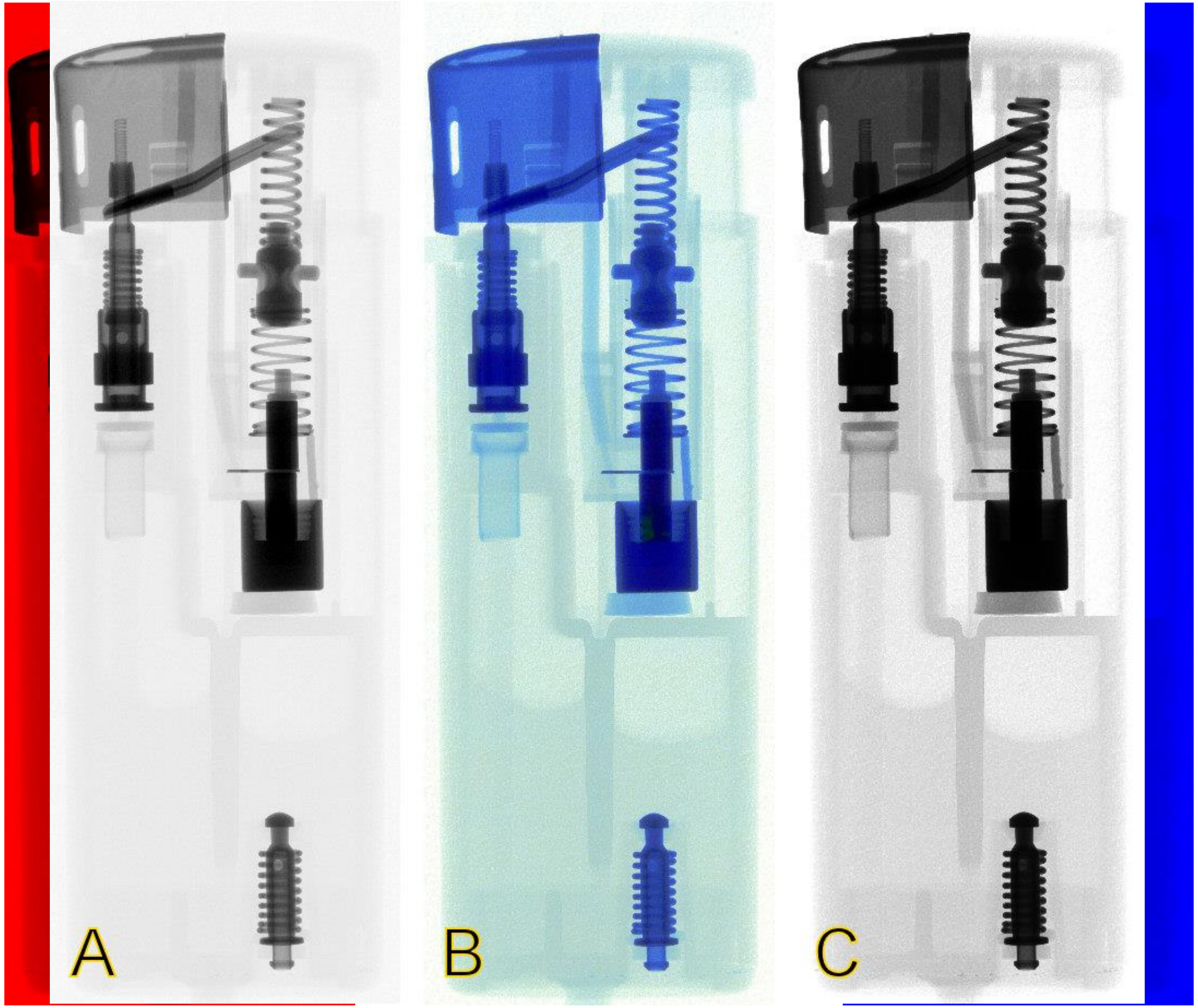

Medipix3 Biological Imaging: Art

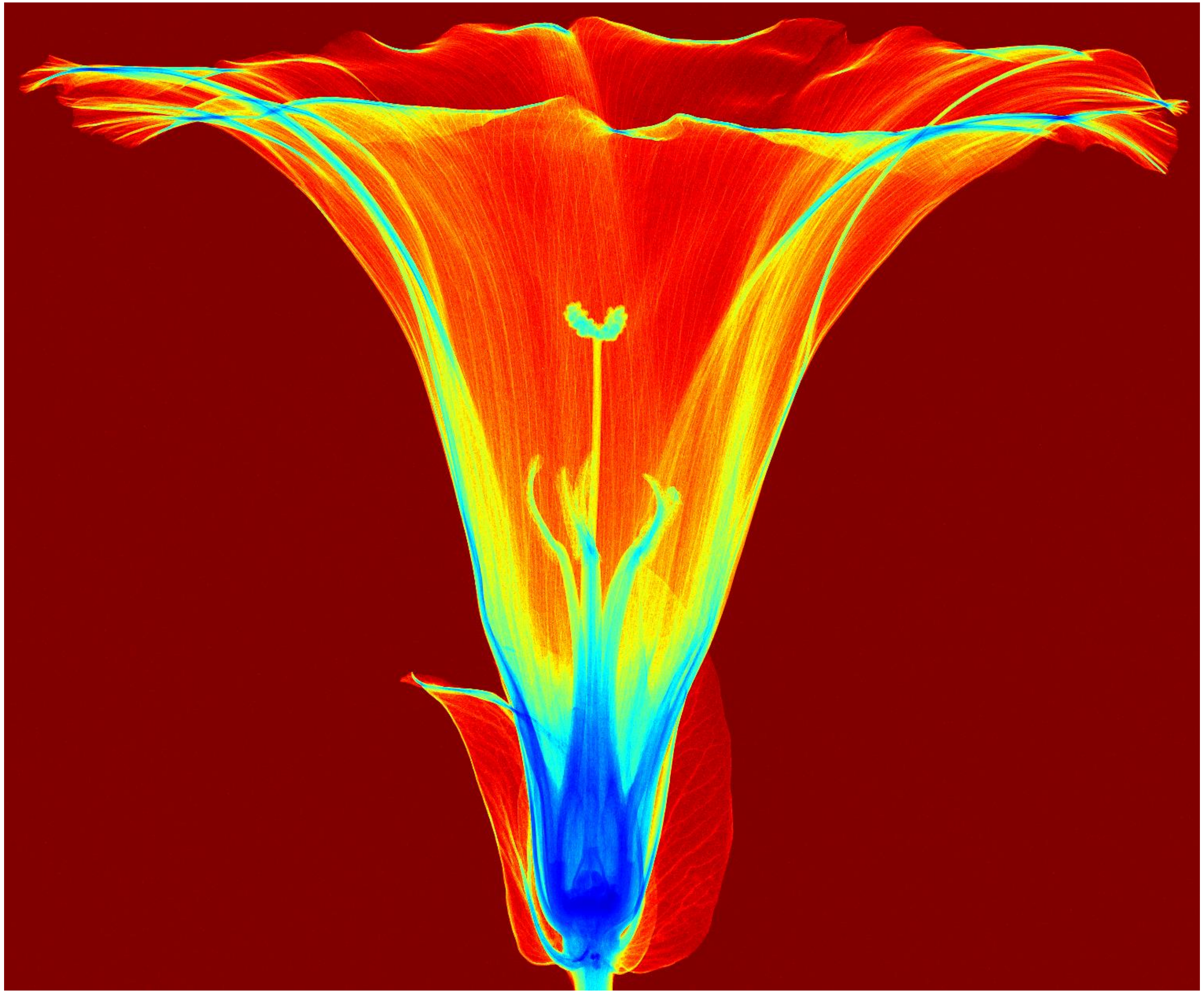

Medipix3 Medical Imaging: Sensor Attenuation Efficiencies

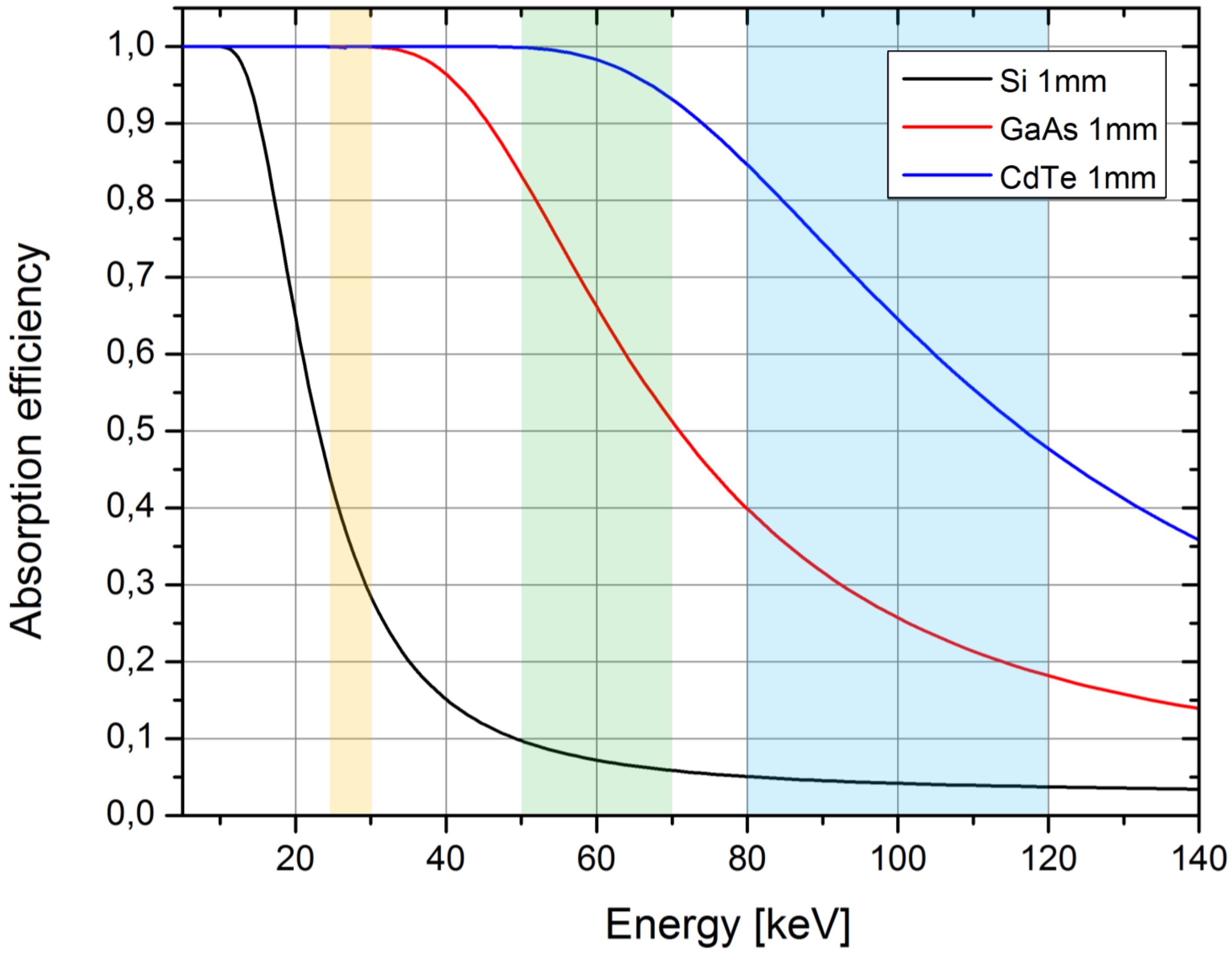

Mammography

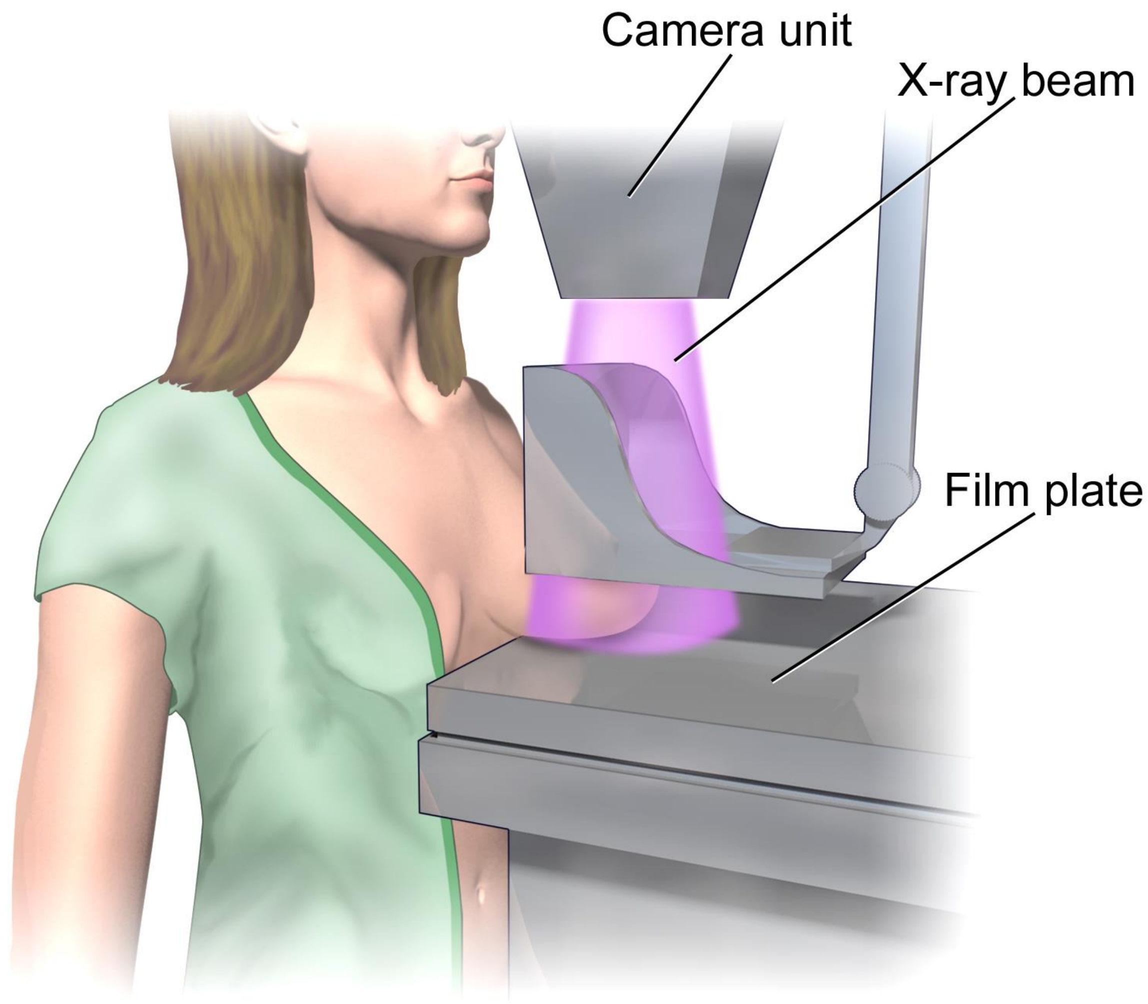

Mammogram

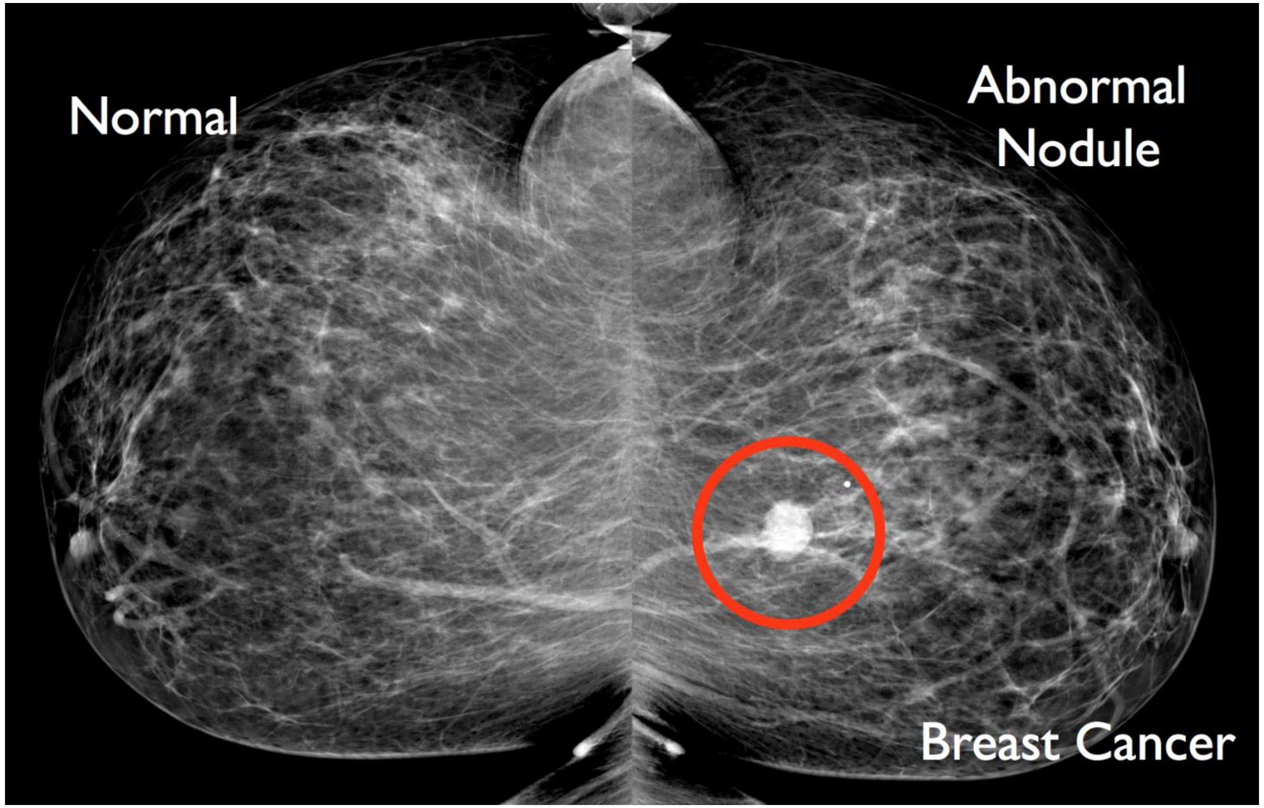

Courtesy of breast360.org
https://breast360.org/wp-content/uploads/filer_public_thumbnails/filer_public/0d/e5/0de59648-ca2e-4005-be2c-b315c3664ddb/bts-_mammo_3.png__1692x1082_q85_crop_subsampling-2_upscale.png

Diagram: Medical gallery of Blausen Medical 2014. WikiJournal of Medicine 1 (2). DOI:10.15347/wjm/2014.010. ISSN 2002-4436

Commercial Mammography Phantom: Radiography

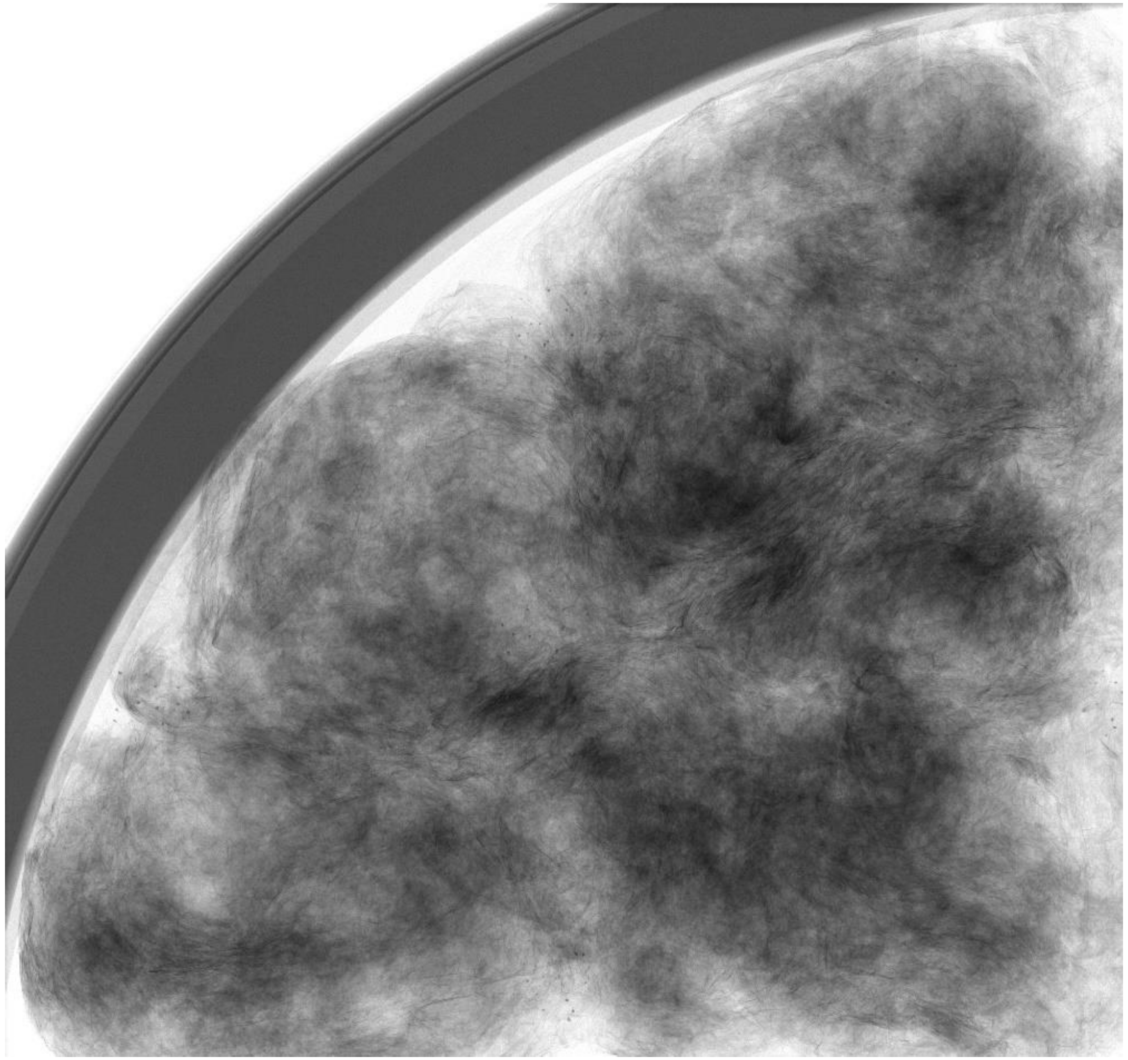

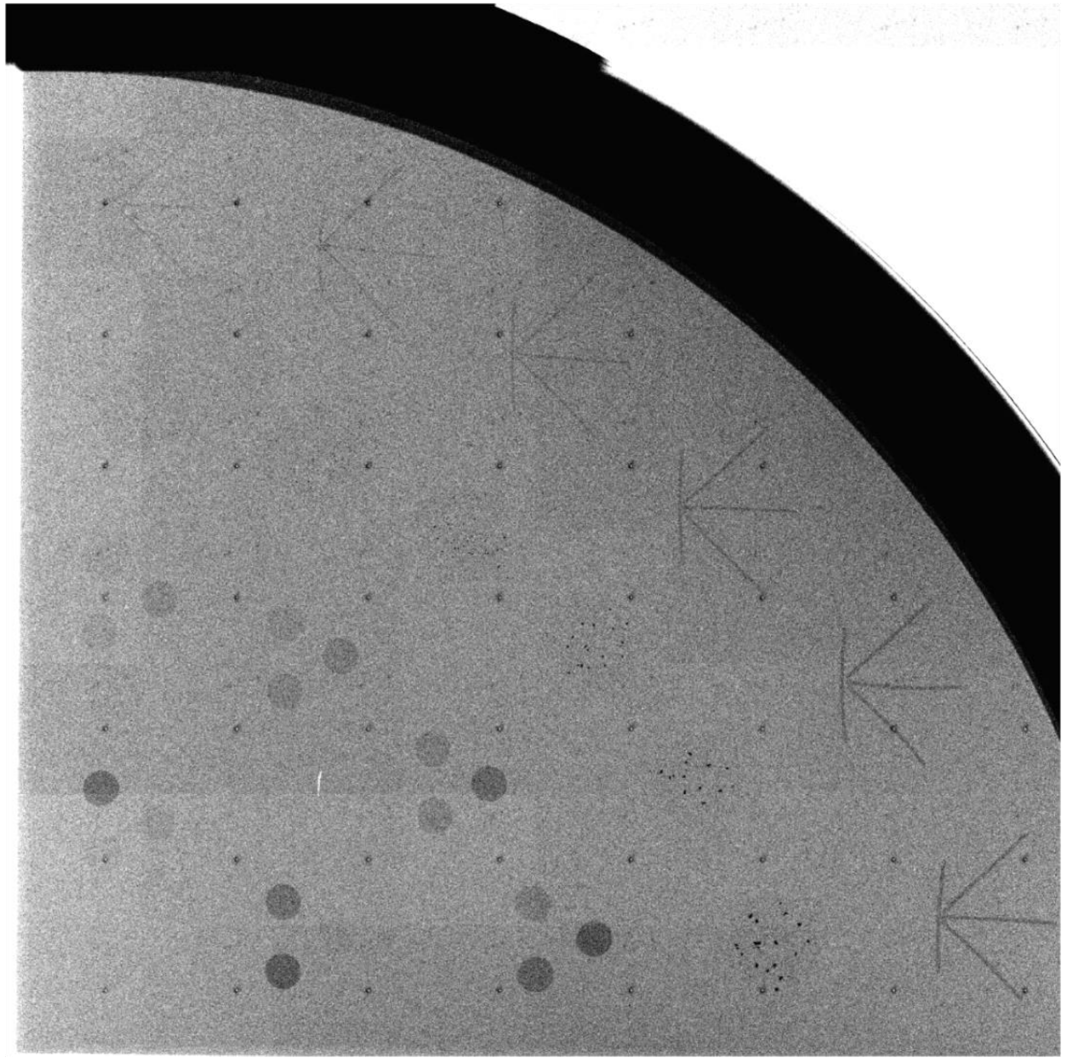

CdTe, threshold 7.5 keV, magnification: 1.15x, 16x8 tiles

Sensor Comparison

0.43 mGy

CNR

4.30 mGy

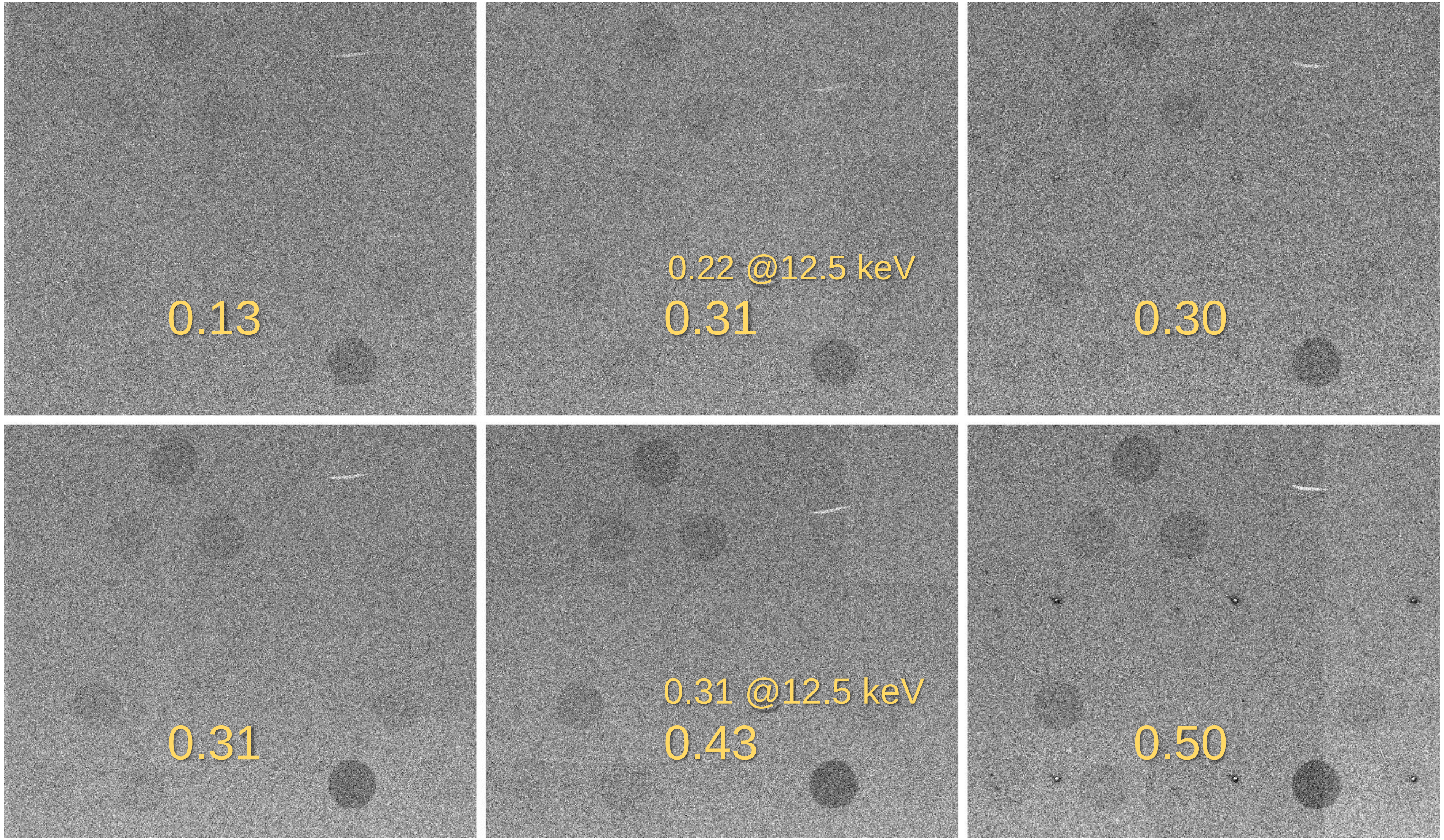

Si 500µm

GaAs 500µm

CdTe 450µm

Source: LeedsTestObjects.com

Spatial Resolution Test

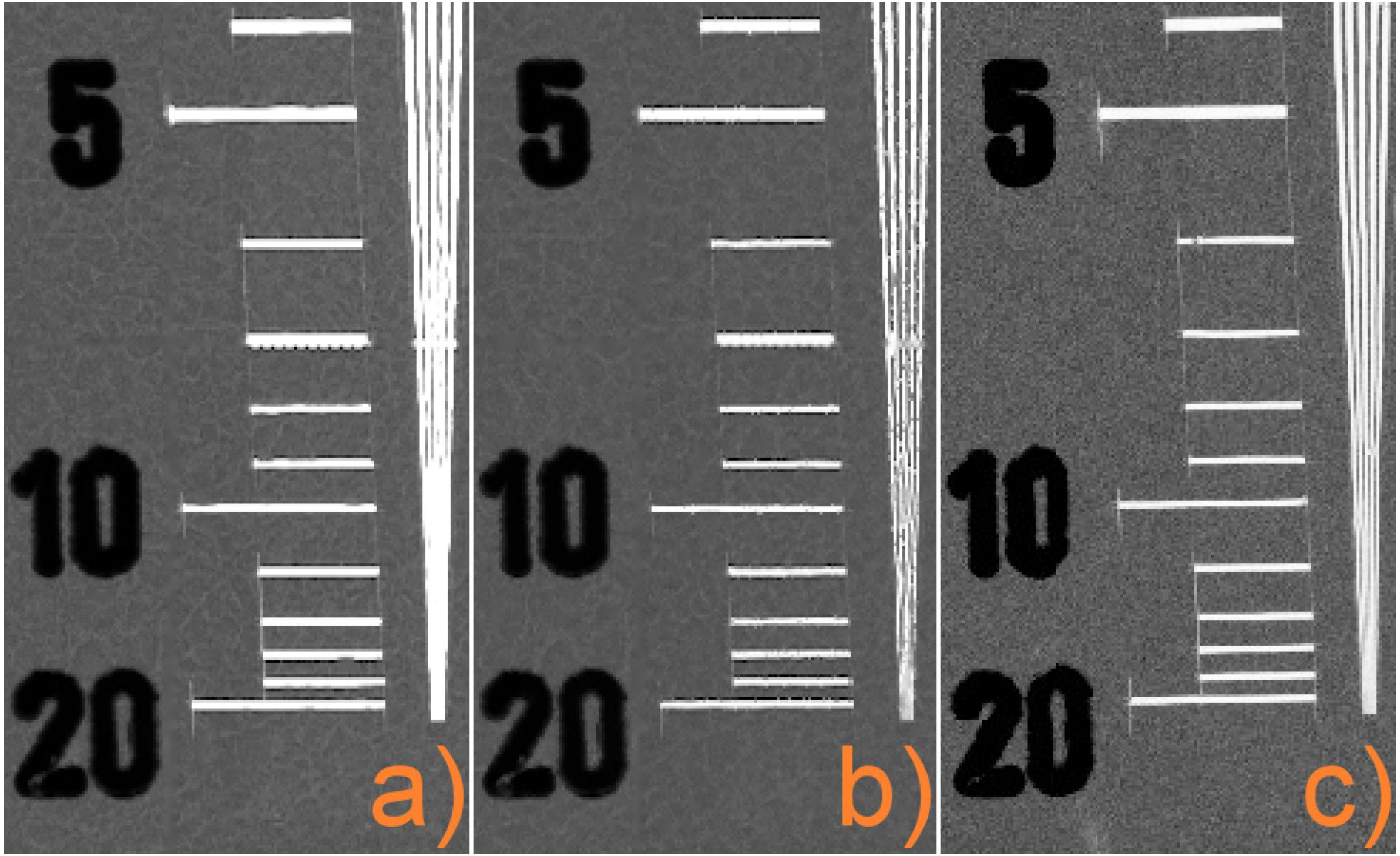

Nyquist limit:
9.1 lp/mm

a) GaAs @ 7.5 keV

b) GaAs @ 12.5 keV

c) CdTe @ 7.5 keV

Human Mammography Phantom Comparison

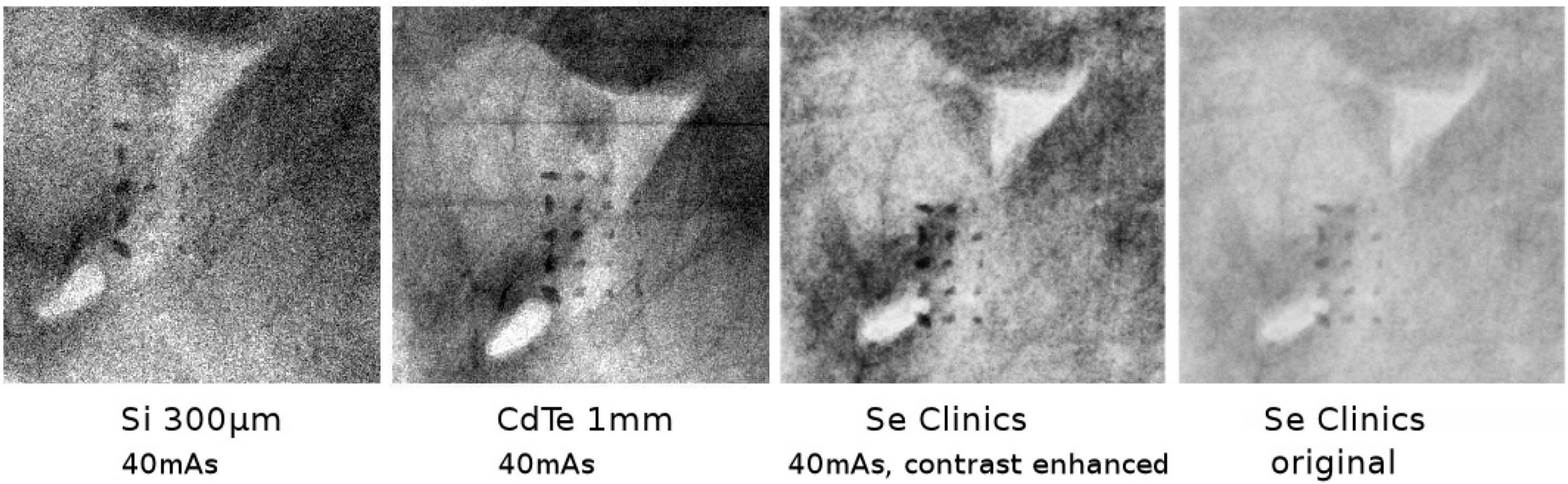

40 mAs = 44 % of standard dose

Small Crystals: CNR to White Backgr. (3σ Fractile)

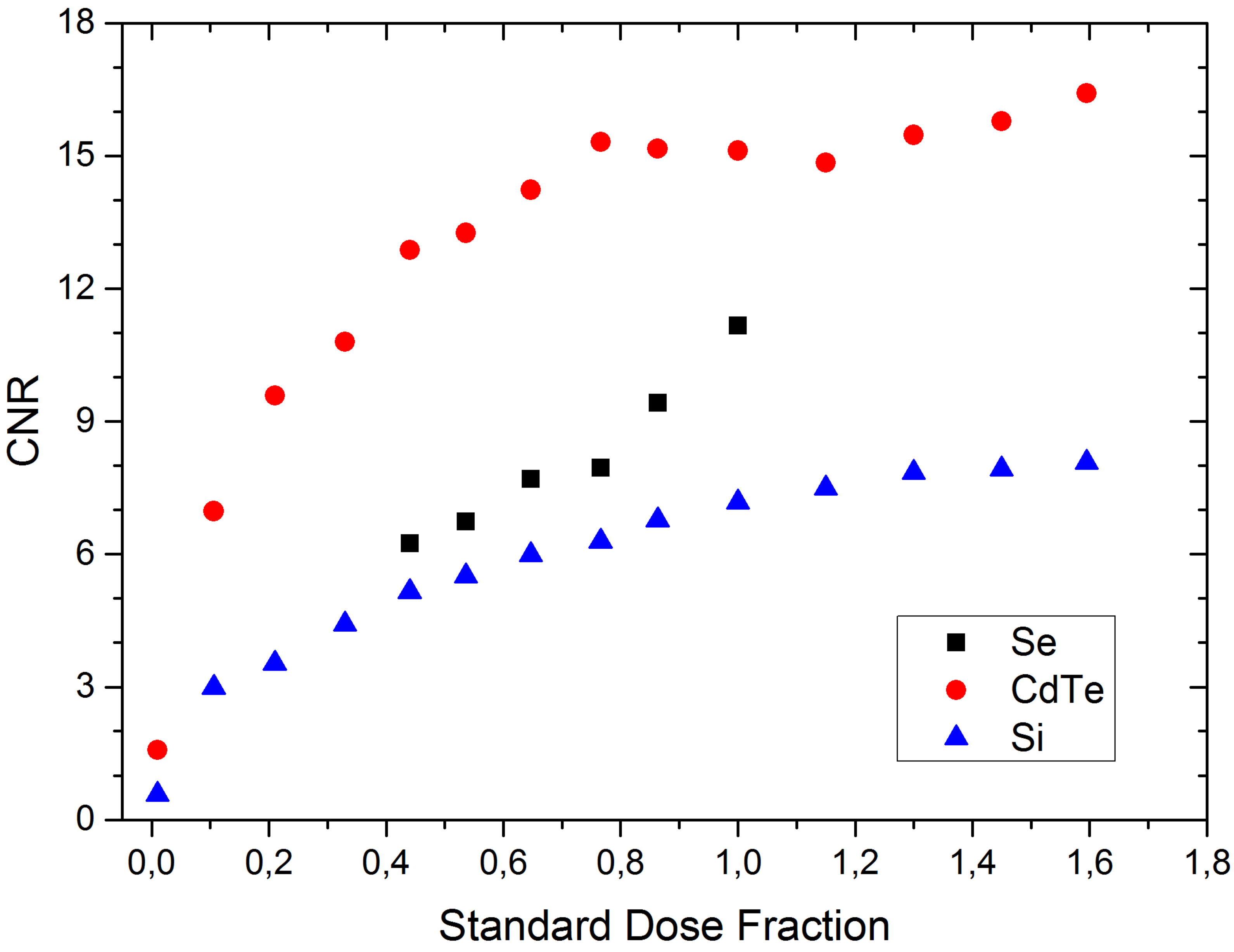

Image Quality: Si vs CdTe

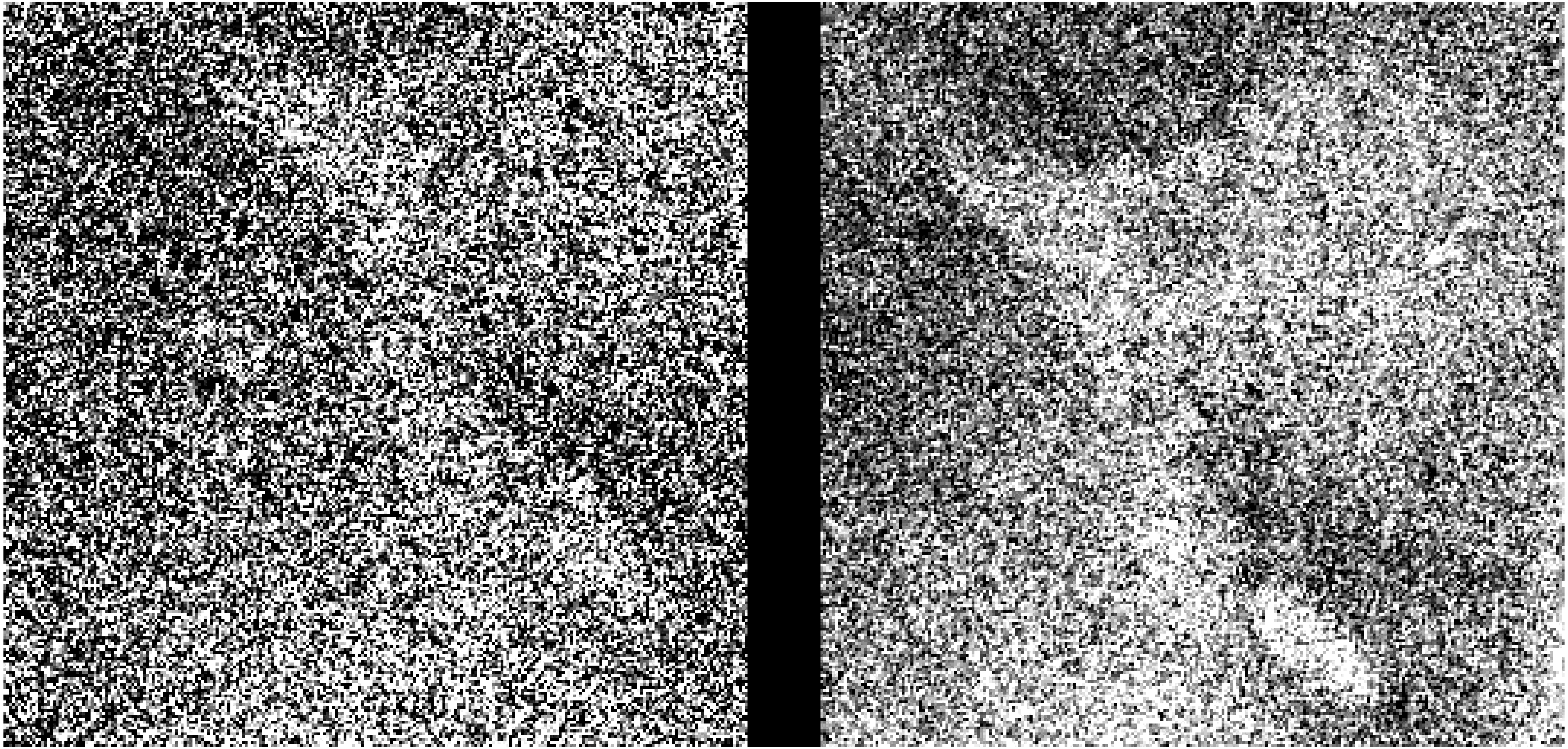

Si 300 µm

CdTe 1 mm

K-Edge Imaging

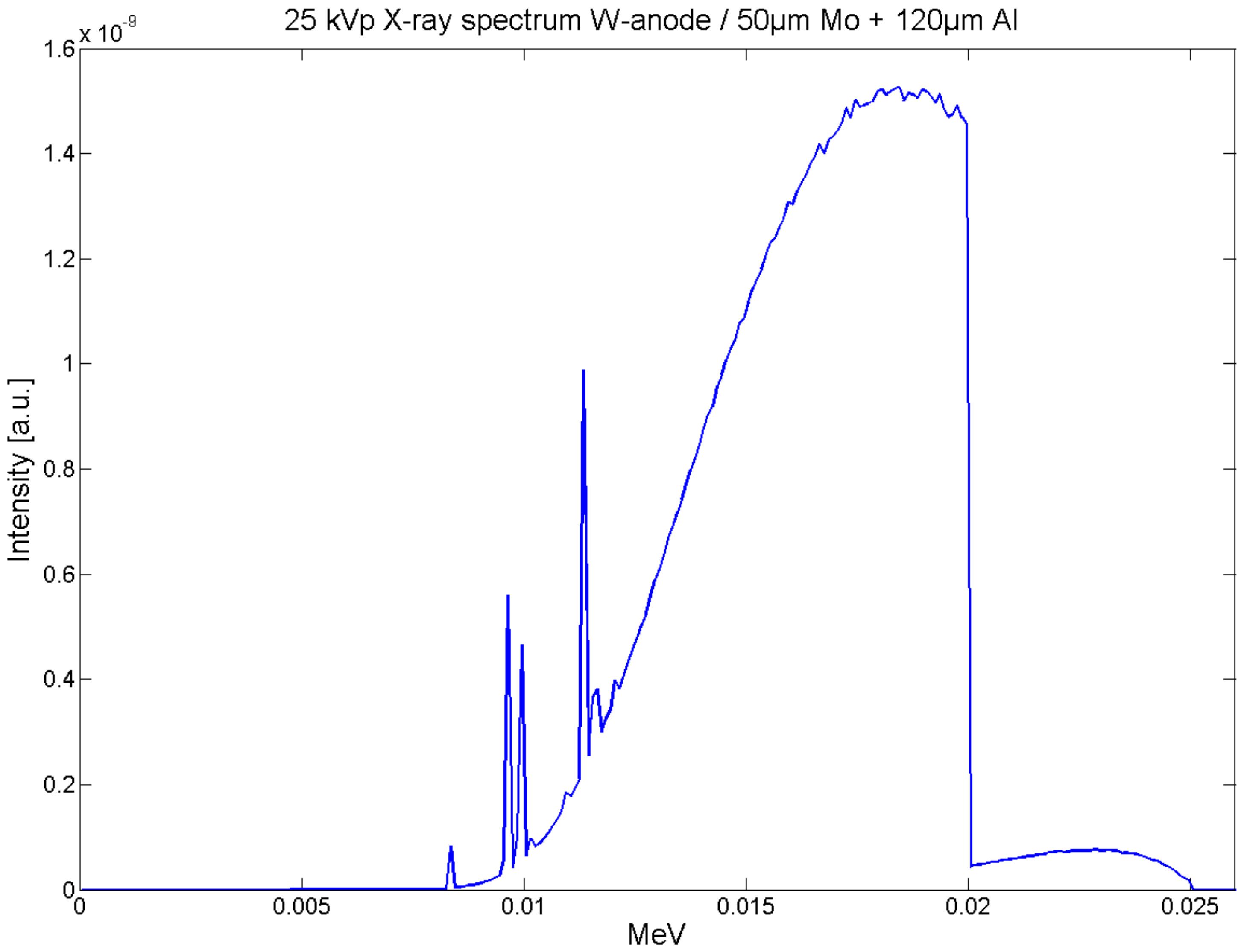

Unfiltered W-anode input spectrum: Simulation of G. Blaj (SLAC)

- Horizontal direction:
  8 Different materials
- Vertical direction:
  Varying thickness
- Lower area:
  3 layers of aluminum in different thicknesses

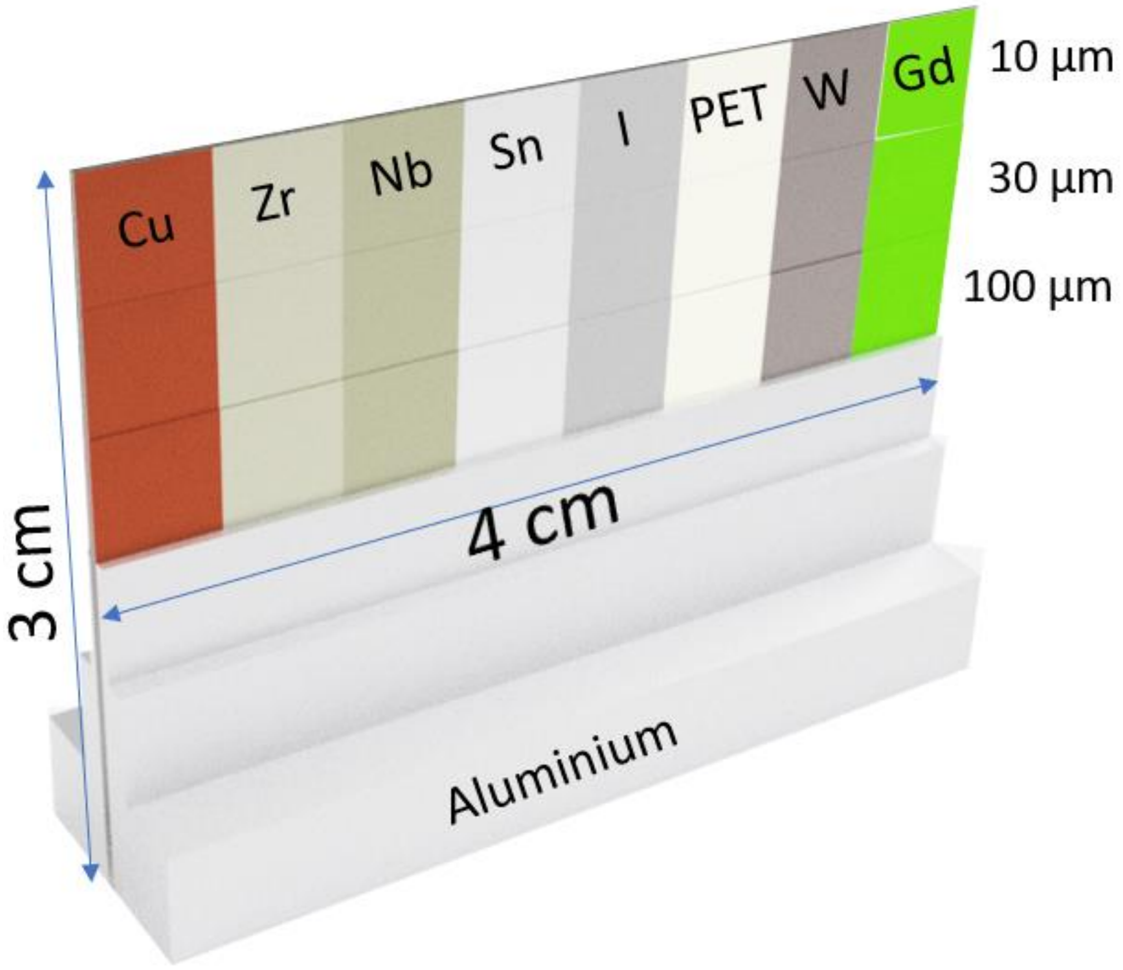

Absorption Phantom Photography

3 cm

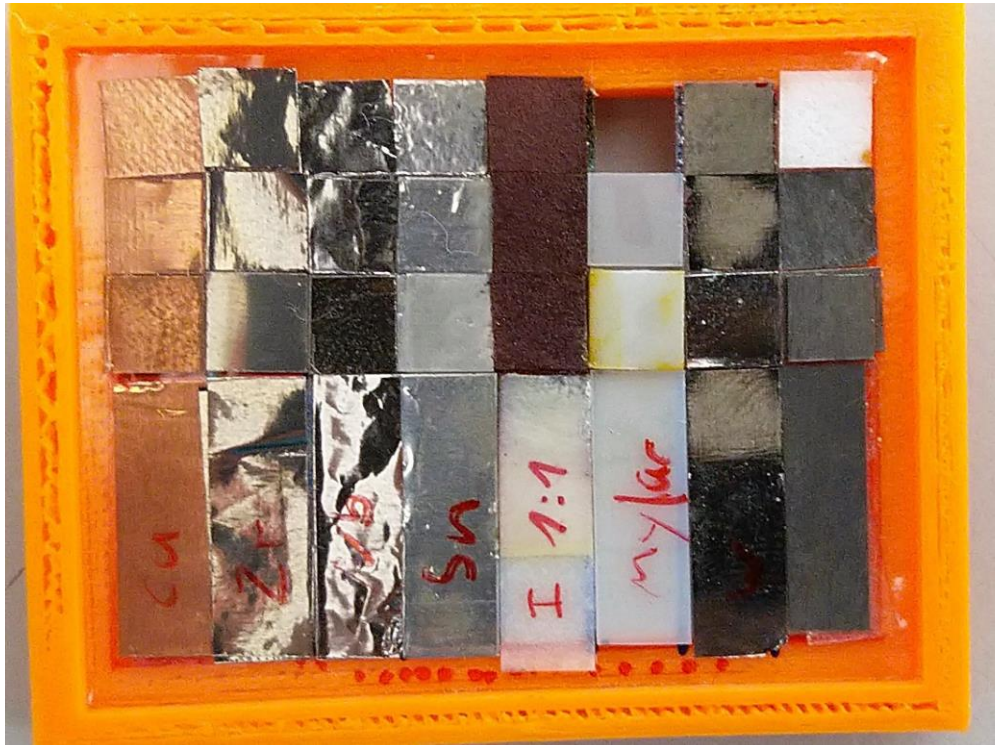

4 cm

Empty field for normalization

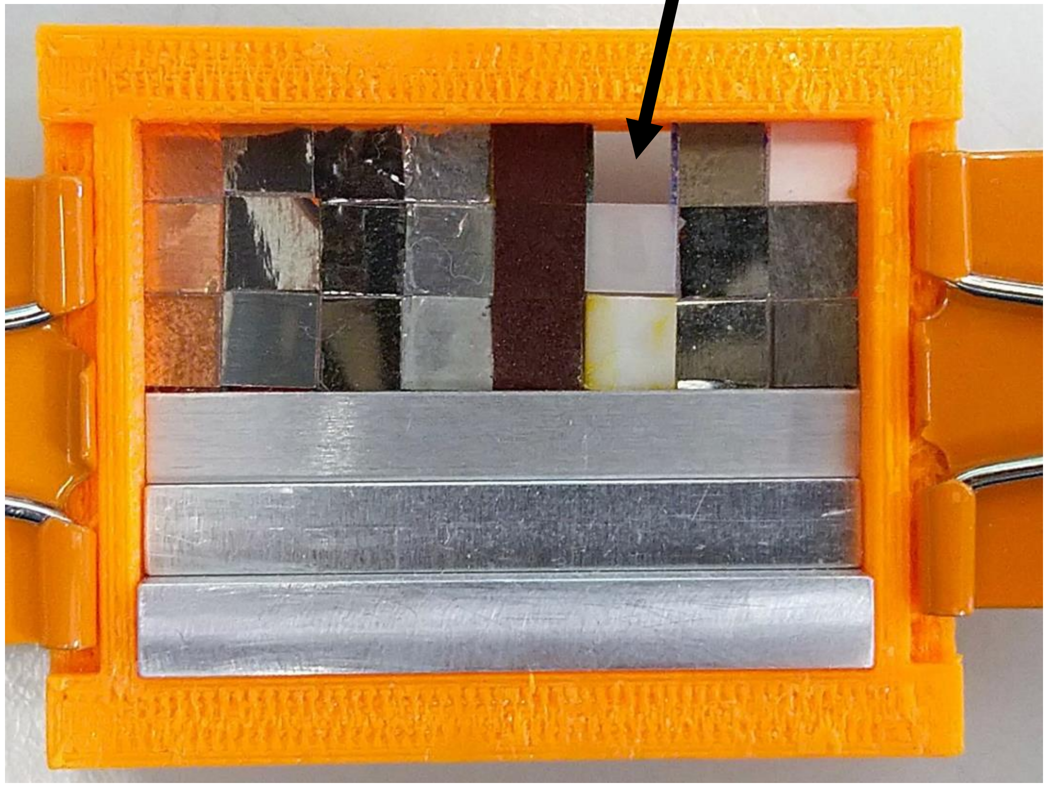

Absorption Phantom – Medipix3RX

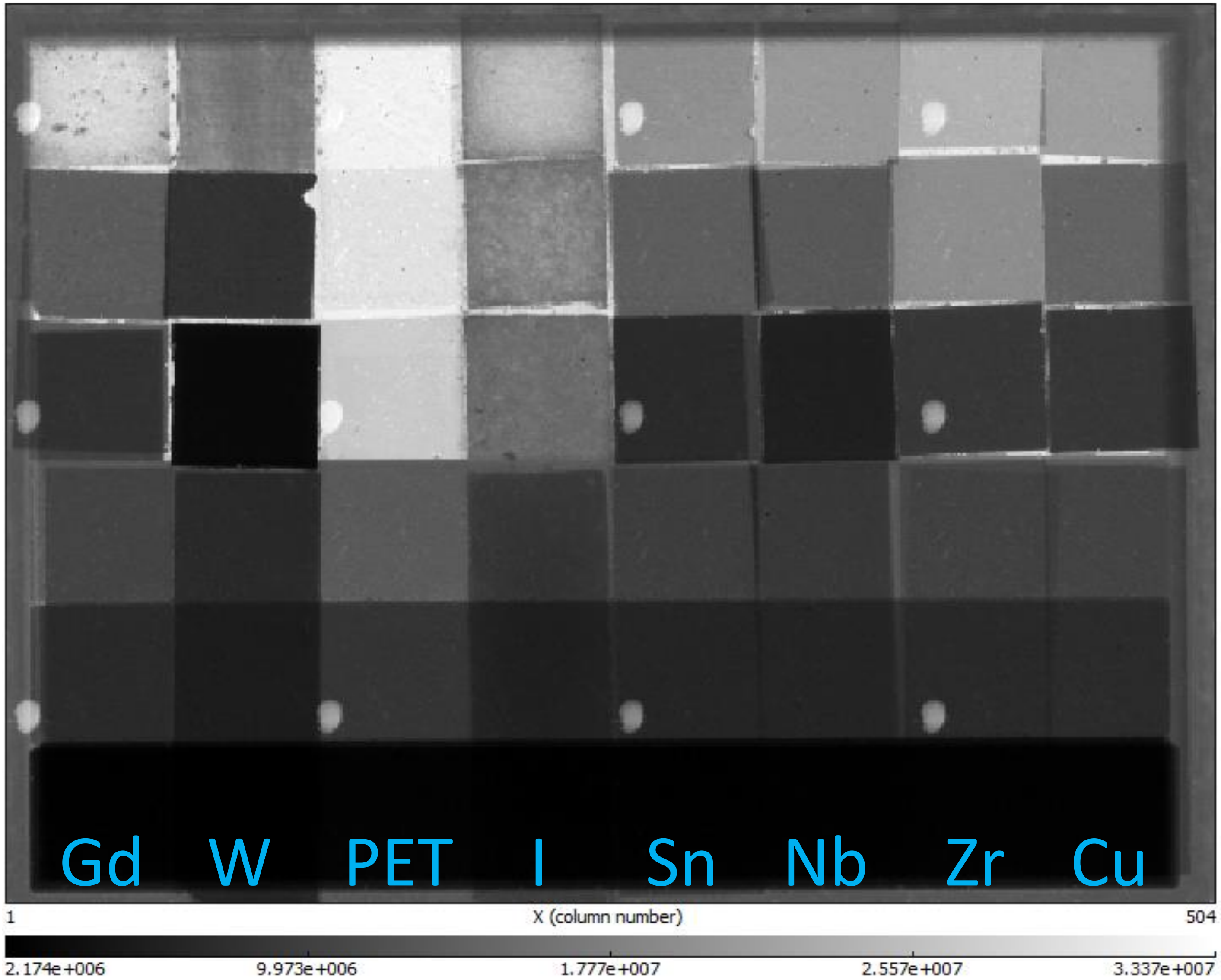

K-Edge Imaging: Evaluation of the Results

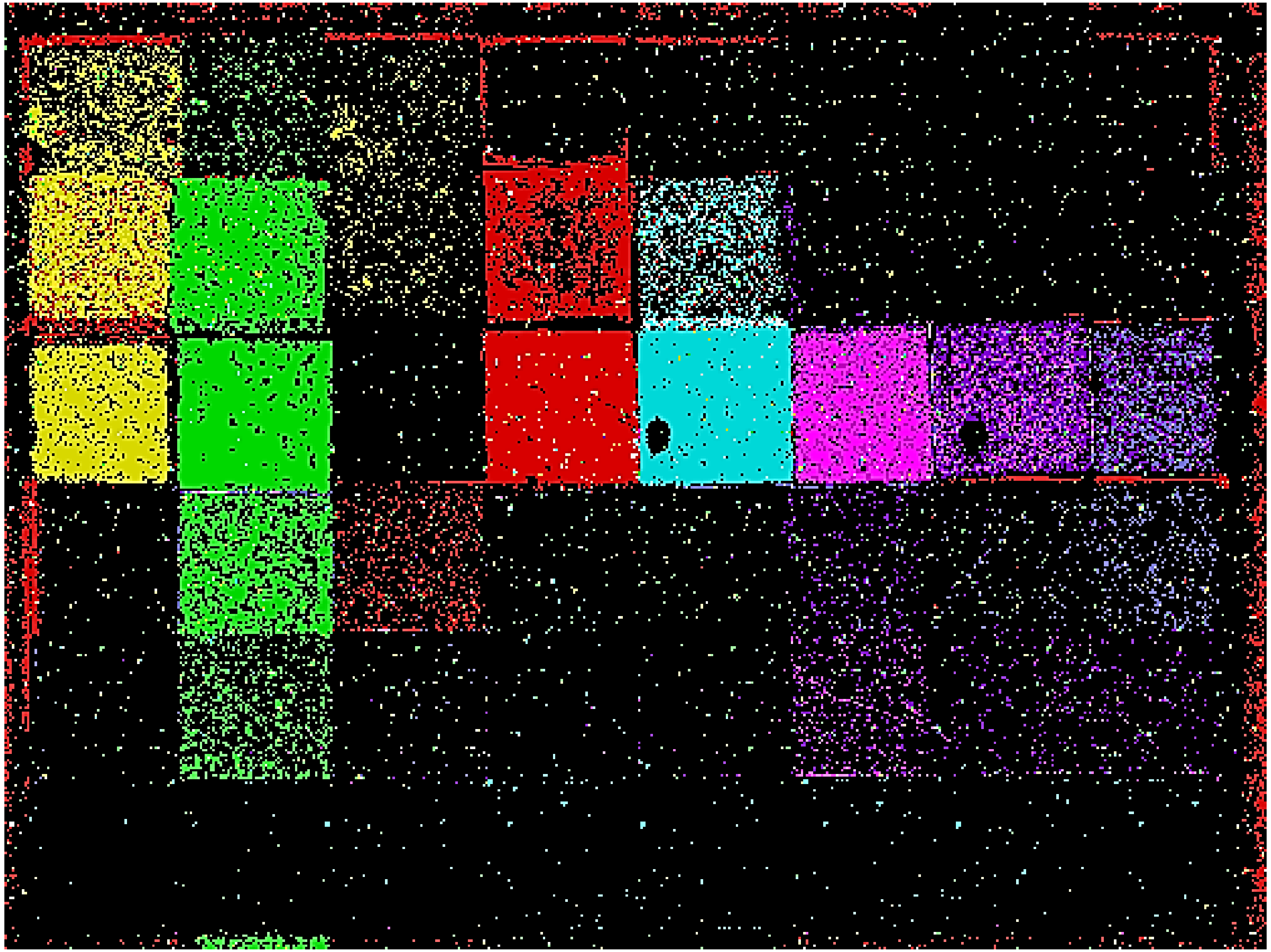

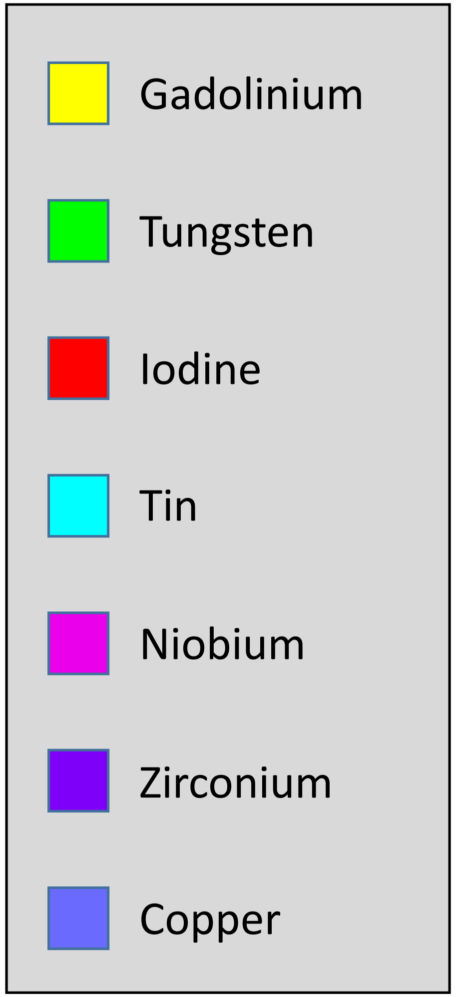

Spectroscopic Detector (Timepix)

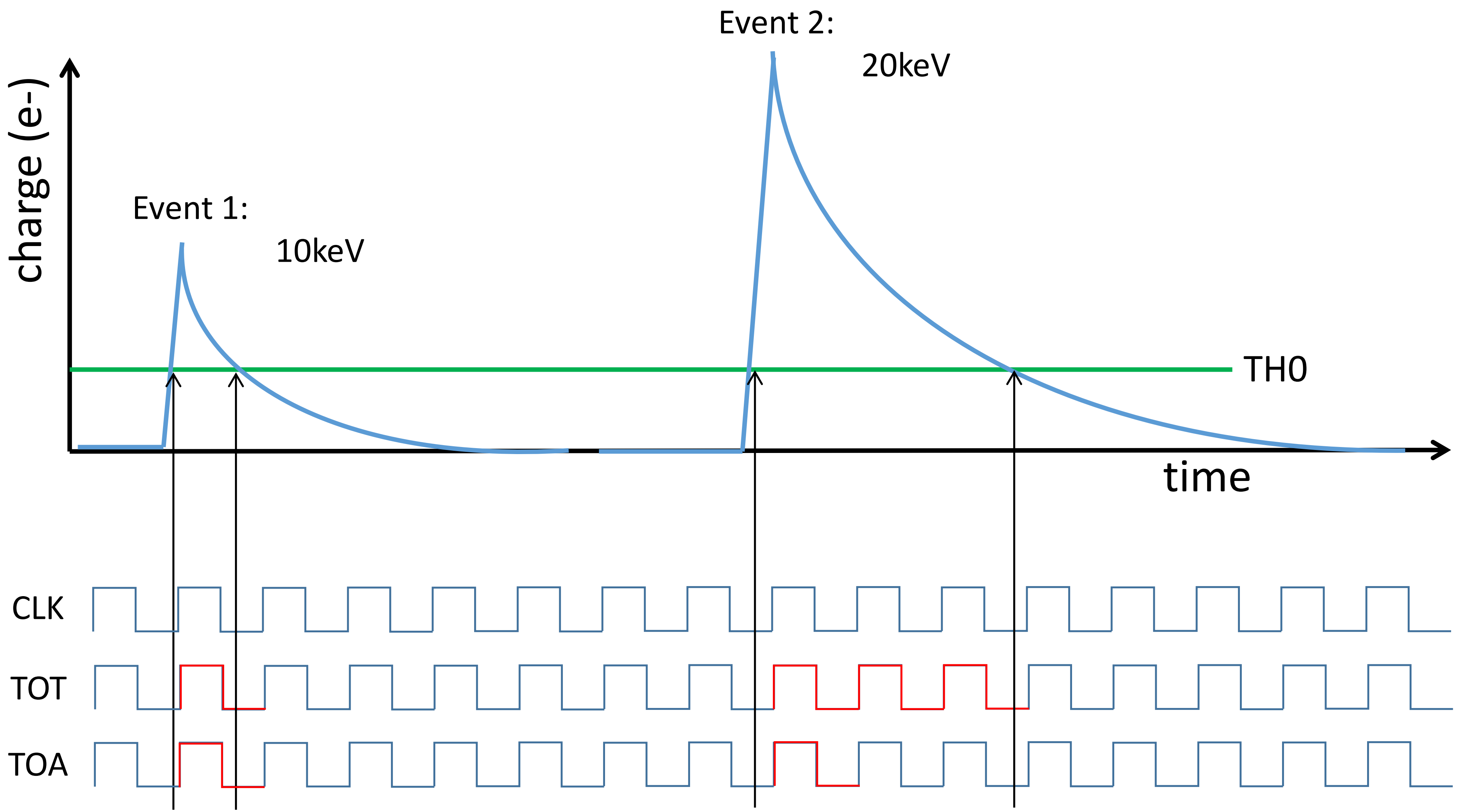

Charge Sharing Effects - Improvement Through Clustering

Higher energy resolution

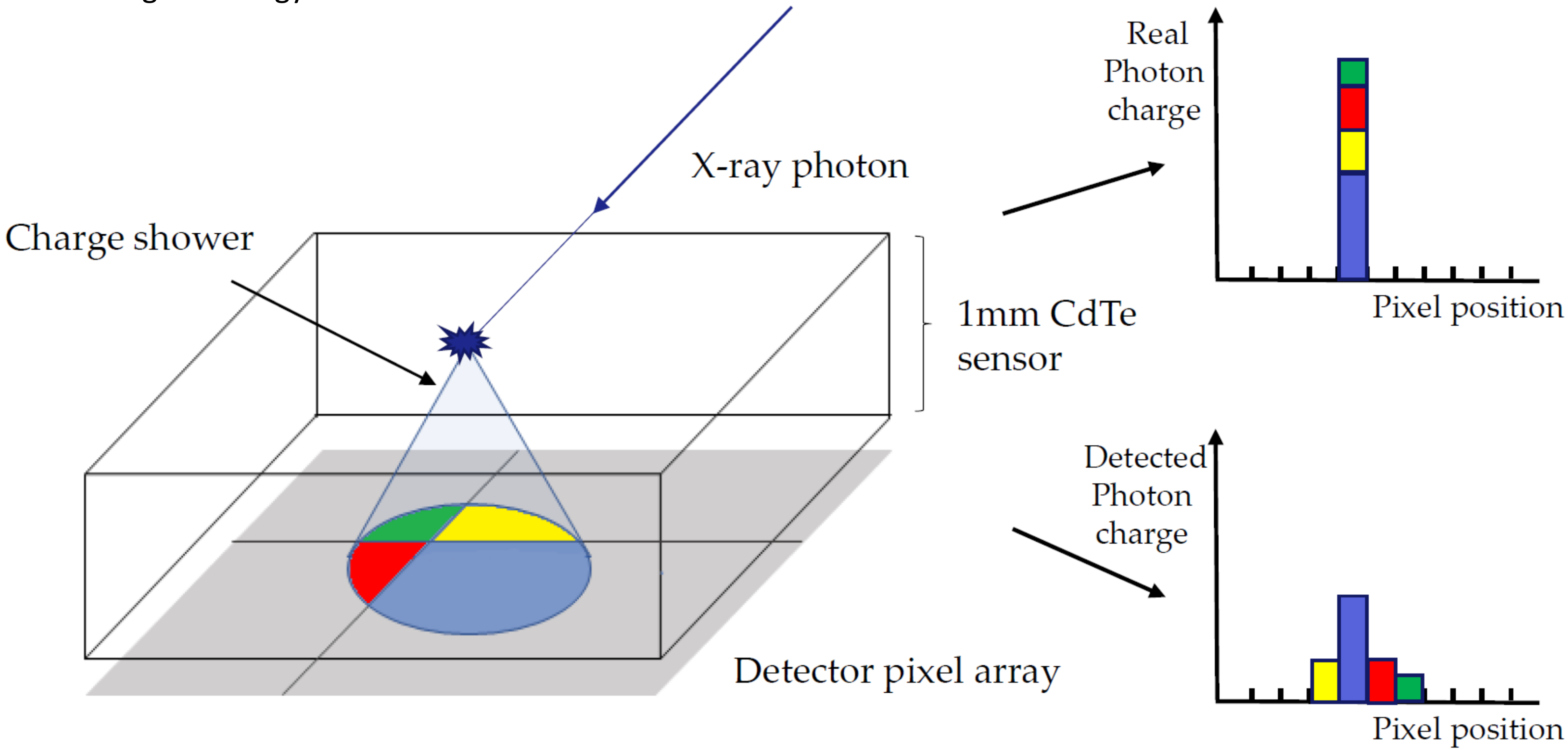

Charge Sharing Mechanisms

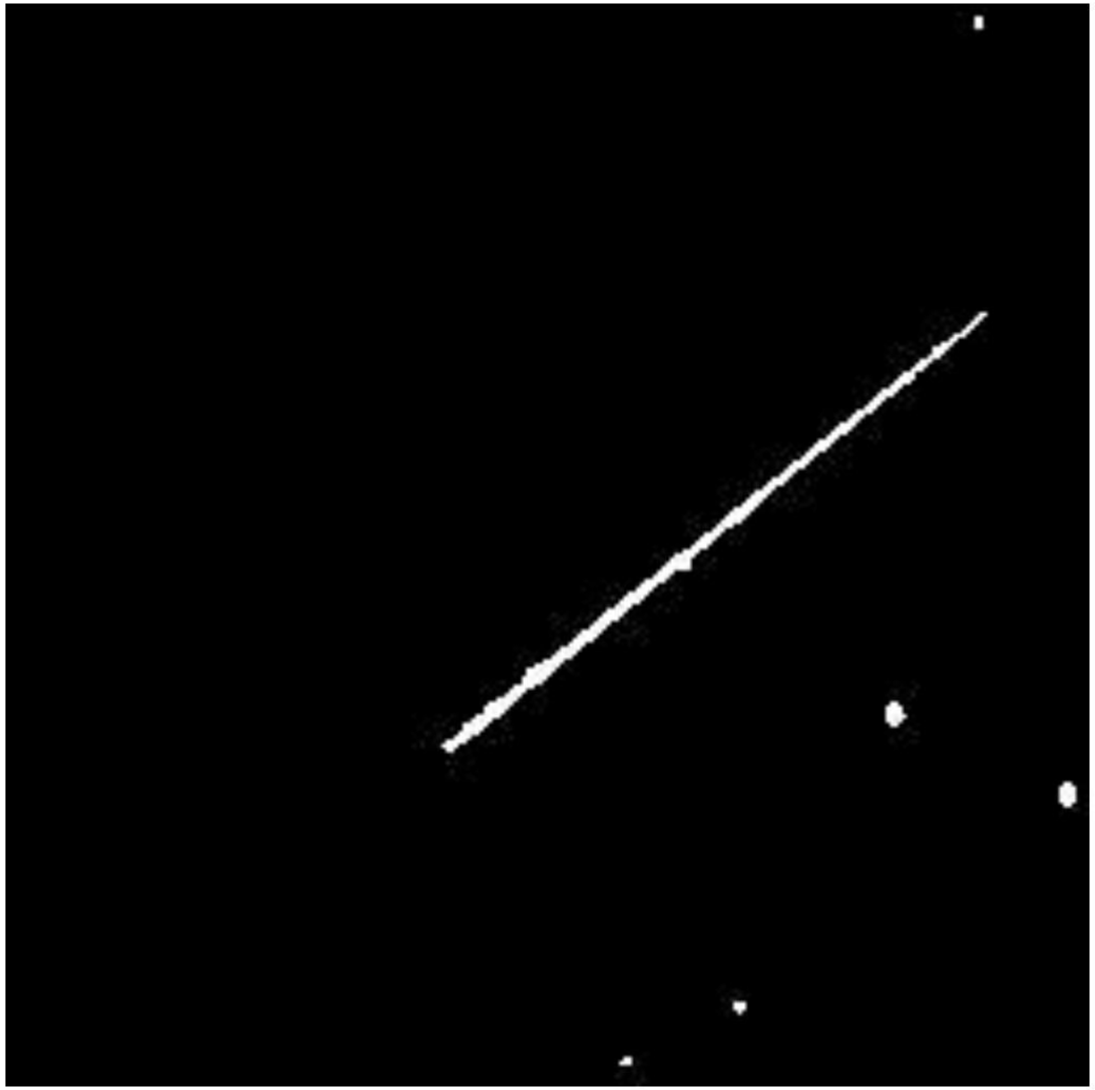

Reduction of Charge Sharing:

- Collecting carriers more quickly
  - Reducing sensor thickness
  - Increasing field strength
  - Using material with higher mobility
- Small pixel effect

Source: R. Ballabriga / CERN

Charge Sharing Effects - Improvement Through Clustering

No Subresolution:
highest counting pixel gets hit

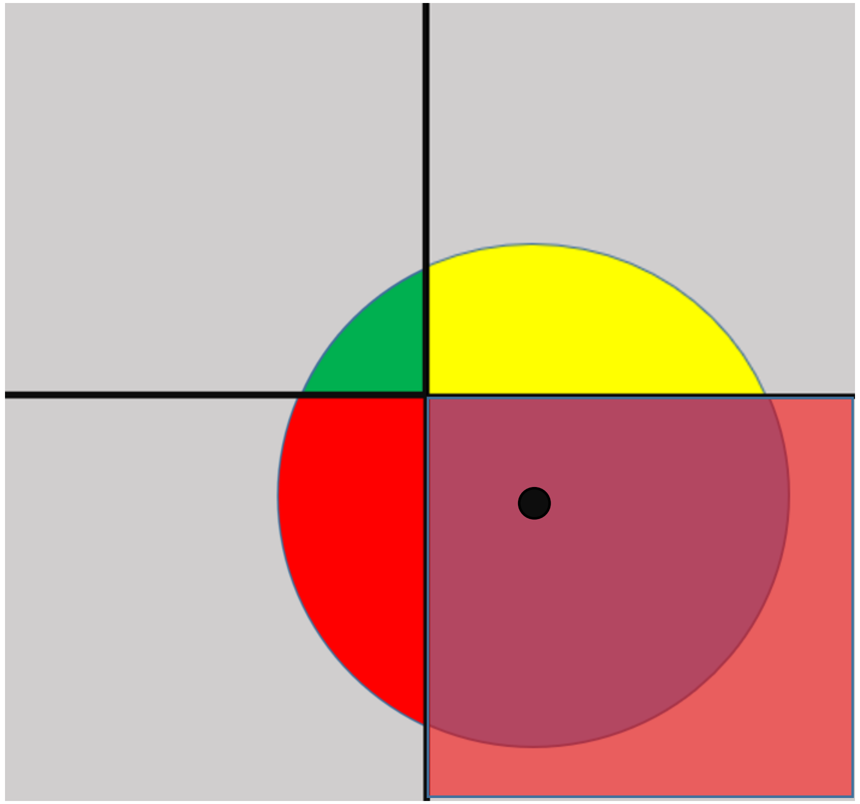

Position:
Pixel (1|1)

Subresolution:
calculated by center of mass

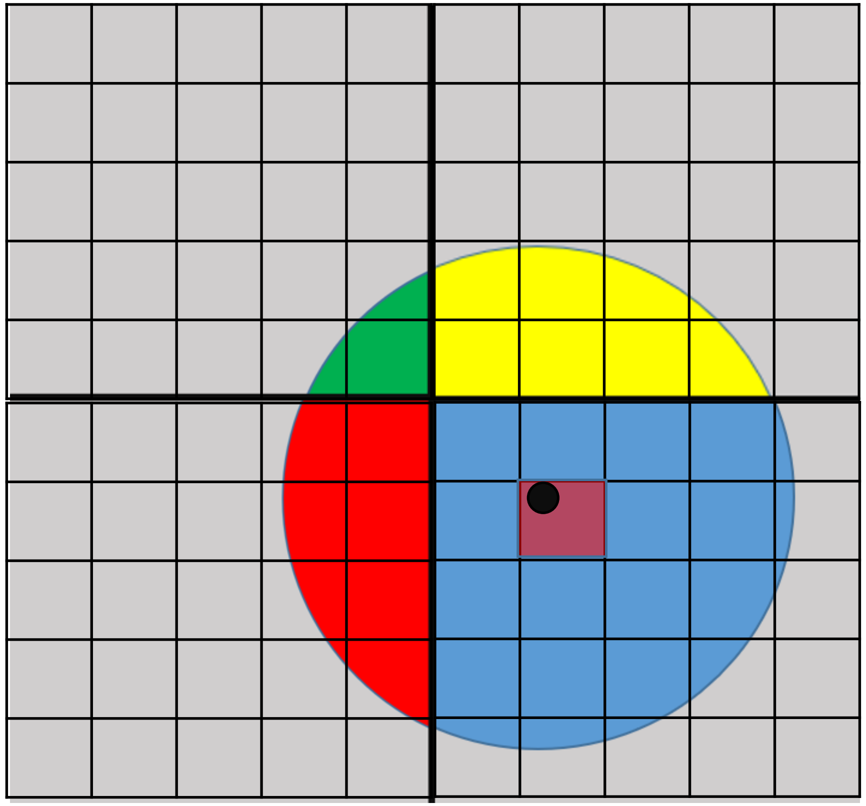

Position:
Pixel (1.2|1.2)

Center of Gravity: Subpixel Spatial Resolution

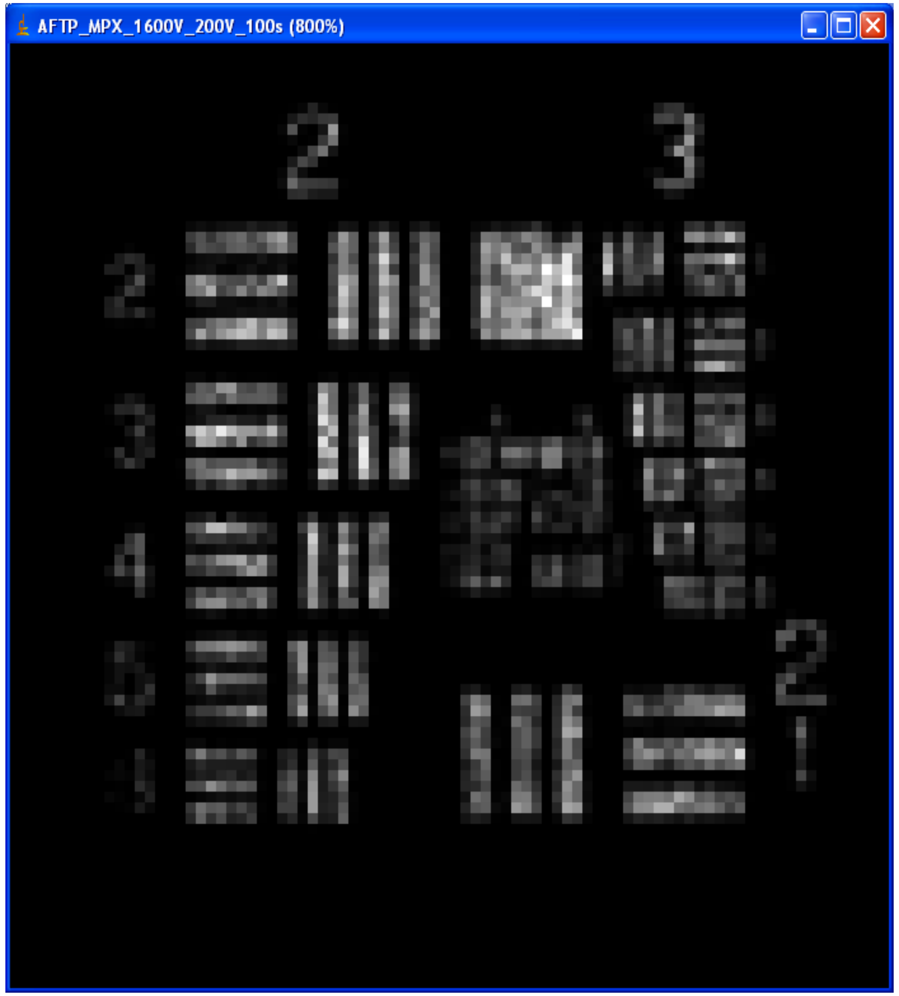

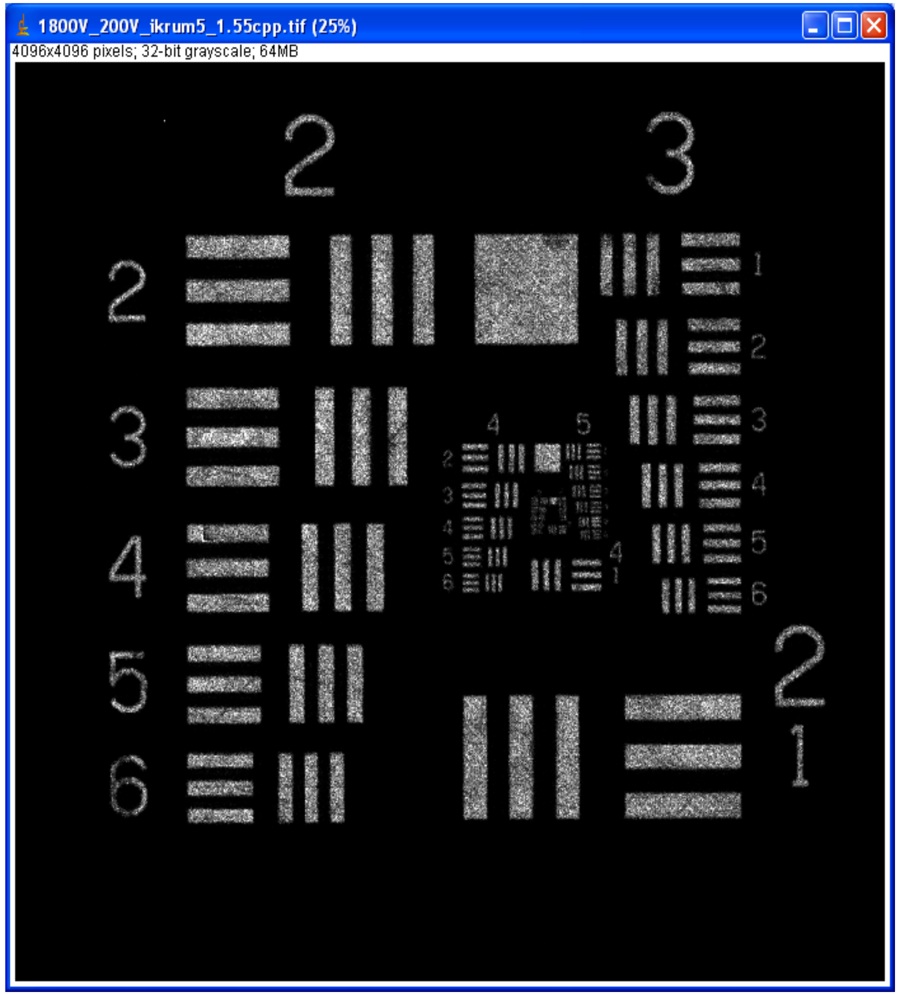

Timepix 1mm CdTe

Left:
No cluster analysis
8.5 LP/mm

Right:
Center of mass calc
57 LP/mm

J. Vallerga and co-workers, UC Berkeley, USA

IPix: Gamma Camera

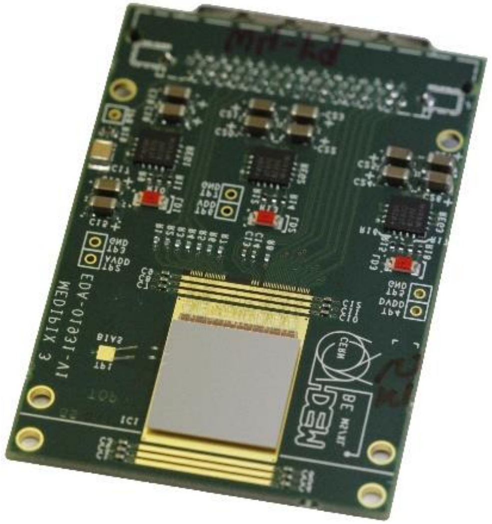

Sensor Data

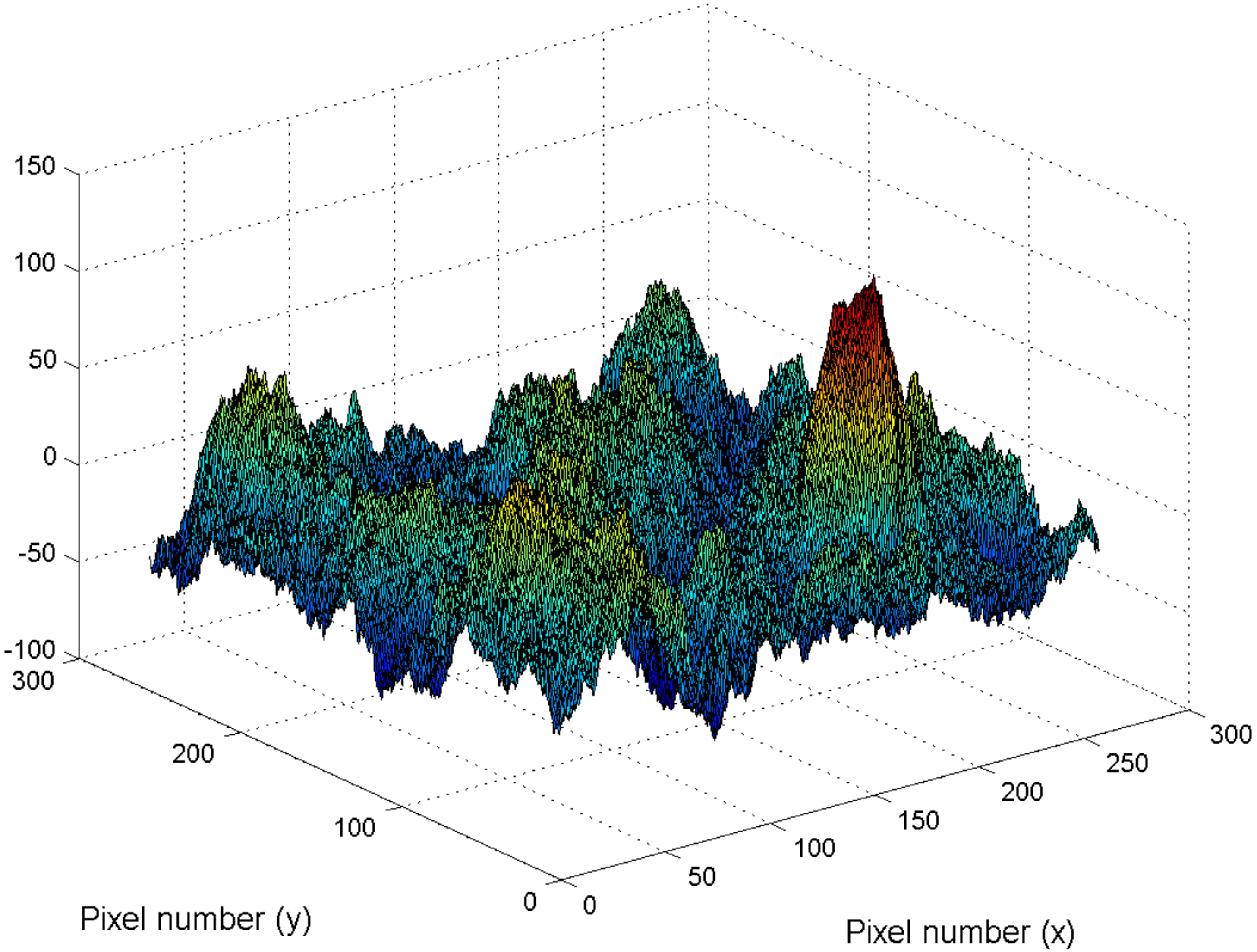

150
100
50
0
-50
-100
300
200
100
0
Pixel number (y)
0
50
100
150
200
250
300
Pixel number (x)

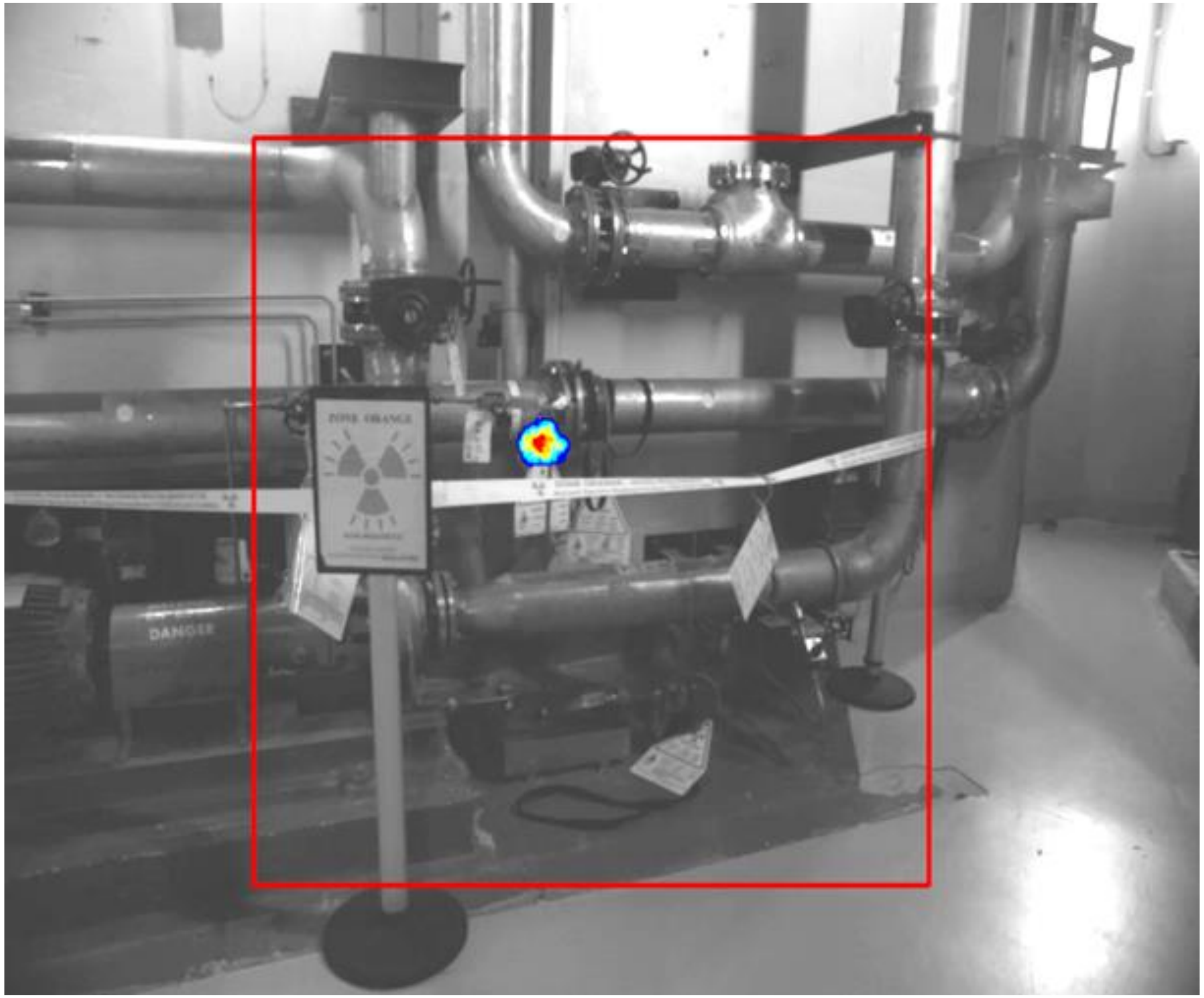
ZONE ORANGE
DANGER

Measurement Contest Nuclear Power Plant*

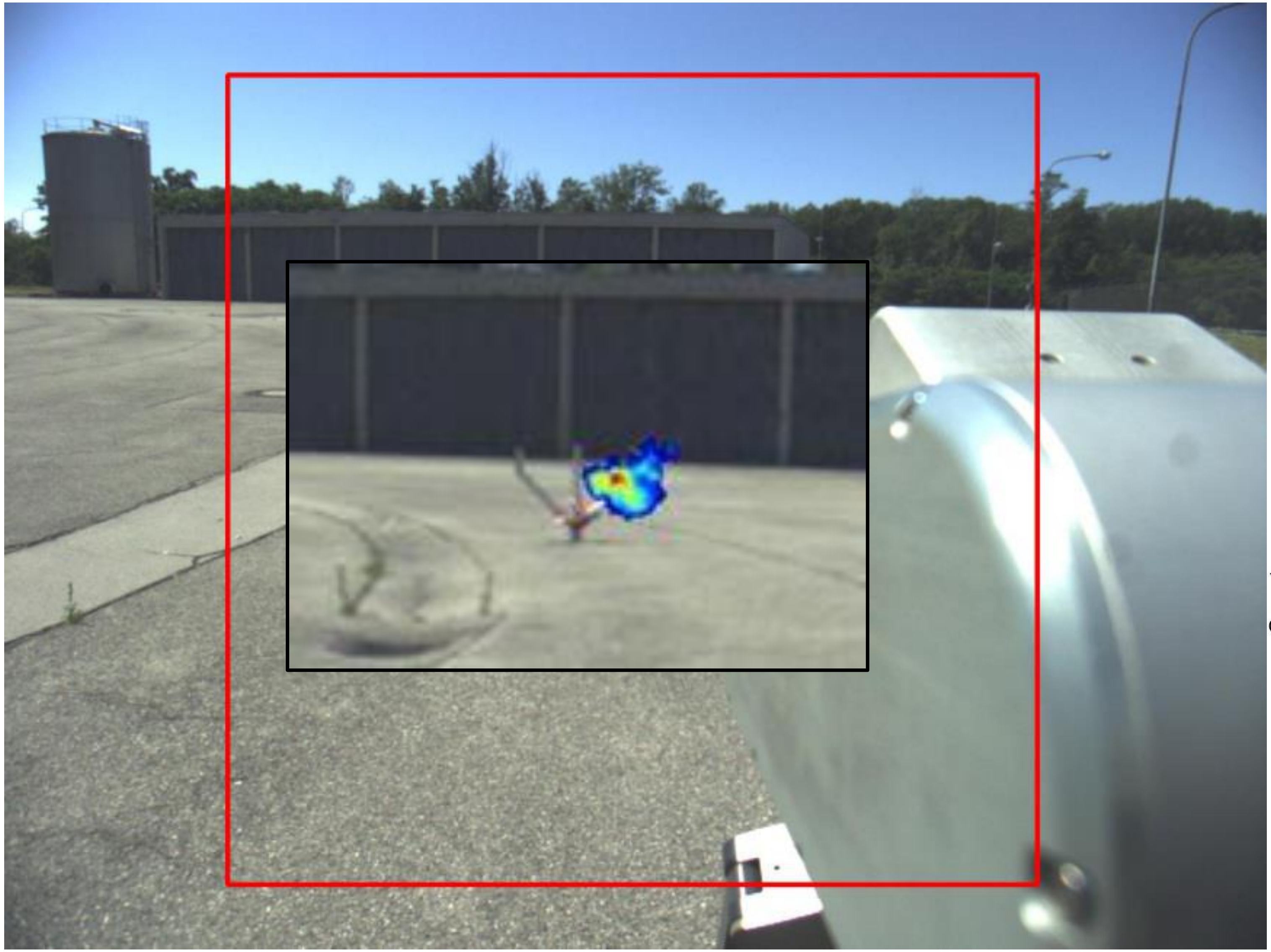

- Co60, 21 Cps, acq. time for loc. 115s
- Distance: 15 Meter
- 3mm @-660 V

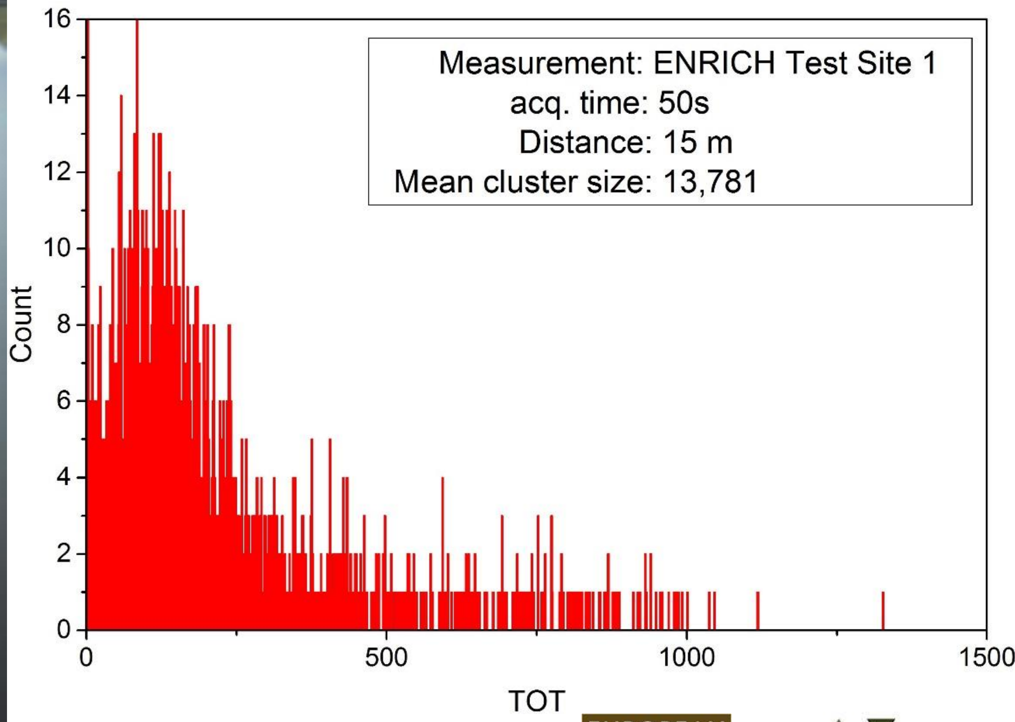

*2nd European Robotics Hackathon, EnRicH 2019 Zwentendorf Nuclear Power Plant (NPP) Austria July 1st - 5th, 2019

Signed
Vincent van Gogh

La Crau with Montmajour in the backgroud

~1888

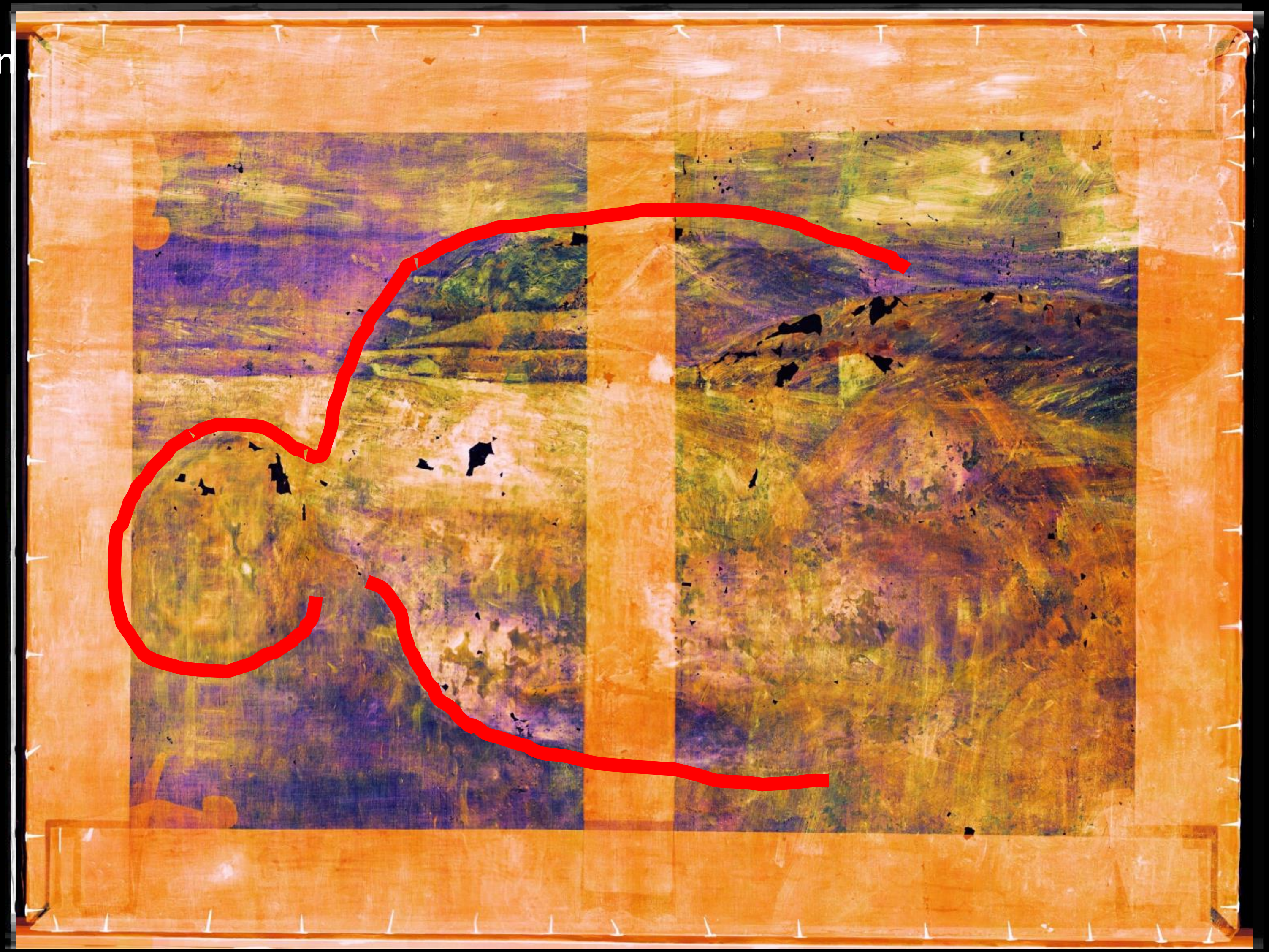

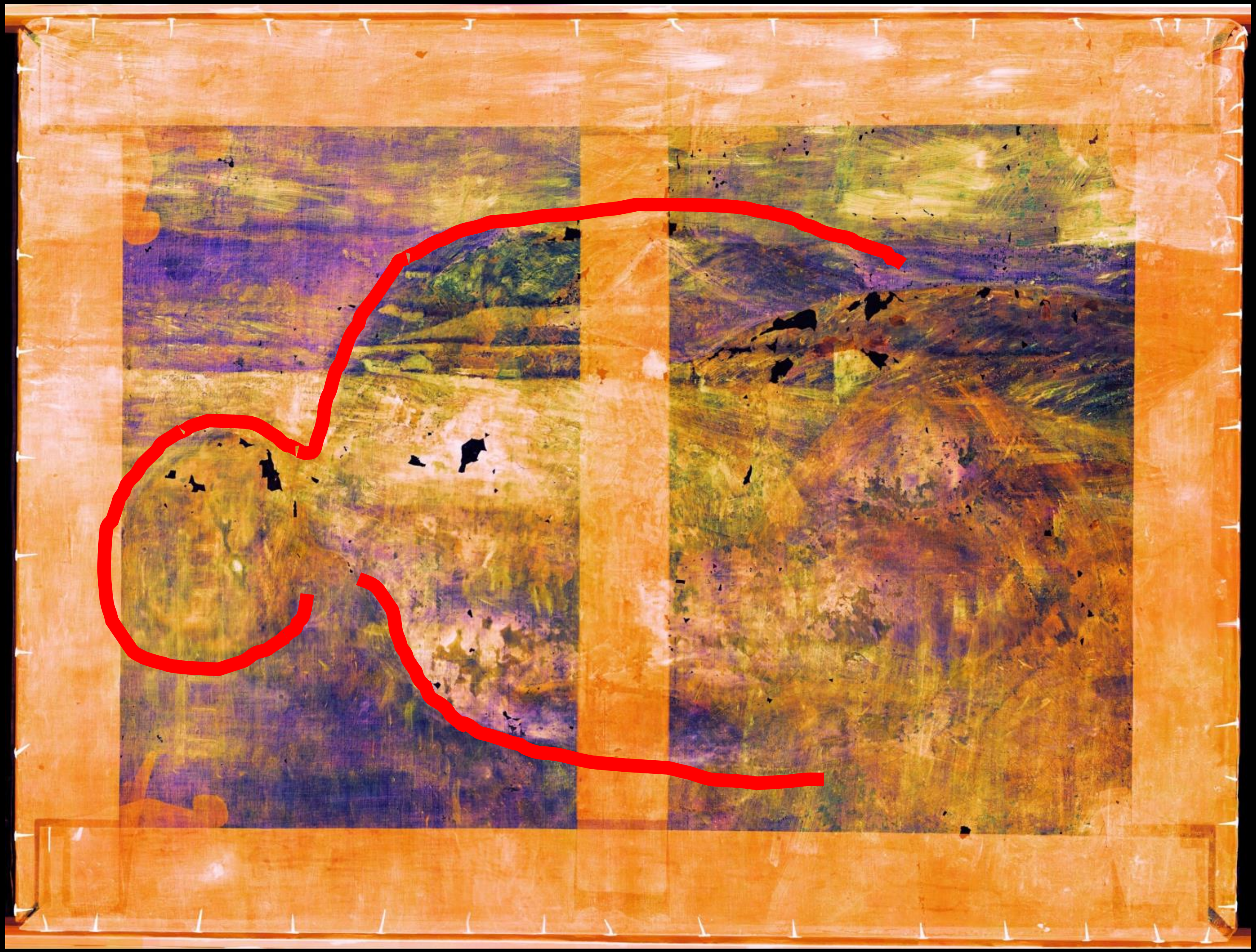

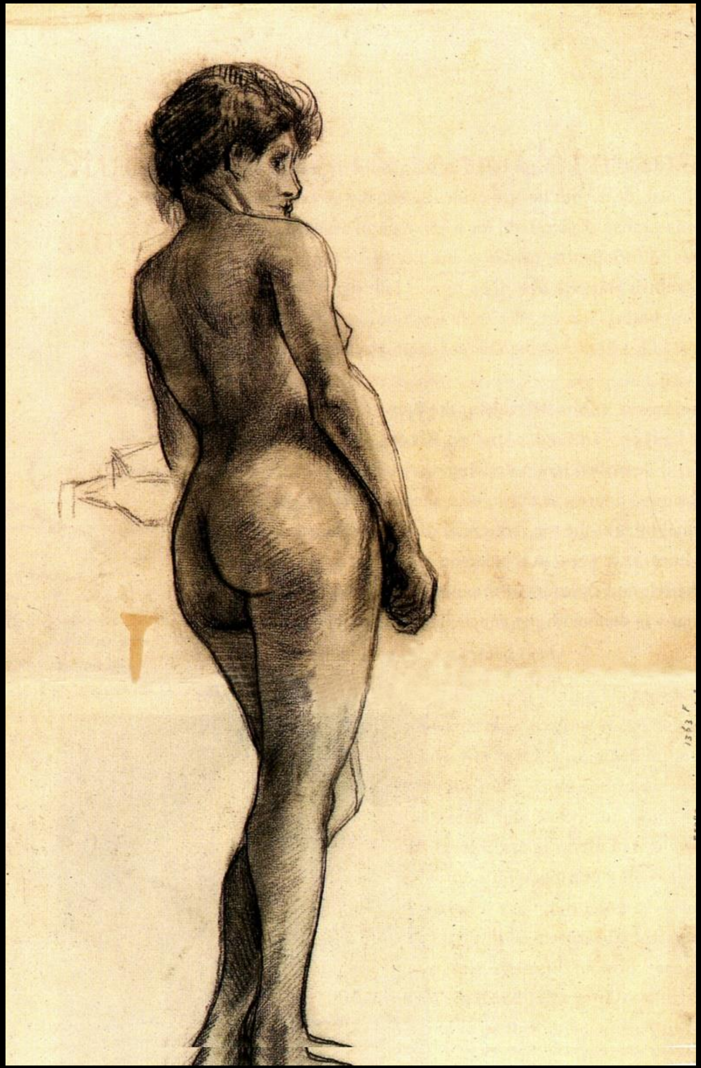

INSIGHTART

Timepix3 Particle Track Measurement

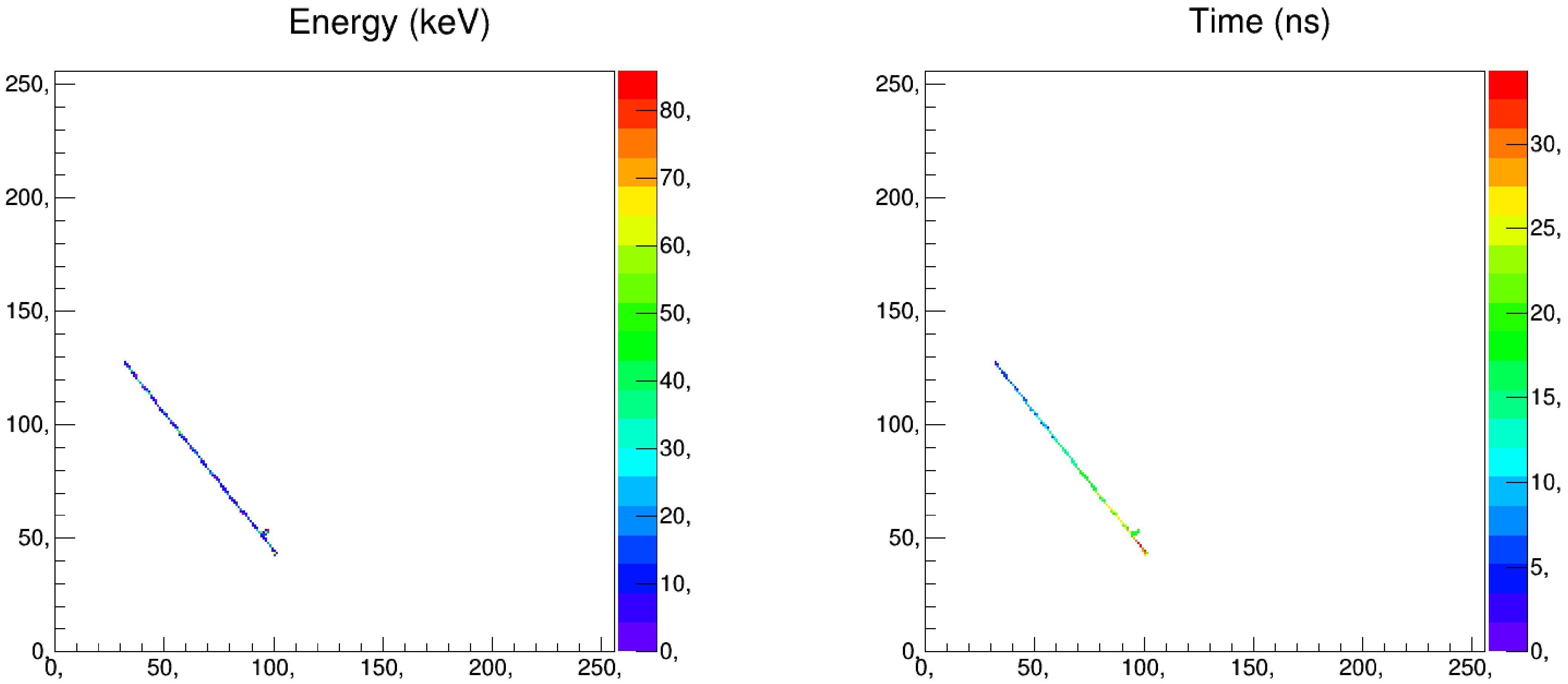

Bias 100V, Ikrum 5, with time walk correction

Timepix3 Particle Track Measurement

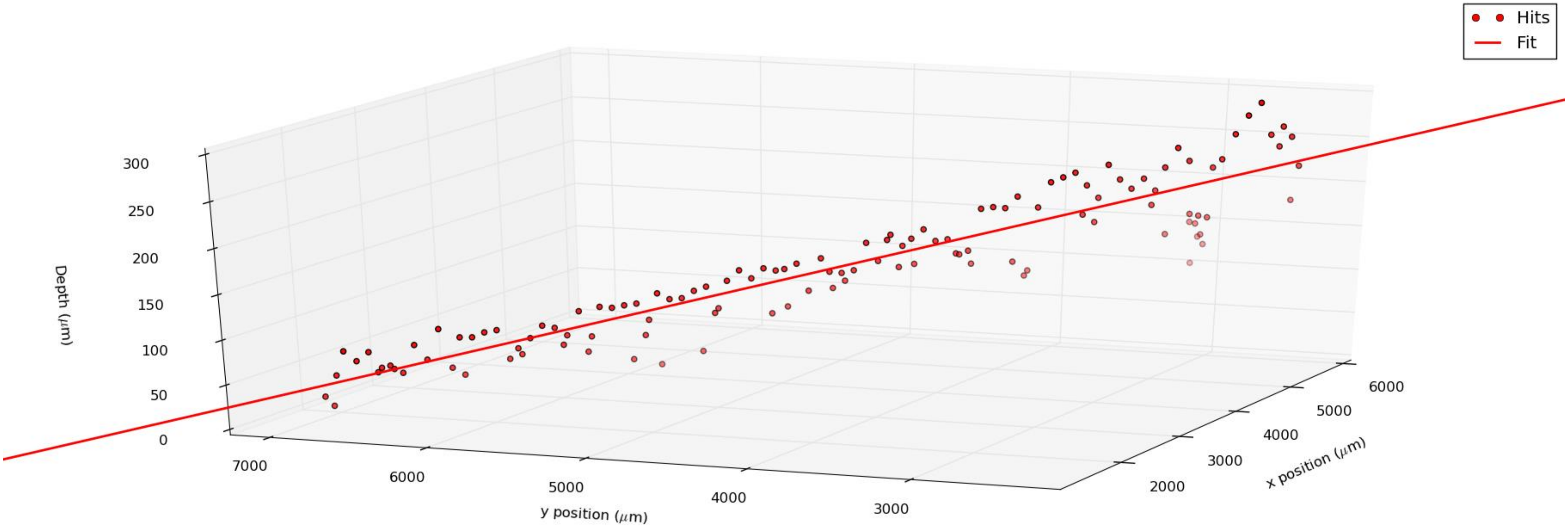

Note: Not to scale!

Bias 100V, Ikrum 5, with time walk correction

Test with 120GeV/c Pion Track

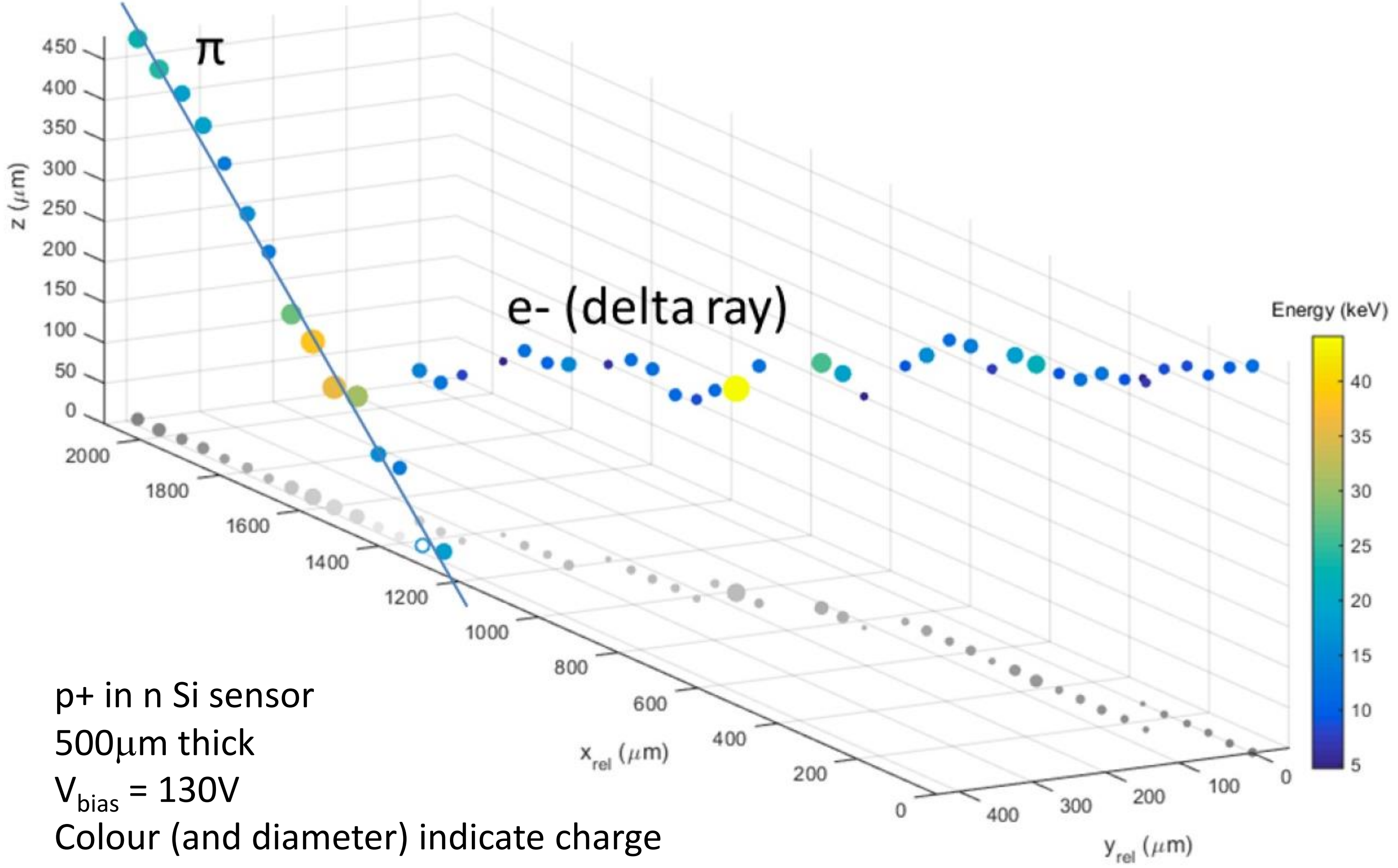

p+ in n Si sensor
500μm thick
V_{bias} = 130V
Colour (and diameter) indicate charge
Measured z resolution ~50μm

Source: B. Bergmann & S. Pospisil, CTU Prague

Timepix in Space at ISS

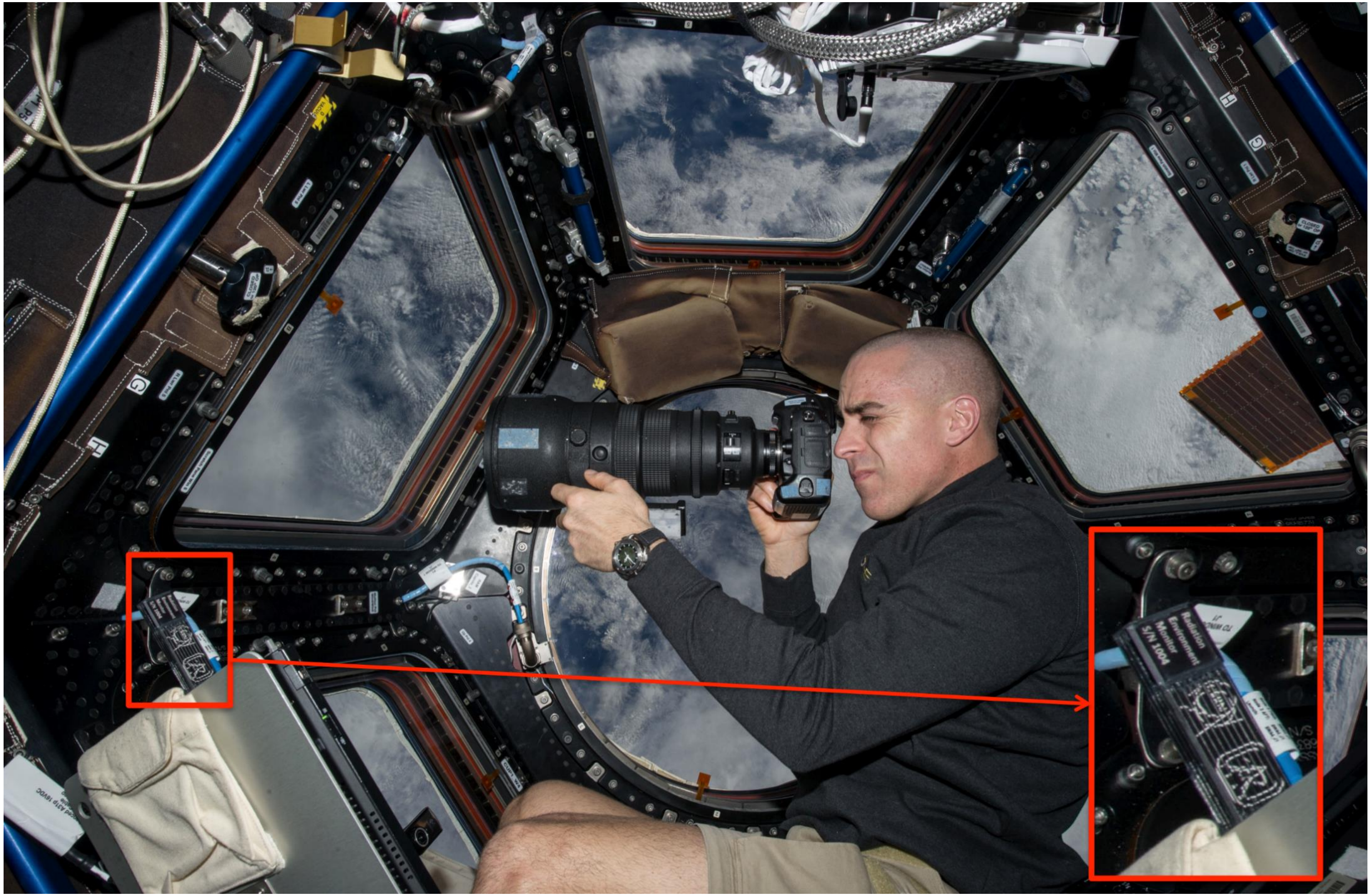

Source: Courtesy of NASA, photo ref. no. iss036e006175

REM Dose Rate Data (μG/min)

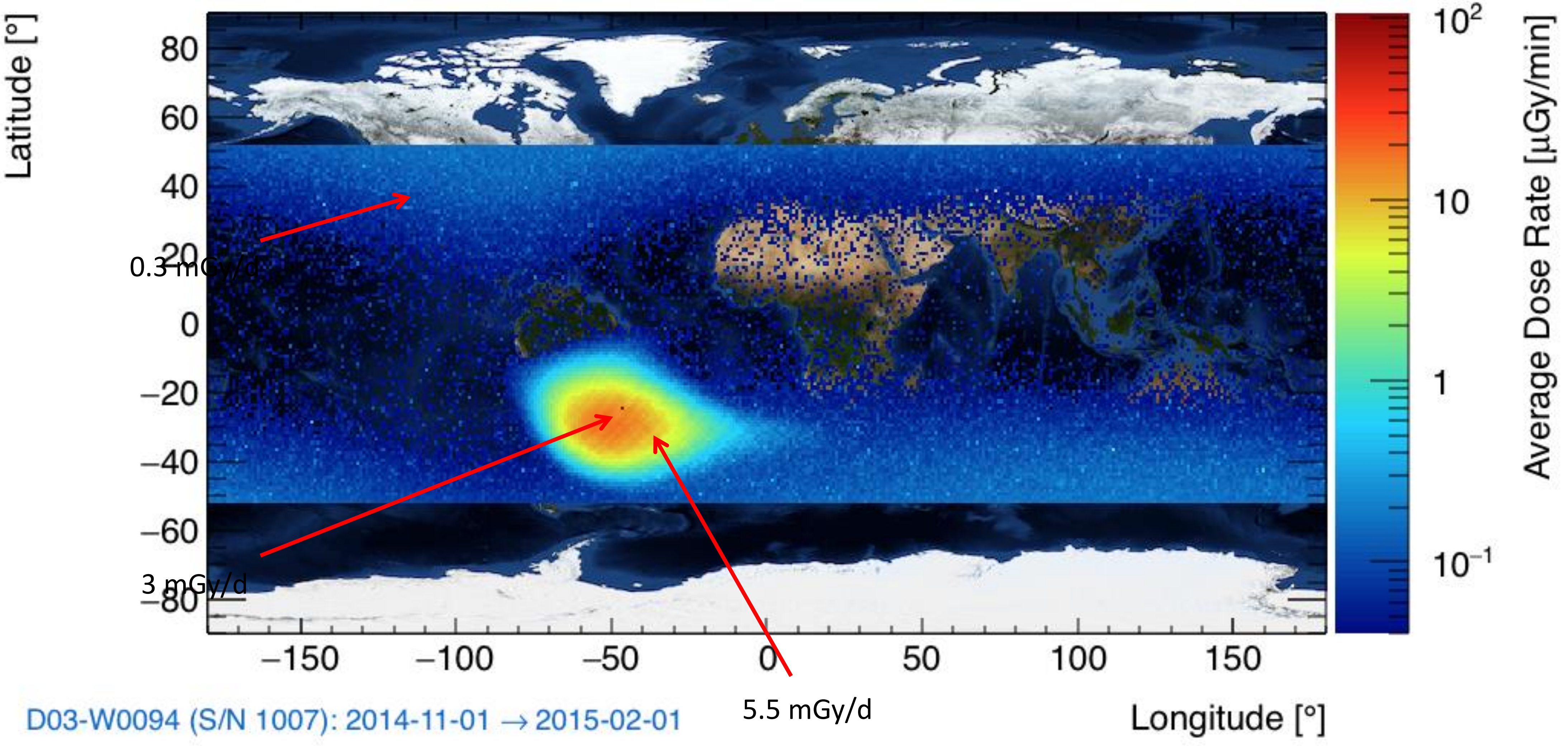

Source: University of Houston / IEAP Prague / NASA

Timepix - 4s Exposures in Space

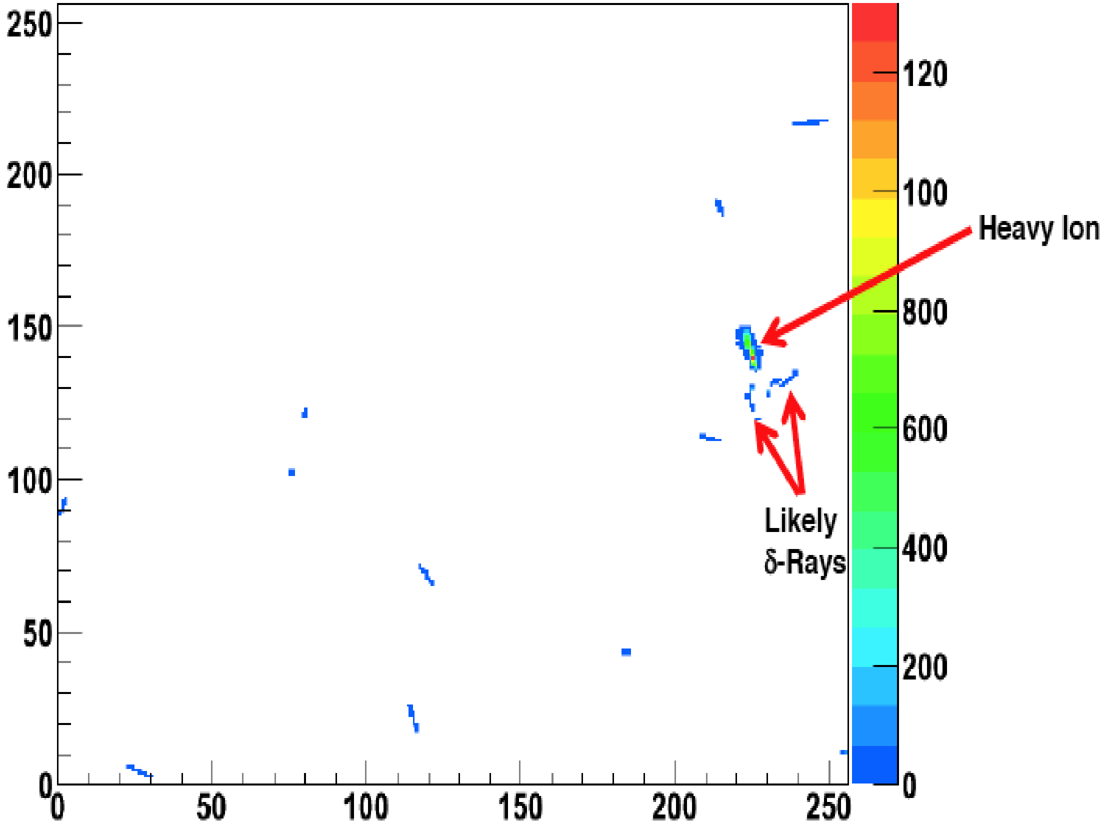

South China Sea

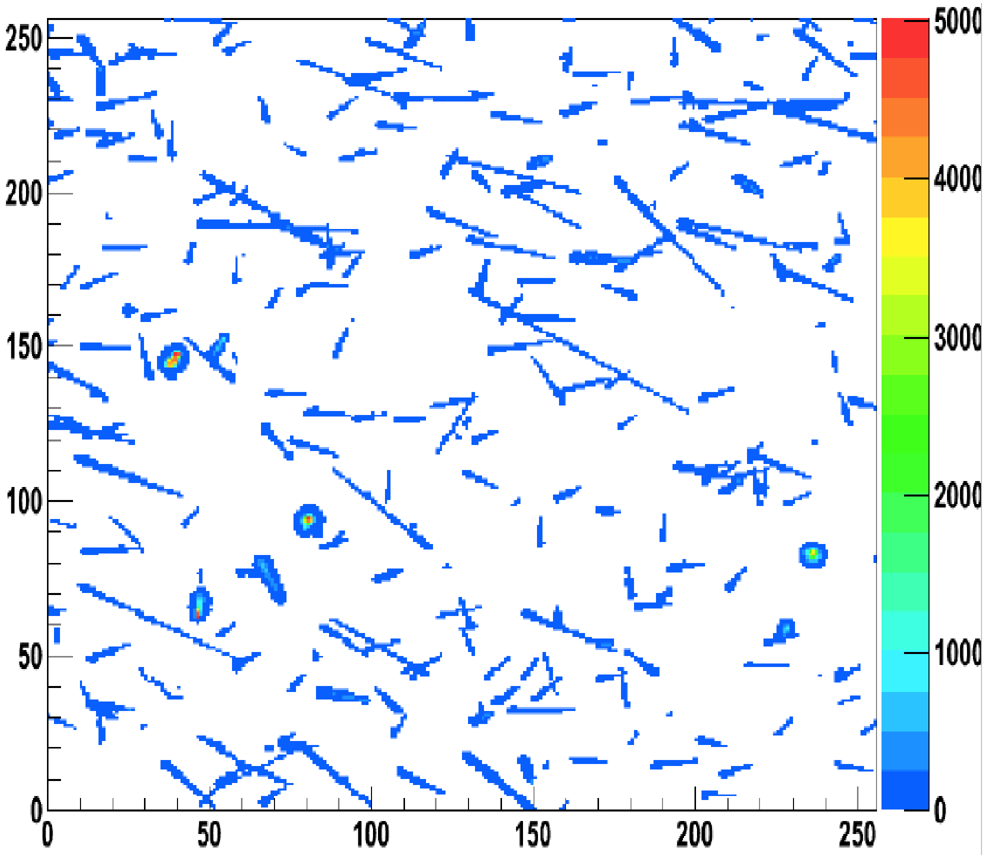

South Atlantic Anomaly

Source: University of Houston / IEAP Prague / NASA

Summary, Conclusions and Outlook

- Semiconductor detectors: important role in HEP, medical imaging, X- and γ-ray imaging, …
- High quality sensors necessary for high SNR, high-Z for high quantum efficiency
- Single photon analyzing detectors (Timepix) will offer totally new options
- New algorithms and ASICs are necessary for calibration, data processing, data analysis, visualization

10

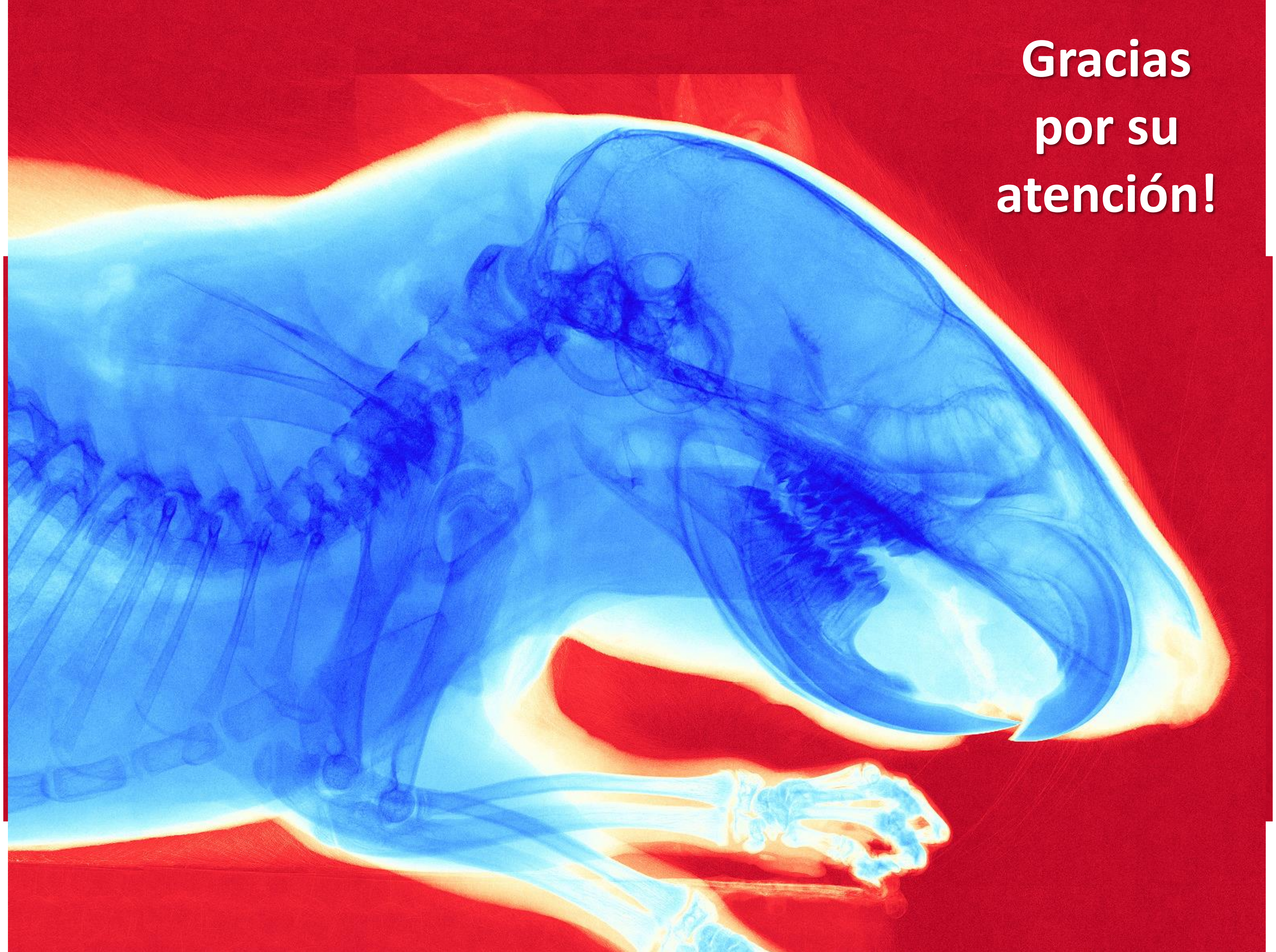

Per Pixel Calibration

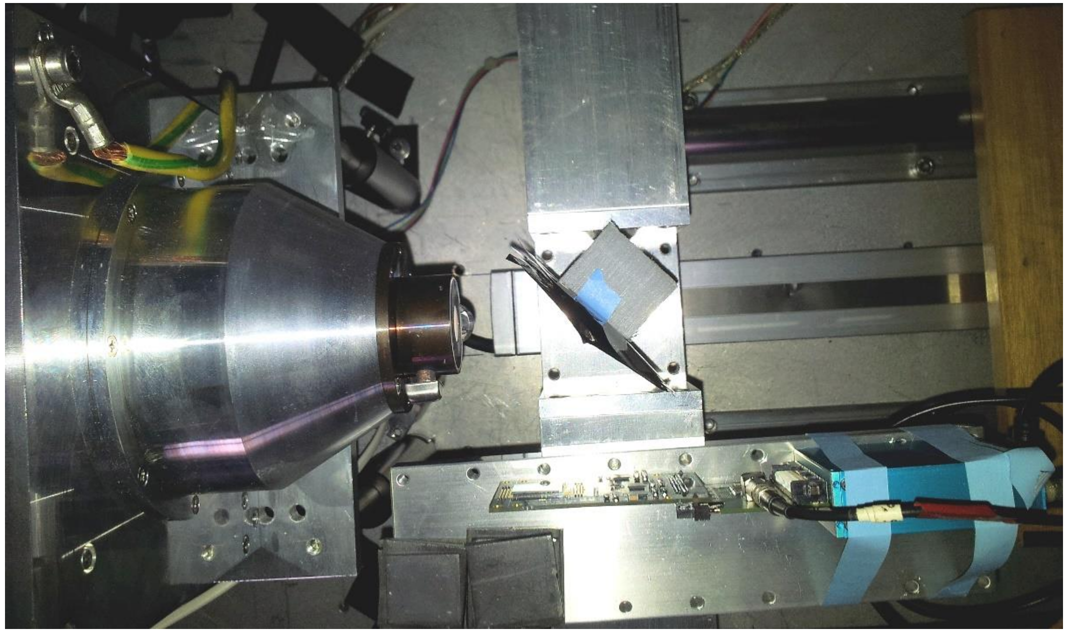

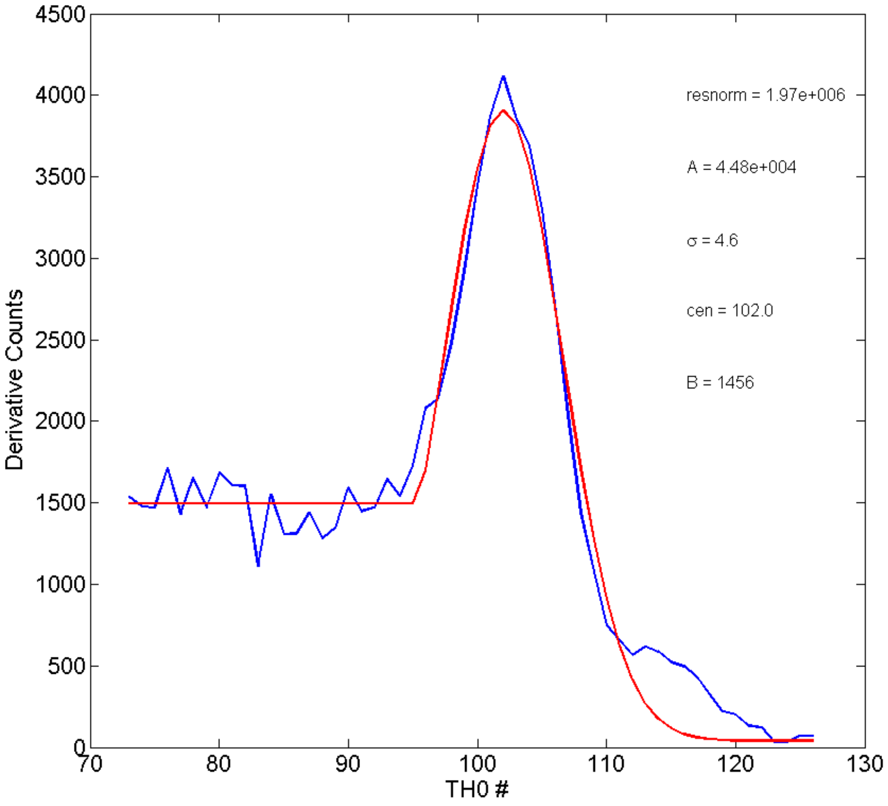

Equalization methods:

- noise floor
- test pulse
- counter adjustment
- spectral line

$$C + A \cdot \frac{1}{\sigma\sqrt{2\pi}} \cdot e^{-\frac{1}{2}\left(\frac{x-x_C}{\sigma}\right)^2}$$

$$+ \left(B - A \cdot \frac{1}{\sigma\sqrt{2\pi}} \cdot e^{-\frac{1}{2}\left(\frac{x-x_C}{\sigma}\right)^2}\right) \cdot \Theta\left(x_c - 1.4\sigma - x\right)$$

MPX3 Si Energy Deposition Spectrum

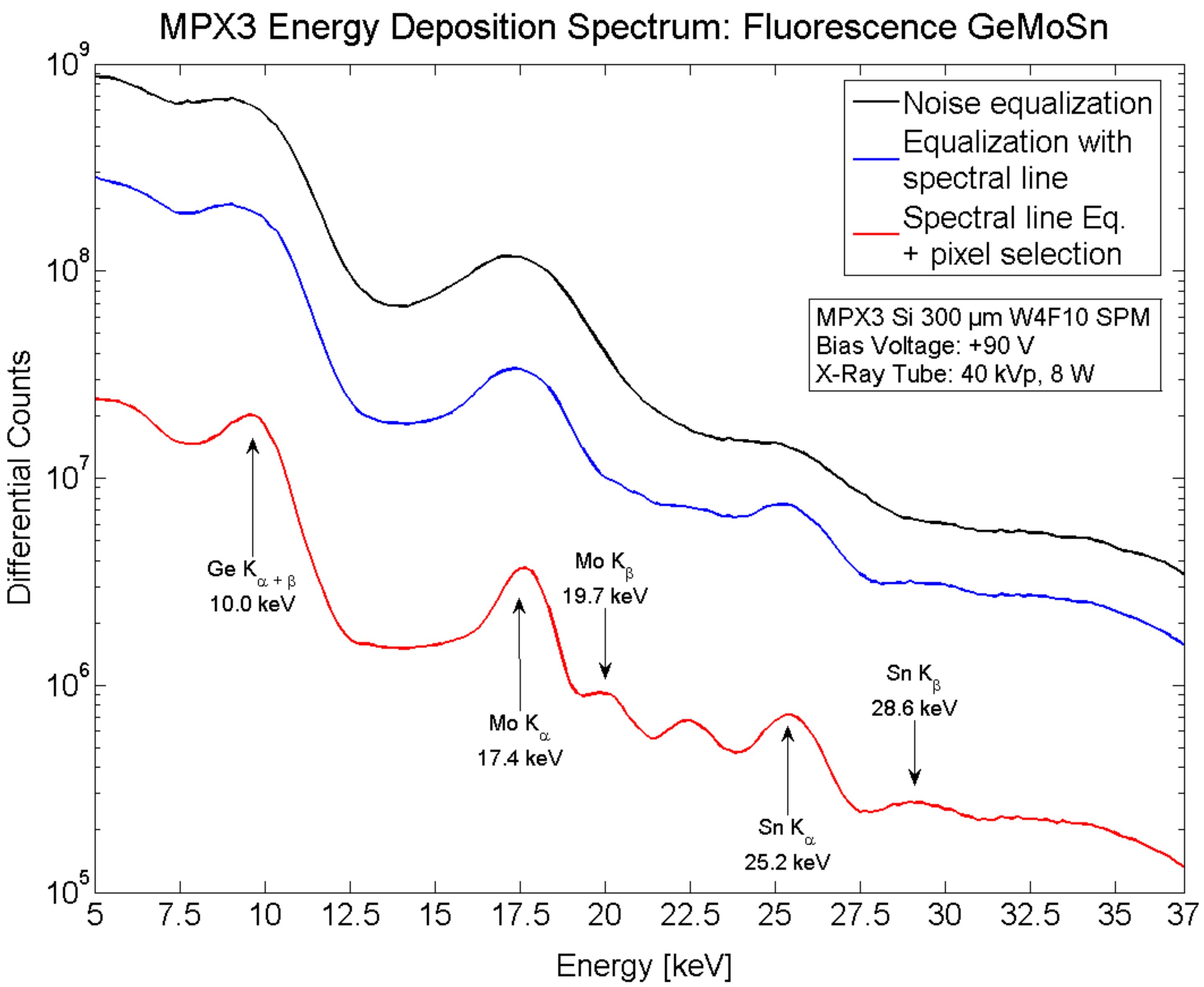

Timepix Energy Calibration

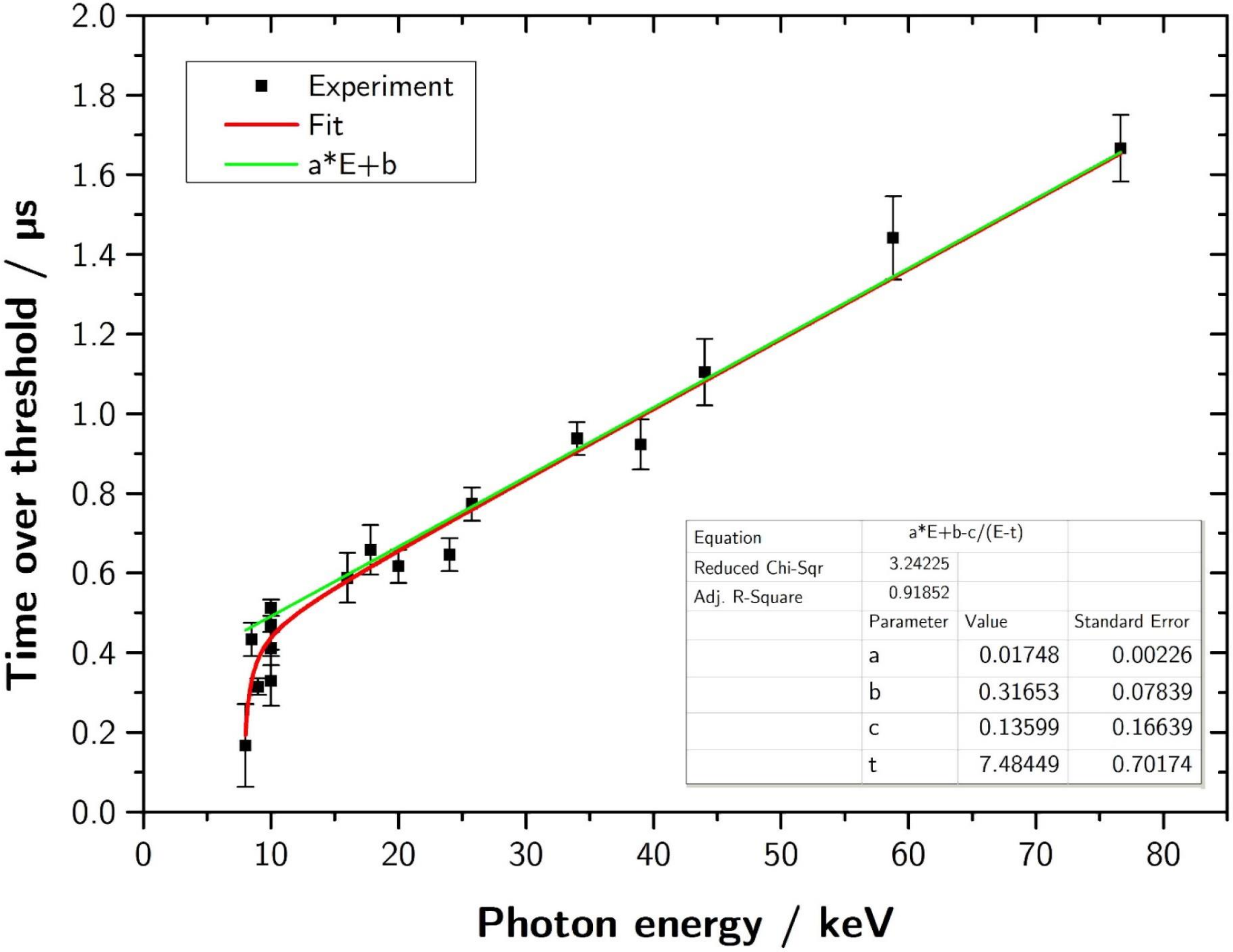

Equation	a*E+b-c/(E-t)		
Reduced Chi-Sqr	3.24225		
Adj. R-Square	0.91852		
	Parameter	Value	Standard Error
	a	0.01748	0.00226
	b	0.31653	0.07839
	c	0.13599	0.16639
	t	7.48449	0.70174

Source: Elias Hamann, Universität Freiburg / Jan Jakubek, Advacam

Medipix & Timepix

	Medipix2	Medipix3	Timepix	Timepix3
Pixel side (μm)	55	55/110	55	55
Technology (nm)	250	130	250	130
# pixels in x and y	256	256/128	256	256
Readout architecture	Frame based Sequential RW	Frame based Continuous RW	Frame based Sequential RW	Data driven/ frame based
Charge summing and allocation mode (CSM)	No	Yes	No	No
# thresholds	2 (window discriminator)	2/4/8 Seq RW 1/4 Cont RW	1	1
ToT/ToA	No	No	ToT (14 bit) OR ToA (14 bit, 10ns precision)	ToT (10 bit) AND ToA (18 bit, 1.56ns precision)
Front end noise (e^- rms)	110	80(SPM) 174(CSM)	100	62
Minimum Threshold (e^-)	900	500 (SPM) 1000 (CSM)	650	500
Peaking time (ns)	150	120	100	30
Max count rate ($Mc/mm^2/s$)* *very sensitive to exact test conditions	826	614 (SPM 55μm) 114 (CSM 55μm) 130 (SPM 110μm) 29 (CSM 110μm)	-	0.43 (data driven)

Source: M. Campbell / CERN

Sensor Homogeneity Comparison

Sensor raw image: GaAs

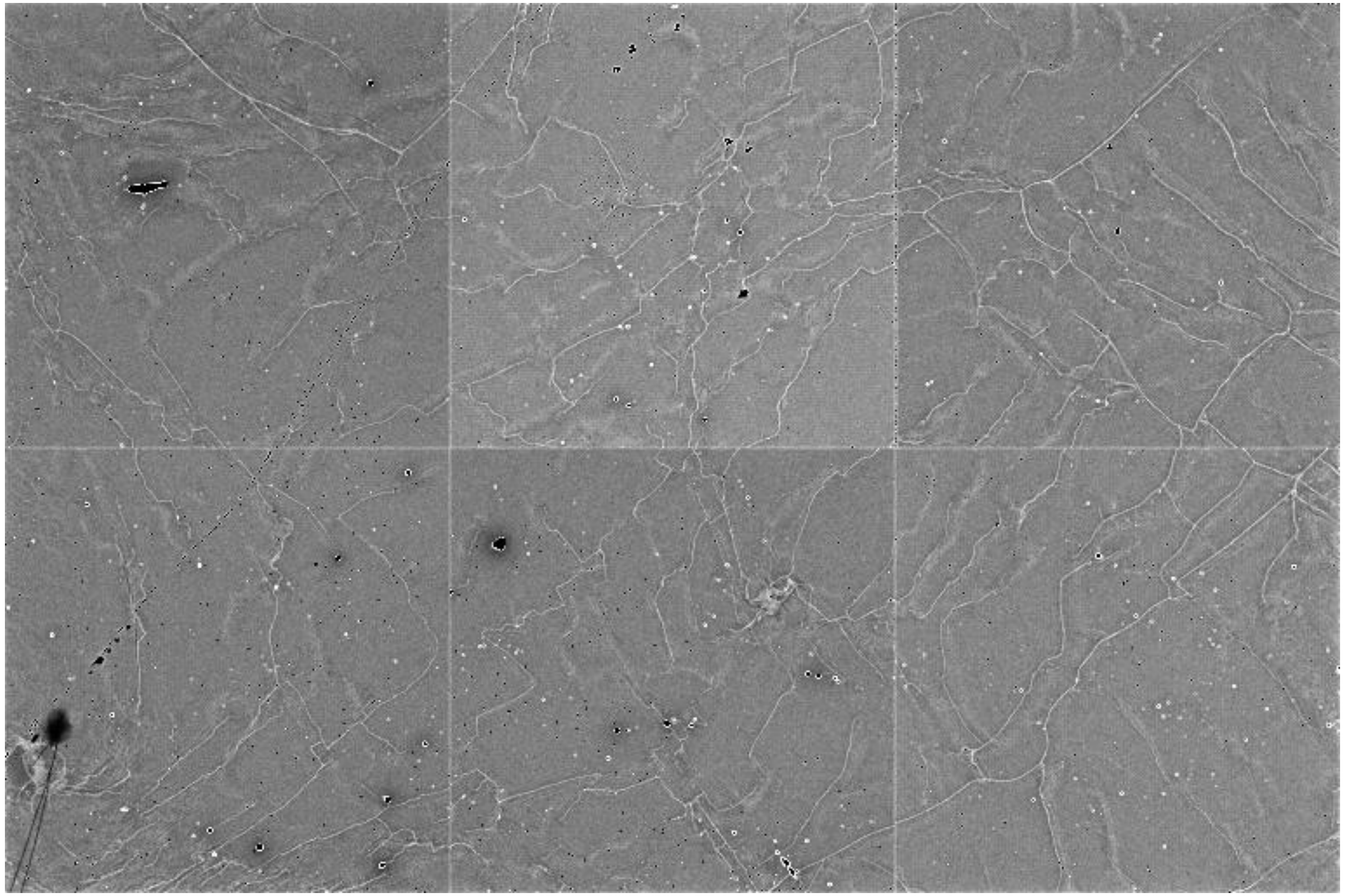

GaAs 500 µm

Medipix 3RX / Timepix Hexa

HV: +180 V

Defective pixels:

[illegible]

[illegible]

GaAs sensor
by Tomsk State University

Courtesy of D. Pennicard / H. Graafsma (DESY)

82

Dose Reduction: Simulations

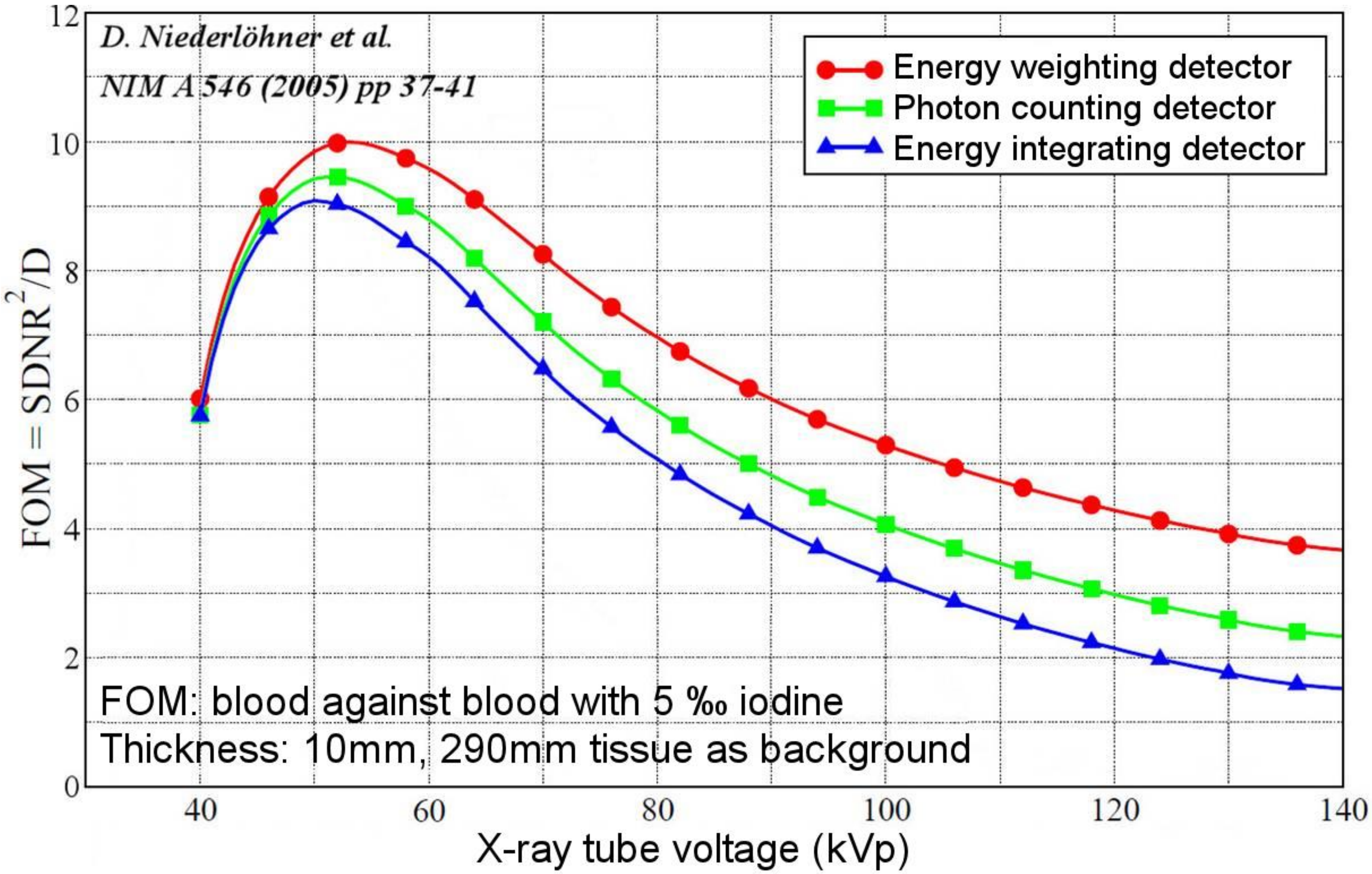

D. Niederlöhner et al.,"The energy weighting technique: measurements and simulations", NIM A, 2005

Single Layer Compton Camera with MiniPIX TPX3

^{131}Iodine gamma source

- 3 different Iodine solution in small bottles positioned in a room at different positions
- Distance from detector 3.5 m (activity 10's of MBq)
- Mapped on photograph of the room
- Sources located correctly within minutes
- Image took hours to collect

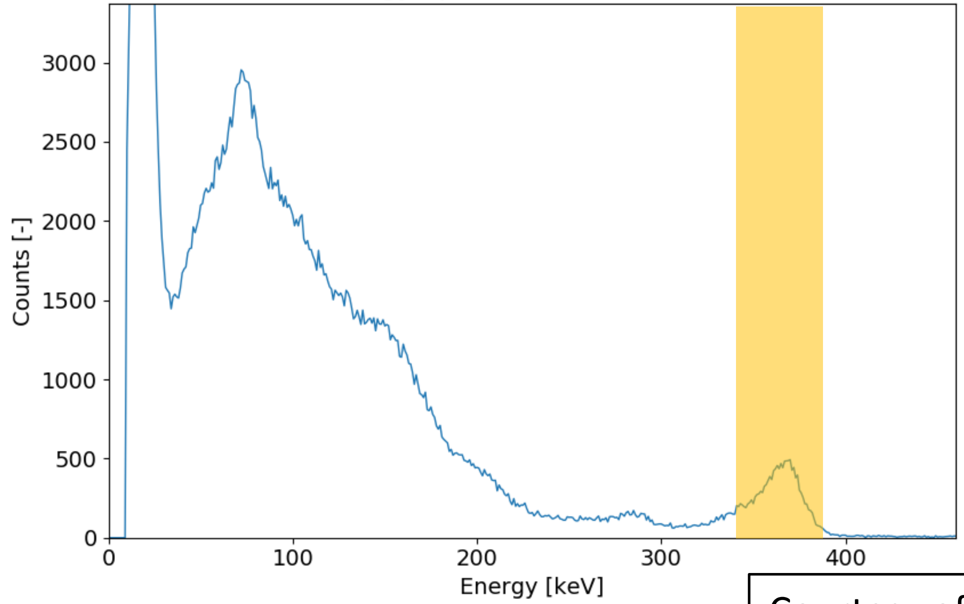

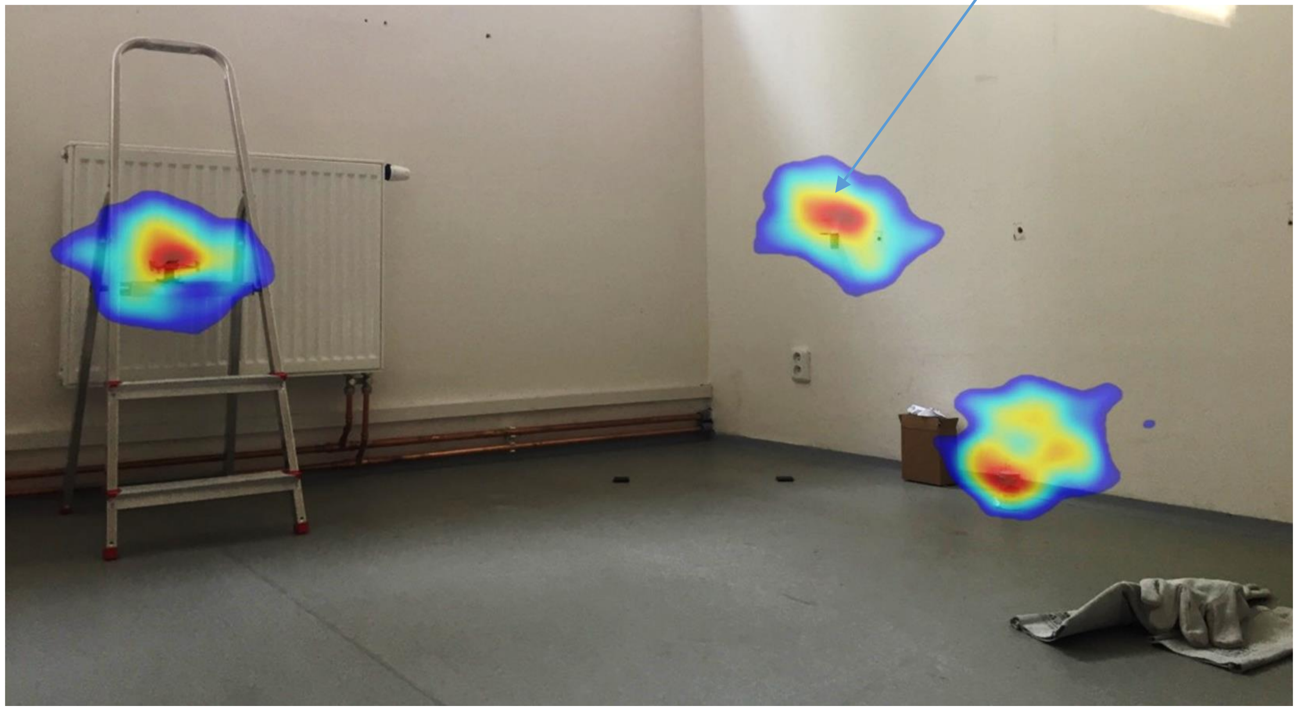

Reconstruction of position of three ^{131}I gamma sources (364 keV)

Courtesy of D. Turecek, Advacam s.r.o